R-04-58

Characterisation, design and execution of two grouting fans at 450 m level, Äspö HRL

Ann Emmelin, Svensk Kärnbränslehantering AB

Magnus Eriksson, Kungliga Tekniska Högskolan

Åsa Fransson, Chalmers tekniska högskola

September 2004

Svensk Kärnbränslehantering AB
Swedish Nuclear Fuel
and Waste Management Co
Box 5864
SE-102 40 Stockholm Sweden
Tel 08-459 84 00
+46 8 459 84 00
Fax 08-661 57 19
+46 8 661 57 19

ISSN 1402-3091
SKB Rapport R-04-58

Characterisation, design and execution of two grouting fans at 450 m level, Äspö HRL

Ann Emmelin, Svensk Kärnbränslehantering AB

Magnus Eriksson, Kungliga Tekniska Högskolan

Åsa Fransson, Chalmers tekniska högskola

September 2004

Summary

During June 2003 a grouting field experiment was carried out at Äspö HRL, in connection with the construction of a tunnel (TASQ) for the Äspö Pillar Stability Experiment (APSE). The tunnel is situated in connection to the elevator shaft landing at 450 m depth and runs in direction N/E. The grouting was carried out as part of the ordinary construction work, but was accompanied by extra investigations and analyses during operations and an active adaptation of a basic grouting design to the encountered conditions.

The main objectives of this set-up were to

- Investigate what can be achieved with best available technology, material and knowledge under the current conditions, i.e. a relatively tight crystalline rock mass at great depth.
- Collect data and evaluate theories resulting from previous research projects on characterisation and predictions on grout spread.
- Collect data to further develop those above mentioned theories.
- Contribute to the achievement of good conditions at the experimental site for the pillar stability experiments.

The characterization method is based on analyses of stepwise investigations consisting of investigations in an initially drilled core-drill hole followed by probe and grouting boreholes with pressure-build-up tests and measuring of inflow during drilling, all aiming at identifying the singular fractures that are to be sealed.

The decision about grouting design is based on the successively up-dated rock description from the characterization and iterative selection and testing of grouting design and grout in a numeric model, resulting in an expected grout spread and sealing effect.

Based on investigations and analysis of results from investigations of a core-drilled hole at the site, a basic design was set up, together with conditions for application. Probe boreholes covering the first anticipated fan gave substantially larger inflows than expected, and subsequently the design was changed. A first round was drilled and grouted, sealing off the larger fractures. This was followed by a round drilled and grouted according to the basic design, taking care of the smaller fractures. The other fan carried out was grouted according to the basic design. The sealing effects in both fans were high and according to calculations.

The application of the coupled methodology for characterisation and design implied that a systematic pre-grouting could be avoided due to a detailed characterisation and that an early assessment could be made concerning what is a suitable grouting methodology.

Sammanfattning

I juni 2003 utfördes en injekteringsstudie i Äspö HRL, i samband med byggandet av en tunnel (TASQ) för APSE – Äspö Pillar Stability Experiment. Tunneln är belägen i anslutning till hisschaktet på 450 m djup och dess riktning är N/E. Injekteringsstudien utfördes som en del av den egentliga produktionen, men denna åtföljdes av extra undersökningar och analyser under genomförandet som låg till grund för en basdesign och en anpassning av injekteringsutförandet i varje läge utifrån resultaten av analyserna.

Den egentliga anledningen till att bygga APSE-tunneln var således att åstadkomma en experimentplats för spänningsrelaterade experiment (Äspö Pillar Stability Experiment). För injekteringsstudien var syftet att:

- Undersöka vad man kan uppnå med bästa tillgängliga teknik, material och kunskap under aktuella förhållanden, dvs relativt tätt berg på stort djup.
- Samla data och utvärdera en tidigare framlagd metodik för karakterisering kopplad till injekteringsprognos.
- Samla data för att kunna vidareutveckla metodiken.
- Bidra till en god försöksplats för pelarstabilitetsexperimenten.

Karakteriseringsmetoden innebar stegvisa analyser utifrån undersökningar i ett initiellt borrat kärnborrhål följt av sonderingshål och injekteringshål. Undersökningarna, som utgjordes av bland annat inmätning av inflöde under borrning och tryckuppbyggnadstester och som syftade till att identifiera de enskilda strukturer som skulle tätas, resulterade i successivt uppdaterade beskrivningar av bergförhållandena.

Beslut om injekteringsutförande baserades på iterativa beräkningar i en modell där beskrivningen från karakteriseringen utgör indata, injekteringsutförande inklusive bruksegenskaper kan ansättas och resultatet visar bruksspridningen och tätningseffekt.

Baserat på undersökningarna i det initiellt borrade kärnborrhålet förutsågs två skärmar samt ansattes en basdesign för injekteringen med tillhörande kriterier för tillämpning av denna. De sonderingshål som täckte den första förutsedda injekteringsskärmen gav betydligt större inflöden än förväntat, och injekteringsutförandet anpassades så att injekteringen utfördes i två omgångar i detta läge. Den första omgången utfördes i syfte att täta de större inläckagen, varefter den andra utfördes enligt basdesignen i syfte att täta de mindre inläckagen. Tätningseffekten i båda de skärmar som kom att utföras var hög och i enlighet med beräkningarna.

Tillämpningen av denna kopplade metodik för karakterisering och design innebar dels att systematisk förinjektering kunde undvikas tack vara en detaljerad karakterisering, dels att en tidig bedömning av lämplig injekteringsmetodik kunde göras.

Notations and symbols

Roman letters

Symbol	Unit	Explanation
b	µm	hydraulic aperture
$b_{average}$	µm	arithmetic mean aperture
$b_{critical}$	µm	critical limit on aperture for filtration of grout
b_{min}	µm	minimum aperture for grout penetration
c	%	amount of contact
dL	m	step length for Posiva Flow Log
dh	m	difference in hydraulic head
g	m/s^2	acceleration due to gravity
L	m	test section for Posiva Flow Log
Q	L/min	flow
Q/dh	m^2/s	specific capacity
Qmax	L/min	the largest total inflow to a section of a borehole
Qtot	L/min	the total inflow to a borehole
r	m	radial distance
s”	m	recovery
S	–	storage coefficient
t_e	s	adjusted time
t_P	s	injection or flow time for pressure build-up test
t_{PB}	s	time since recovery started or the Pressure build-up time
T	m^2/s	transmissivity

Greek letters

ρ	kg/m^3	density
µ	Pa s	viscosity
μ_B	Pa s	viscosity in Bingham fluids
τ_0	Pa	yield value in Bingham fluids

Abbreviations

BIPS	Borehole Image Processing System
Fan 1:2	Grouting Fan 1, round 2
HMS	Hydro Monitoring System, permanent installation in Äspö HRL, for automatic registration of groundwater pressure.
PBT	Pressure build-up test
PFL	Posiva Flow Log
RVS	Rock Visualisation System
w/c ratio	water to cement ratio (in weight)
Äspö HRL	Äspö Hard Rock Laboratory

Positioning

Throughout this report, data, analyses and results from probe- and grouting boreholes are related to the length of the core borehole. However, names of boreholes and fans are related to the length used for the construction work. The difference between the length for the construction work and the core borehole length is approximately 11 m. Consequently, probe borehole SQ0049B starts at approximately 38 m along the core borehole (49–11=38 m). When using the Rock Visualisation System (RVS) to present 3D-images this is of no importance since the borehole coordinates (X,Y,Z) are used to compile data.

Contents

1 Introduction

1.1 Background

SKB grouting research aims at knowledge, methods, grout and equipment to handle all inflow situations, taking into account the special demands made by the deep repository. To achieve this it is essential to get a thorough understanding of the system rock – grout – grouting technique. In the 1990s SKB initiated a rock grouting research programme. Two doctoral studies within the programme were concerned with the task how to characterise the rock in such a way that it can be used as the basis for prediction of grout spread and subsequent grouting design. Resulting models were tested in laboratory and in a small field experiment and proved reasonable /Fransson 2001; Eriksson 2002/. However, to be able to make use of the theories in a real production situation, they need to be verified through testing under controlled circumstances in different situations and also further developed, and a methodology that is compatible with an effective production needs to be worked out.

Taking part in the construction and sealing of the tunnel being built for the Äspö Pillar Stability Experiment (APSE) presented itself as a good opportunity to test theories and practices under controlled circumstances, and to collect data for further development of the methodology. Thus a special project "APSE Grouting" (SKB project no SU308) was initiated.

1.2 Objectives

The main objectives of the APSE Grouting project were to

- Investigate what can be achieved with best available technology, material and knowledge under the current conditions, i.e. a relatively tight crystalline rock mass at great depth.
- Collect data and evaluate theories resulting from previous research projects on characterisation and predictions on grout spread.
- Collect data to further develop those above mentioned theories.
- Contribute to the achievement of good conditions at the experimental site for the pillar stability experiments.

It should be noticed that there was no level set for what would be the accepted inflow after sealing work.

One aspect to consider when setting up strategies for the work, was the amount of grout to be consumed. In the deep repository it will be desirable to keep the amount of foreign matters as low as possible. This goal was also to be applied at the APSE tunnel, and thus the qualitative goal was to get the tunnel "tight" with as little grout as possible.

1.3 Overview preparations and field experiments

1.3.1 Site selection and grouting research ambitions

At the time of involvement of the grouting research team three potential sites in the Äspö HRL were under consideration, and preparation of tender documents for the construction work was under way. Results, including pressure build-up tests, from core-drilled holes at two sites existed; those sites were under discussion as there was a risk of disturbing other experiments. A third site was under investigation, pressure-build-up tests not yet carried out, but with a relatively low flow from the core-drilled hole and presumably lower risk.

Based on the knowledge at the time, the grouting research team set up three alternative ambition levels 1–3 for the work to be carried out, depending on the site selection and the conditions there.

1. Make a general review of draft to tender documents and possibly suggest improvements, with regard to grouting operations. In construction work include registration of inflows and collect those and other grouting data (amount of grouting, flow, pressure) for later analyses. No active involvement during construction.
2. As level 1, plus evaluation of pre-investigations as a basis for adjustment of the grouting design described in the draft to tender documents (setting-up of a basic grouting design). Make a prediction of grouting outcome. No active involvement during construction.
3. As level 2, plus active involvement during construction meaning stepwise interpretation of tests and measurements during construction and a subsequent review and possibly adjustments in the application of the basic grouting design.

Level 3 would only be carried through if the rock mass – as interpreted from pre-investigations – could be judged as "groutable", meaning if waterbearing fractures larger than approximately 100 µm were predicted.

As it turned out, the third new site proved suitable for the pillar stability experiment, the risks judged under control and thus this site was chosen. The inflows registered during drilling indicated that there was a water-bearing stretch at 50–57 m with fractures estimated to approximately 100 µm, while the rest of the rock along the core-hole was dry.

The ambitions for the grouting research was thus set generally at level 2, but with the higher level 3 for the stretch at 50–57 m, where it was already shown necessary to grout.

1.3.2 Preparation of tender documents and basic grouting design

The first draft to tender documents implied a pregrouting with 12–15 m long grouting fans with 3 m overlap and a distance of 3.5 m at the most between grout holes in a fan. The concept included 35 m long probe boreholes drilled in two groups of three covering the entire tunnel length, with inflow and results of pressure-build-up tests as the basis for decision on whether drilling for grouting was to be carried out. It was specified that microcement was to be used and requirements on grout properties were set. Based on the knowledge at the time, a preliminary grout spread analysis showed that the hole distance should be smaller, and that it then could be possible to seal the rock mass, using a Ultrafine 12 grout mix with high w/c ratio.

Rock conditions were discussed with grout manufacturer Cementa who given the choice between Ultrafine 12 and Ultrafine 16 (UF 16) recommended the not so widely used UF 16, which was also prescribed in the final tender documents.

Grouting was specified in a combined technical description – bill of quantities, giving recipes for grout and instructions for executions of tests and grouting. In the description was stated that the client would make changes based on the result of grouting work. No special statement was made about level 2 and 3. Tender documents also included drawings of fan design and a control programme specifying tests on grout before and during construction, as well as measurements of inflow and water-loss in probe, grout- and blast holes. A special document was included as informative only, explaining the aims and basics for the investigations that were to be carried out with the main components probe boreholes with pressure build-up tests covering 2–3 possible grout fans, and inflow measurements in 3 m sections in every drilled hole. Pressure-build-up tests were to be executed by the client and were described in detail in a separate activity plan.

1.3.3 Procurement and preparations for field work

During the contract discussions with the contractor-to-be, it was decided to abandon the bill of quantities included in the tender documents, which was based on production units such as number of drilled holes etc. Instead a new list was established based on costs per hour for workers and equipment and costs for amounts of materials used, and it was agreed to use this as a means for settling the accounts for the work. The main reason for this agreement was that given the relatively large cost for the contractor to establish itself on the site and the relatively small scope of the actual production work under the special conditions that rule work at the Äspö HRL, it seemed hard to establish fair production unit prices. It also seemed advantageous to be able to make adjustments to the plans presented in the tender documents with the research aims in focus, without discussions about prices for new or substituted work items.

After the final version of tender documents, pressure-build-up tests were carried out in the core-drilled hole and a more detailed description of the rock mass and its water-bearing fractures was achieved. Pre-testing at KTH lab was done on different UF 16-mixes to establish grout properties. A number of combinations of grout and grouting strategies were tested numerically. The basic grouting strategy was confirmed and details added. With regard to grout spread, it was decided that maximum grout hole distance should be 2 m, and that grouting should start with a high wcr grout, if needed followed by stiffer grout at a certain volume.

Probe boreholes were planned to be drilled in four pairs starting at 0 m, 24 m, 38 m and 62 m. The start position and length of holes were set from the information from the core borehole, so as to cover two or three possible grout fans and to cover all of the wet stretch with probe boreholes pair no 3.

The instructions for grouting were worked out in more detail, and it was distinguished between the stretch with water-bearing fractures (level 3) and the drier stretches (level 2). For level 2 stretches the basic design would be applied, meaning grouting according to the pre-set design was to be carried out, under condition that there was an inflow to probe boreholes amounting to a set value. The pre-set inflow was related to the prediction of what fracture-sizes were groutable. If inflows were larger than a certain value, the client would be contacted for instructions. For the level 3 stretch two grouting fans were anticipated. The research group would carry out immediate analyses of hydrotests in the probe boreholes as a basis for any adaptation of the pre-set design and no further drilling be carried out before notification from the client.

The adjusted descriptions were presented in a revised description and discussed with the contractor in written and at a special start meeting where the grouting personnel were introduced to aims and means of the execution of grouting and experiment.

1.3.4 Execution of grouting and analyses

It was anticipated that there might be interest conflicts between the "main" pillar stability experiment, the grouting research and a third research task concerning the disturbed zone. A SKB project manager was appointed to carry through the contract, being responsible for priorities and budget. Although informal discussions were held between the contractor and the grouting research group, all major decisions were formally taken by the client represented by the project manager and delivered to the contractor by the client's contact person.

This also meant that for the "level 2 stretches" – if the inflow was so large that the basic design was not applicable and the contractor was supposed to contact the client, the grouting research group would only be contacted if the project manager found it necessary.

When the contractor and equipment were established on site, the specified pre-testing of grout properties was carried out. Those included Marshcone-time, density, penetrability with filter-pump and setting. Based on results the conditions for approval of grout batches were set; those were limited to penetrability and density.

When excavation works started, there were a number of mishaps resulting in a gross delay in the time schedule. To potentially save time, the pre-set inflow values constituting the conditions for drilling for grouting or for continued blasting were increased. One of the time-consuming problems was the actual blasting and excavation of the tunnel and probe boreholes pair no 1 was drilled from position 5 m in order to fit in with the other work.

Probe boreholes pair 1 and 2 showed practically no inflow, i e according to predictions, and no grouting was carried out.

Probe boreholes pair no 3, covering the earlier identified water-bearing stretch at 50-57 m gave inflows larger than expected, and beyond the limits for the applicability of the basic grouting design. It was also judged probable that the fracture size ranged above the estimated 100 µm on which the basic grouting design was based. Two grouting fans (Fan 1, Fan 2) were planned to cover the water bearing structures, the first one covering the position of the large inflow. A number of possible strategies following two main ideas were modelled in the grout take model to get a basis for the decision on how to cope with this unexpectedly large inflow. The two main ideas were either to use only the drilling geometry of the basic design, or to start out the grouting with an extra round of drilling and grouting in order to first seal the larger fractures. The alternative with an extra drilling and grouting round was chosen, although this meant a certain use of resources and time. The new working order was documented and signed by the client's contract person. The first round was drilled and grouted with a relatively stiff grout (Fan 1:1). When drilling the second round (Fan 1:2), inflow had decreased to the initially expected level, and grouting was carried out according to the basic strategy. Control holes gave inflows below the limit value and excavation was continued.

When the second planned fan (Fan 2) was to be executed other ideas were also presented as alternatives to the strategies from the grouting research group. With regard to the desire to do the job under controlled circumstances and to limit the amount of grout, and as the conditions at the section to be sealed with this second fan were as judged initially, there was found no reason to change and the fan was carried out according to the basic strategy. Control holes showed also this fan was successful.

Probe boreholes pair no 4, was skipped as the length of the tunnel was shortened compared to the initial plans. Instead one of the grouting holes in Fan 2 was used for pressure build-up tests.

The original programme contained water loss measurements in all drilled holes. These were not to be used for any decisions, but to be collected for evaluation after the completion of contractual works. When the first round of holes in the first fan had been measured, it was decided that water loss measurements would be skipped in order to save time. References to data collected during investigation and production are presented in Appendix A. Registrations from Water loss measurements are found in Appendix B.

When the contractual works started, the initial core borehole running all along the planned tunnel, remained unfilled. The hole was filled before the drilling of the first pair of probe boreholes, so as not to risk uncontrolled connection via any fracture to the core borehole and further to all of the rock mass penetrated by the core borehole. However, this filling was found not very successful as fresh grout was coming out from a leaking fracture at position approximately 10 m, when grouting was carried out at position 40 m. The filling of probe boreholes pair no 3 was equally unsuccessful. When packers were released after time needed for setting of the paste, the flow from the holes was the same as before filling. The possibility to succeed in filling the holes in a second attempt was judged low, and grouting operations were carried out with packers stopping the outflow from the probe boreholes.

An overview of locations and times for drilling, hydraulic measurements and grouting is found in Figure 1-1 and Table 1-1. Positions of probe holes, grouting holes and control holes are found in Appendix C.

Throughout this report, data, analyses and results from probe- and grouting boreholes are related to the length of the core borehole. However, names of boreholes and fans are related to the length used for the construction work. The difference between the length for the construction work and the core borehole length is approximately 11 m. Consequently, probe borehole SQ0049B starts at approximately 38 m along the core borehole (49–11=38 m). When using the Rock Visualisation System (RVS) to present 3D-images this is of no importance since the borehole coordinates (X, Y, Z) are used to compile data.

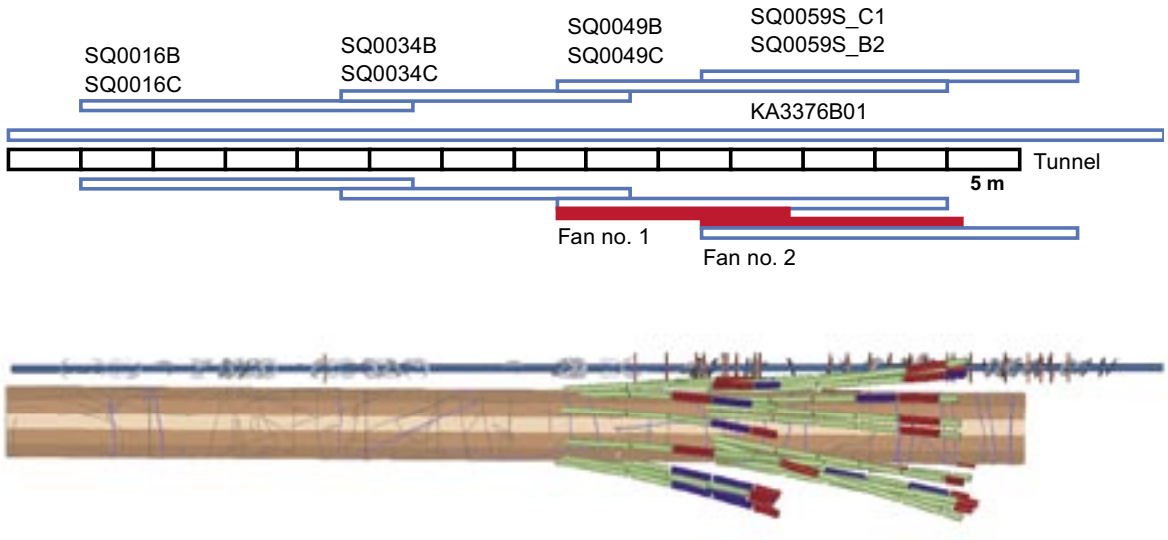

Figure 1-1. *Relative location of core drilled hole (KA), probe holes and grouting fans. Principal sketch with fans marked in red, above, and outcome presented in the RVS system, below (probe holes are found within the tunnel and therefore not visible). Fan no 2 includes one grouting hole (SQ0059_G15) that was also used as a probe hole for hydraulic tests. SQ0059S-C1 and SQ0059S-B2 were only used for inflow measurements. In the lower figure green indicates a flow less than 2 litres/min, blue indicates more than 2 litres/min and red the largest section inflow of a borehole.*

Table 1-1. Activities related to APSE Grouting (drilling, pressure build-up tests, water loss measurement, grouting). During drilling, accumulated inflow was measured every three meters. Time is approximate but corrected to HMS-time.

Activity	Location/borehole	Date
Drilling (acc. inflow)	SQ0016B	2003-05-09, 14:50 – 2003-05-09, 15:26
Drilling (acc. inflow)	SQ0016C	2003-05-09, 17:28 – 2003-05-09, 18:09
Pressure build-up test	SQ0016B	2003-05-09, 19:45 – 2003-05-09, 20:45
Pressure build-up test	SQ0016C	2003-05-09, 21:45 – 2003-05-09, 22:45
Drilling (acc. inflow)	SQ0034C	2003-05-22, 09:15 – 2003-05-22, 09:43
Drilling (acc. inflow)	SQ0034B	2003-05-22, 11:41 – 2003-05-22, 12:08
Pressure build-up test	SQ0034C	2003-05-22, 16:43 – 2003-05-22, 17:43
Pressure build-up test	SQ0034B	2003-05-22, 18:43 – 2003-05-22, 19:43
Drilling (acc. inflow)	SQ0049B	2003-05-27, 12:15 – 2003-05-27, 13:08
Drilling (acc. inflow)	SQ0049C	2003-05-27, 15:30 – 2003-05-27, 16:18
Pressure build-up test	SQ0049B	2003-05-27, 18:21 – 2003-05-27, 19:21
Pressure build-up test	SQ0049C	2003-05-27, 20:51 – 2003-05-27, 21:51
Drilling (acc. inflow)	Fan 1:1 (0049)	2003-06-02, 23:00 – 2003-06-03, 18:01
Water loss measurements	Fan 1:1 (0049)	2003-06-03
Grouting	Fan 1:1 (0049)	2003-06-03, 21:50 – 2003-06-04, 16:52
Drilling (acc. inflow)	Fan 1:2 (0049)	2003-06-05, 14:52 – 2003-06-05, 21:59
Grouting	Fan 1:2 (0049)	2003-06-10, 19:39 – 2003-06-13, 23:30
Drilling (acc. inflow)	Fan 2 (0059)	2003-06-24, 15:40 – 2003-06-25, 17:02
Pressure build-up test	G15 (0059)	2003-06-24, 22:45 – 2003-06-24, 23:45
Grouting	Fan 2 (0059)	2003-06-26, 12:49 – 2003-06-27, 00:44
Drilling (acc. inflow)	SQ0059 S_C1	2003-06-27, 20:00 – 2003-06-27, 20:35
Drilling (acc. inflow)	SQ0059 S_B2	2003-06-27, 20:07 – 2003-06-27, 21:07

2 Methodology

2.1 Overview

The hydrogeological characterisation includes compilation of available data, further hydrogeological investigations and evaluation, compilation and interpretation of data, see Figure 2-1. The information increases successively based on data from core-, probe-, grouting- and control boreholes. The results are continually used to confirm or make an updated grouting design.

Grouting design and prediction of grouting result includes compilation of available data, grouting design and prediction of result followed by descriptions, see Figure 2-1. The main activities are the design of grouting and prediction of result and these activities form an interactive process in the search of a grouting design where the prediction states an acceptable result.

2.2 Hydrogeological characterisation

2.2.1 Hydrogeological investigations

BIPS (Borehole Image Processing System) is used to obtain a digital image along a borehole /Carlsten and Stråhle, 2000; Carlsten et al, 2001/. The resulting image is in colour, continuous along the borehole and shows the entire circumference, i.e. 360°. During core mapping, this image is used to get a correct orientation of the core (at SKB, in combination with the use of the software BOREMAP) to determine strike and dip of fractures intersecting the borehole. Core mapping gives information about rock type, type of fracture (e.g. open, sealed), fracture filling etc. Investigations using BIPS were performed in core borehole KA3376B01, which runs approximately parallel to the constructed tunnel and in the future is referred to as “the core borehole”, see Figure 2-2, Figure 2-3 and /Fransson, 2003/.

A hydraulic test is used to investigate how a geological formation responds to a disturbance in pressure or flow. To use hydraulic tests to describe the rock mass seems reasonable since the aim is to seal the fractures once conducting water with a new fluid, in this case grout. Naturally, there are differences in properties concerning rheology but the fluids are still expected to flow in the same geological medium. In Table 2-2 are compiled the hydraulic tests used to characterise the rock mass.

The tests are assumed to reflect either “local” or “global” hydraulic properties where “local” refers to the rock in the immediate vicinity of the borehole. Pressure build-up tests are performed as transient, time-dependent tests, which give information about the rock further away from the borehole (here referred to as “global” hydraulic properties). The different tests are described more thoroughly below.

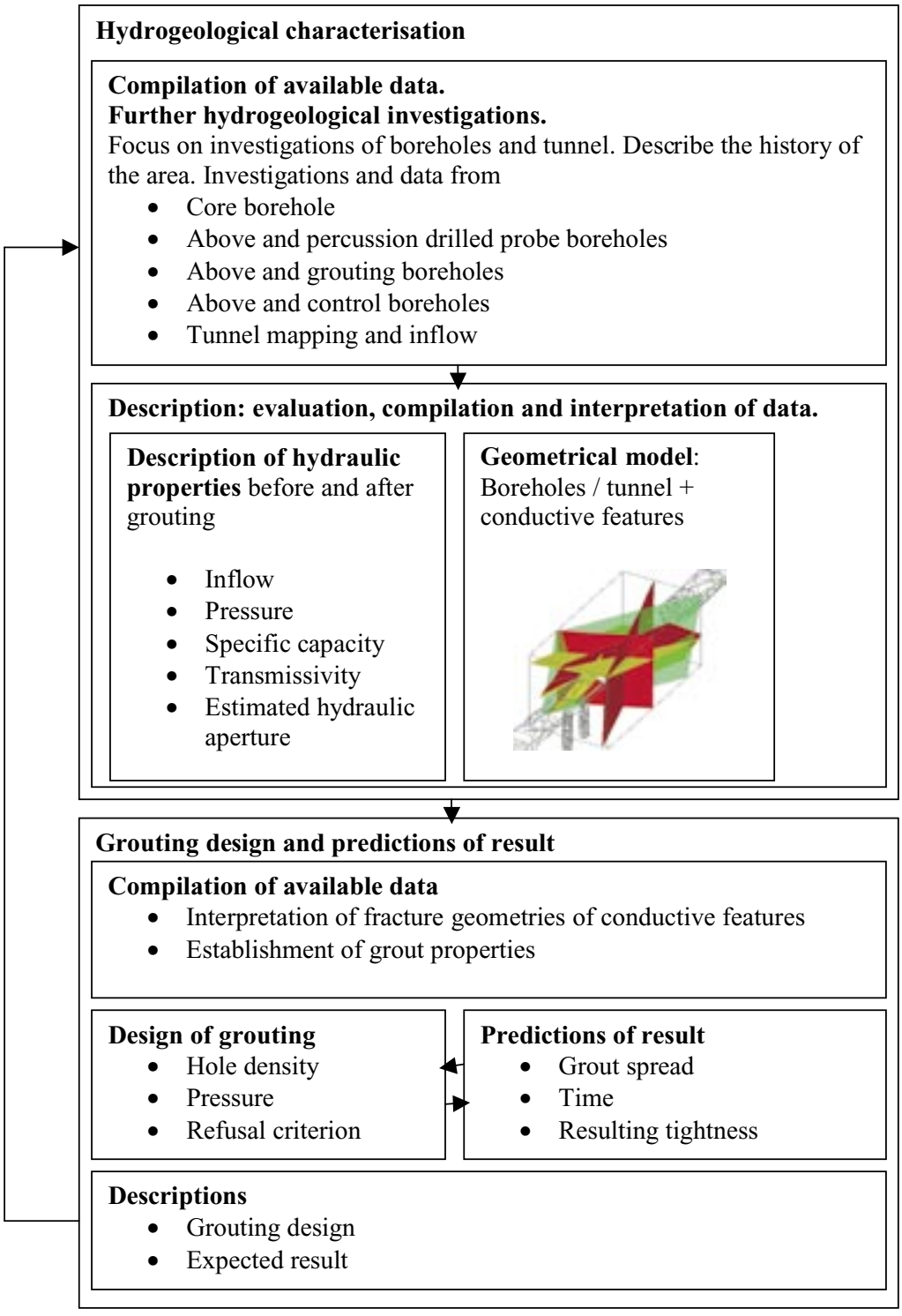

Figure 2-1. *Compilation of activities for the hydrogeological characterisation and the design of grouting.*

Table 2-1. Activities related to borehole KA3376B01 (drilling, Posiva flow logging, and pressure build-up tests), see /Fransson, 2003/.

Activity	Location/borehole	Date
Drilling	KA3376B01	2002-11-08, 15:22 – 2002-11-26, 15:39
Pressure build-up test	KA3376B01	2002-12-11, 13:50
Posiva flow logging	KA3376B01	2003-01-14, 15:15 – 2003-01-15, 08:15
Flowing of borehole (PBT 2, due to disturbances during drilling and Pressure build-up test)	KA3376B01	2003-01-16, 09:59

Table 2-2 Hydraulic tests and pressure monitoring (HMS).

Activity	Location/borehole	Result
Posiva Flow Log	Core borehole	Section tests, inflow along borehole (reflects “local” hydraulic properties).
Inflow during drilling	Percussion drilled probe boreholes and grouting boreholes	Accumulated inflow every 3 m (reflects “local” hydraulic properties).
Pressure build-up tests	Percussion drilled probe boreholes	Flow and pressure as a function of time, specific capacity, transmissivity (reflects “local” and “global” hydraulic properties).
“Water loss measurements” Lugeon test	Grouting boreholes In Fan 1:1.	Short duration test in borehole, flow, pressure (reflects “local” hydraulic properties).
Pressure monitoring (Hydro monitoring system, HMS)	Core boreholes at different locations of the laboratory	Pressure response during drilling, testing and grouting.

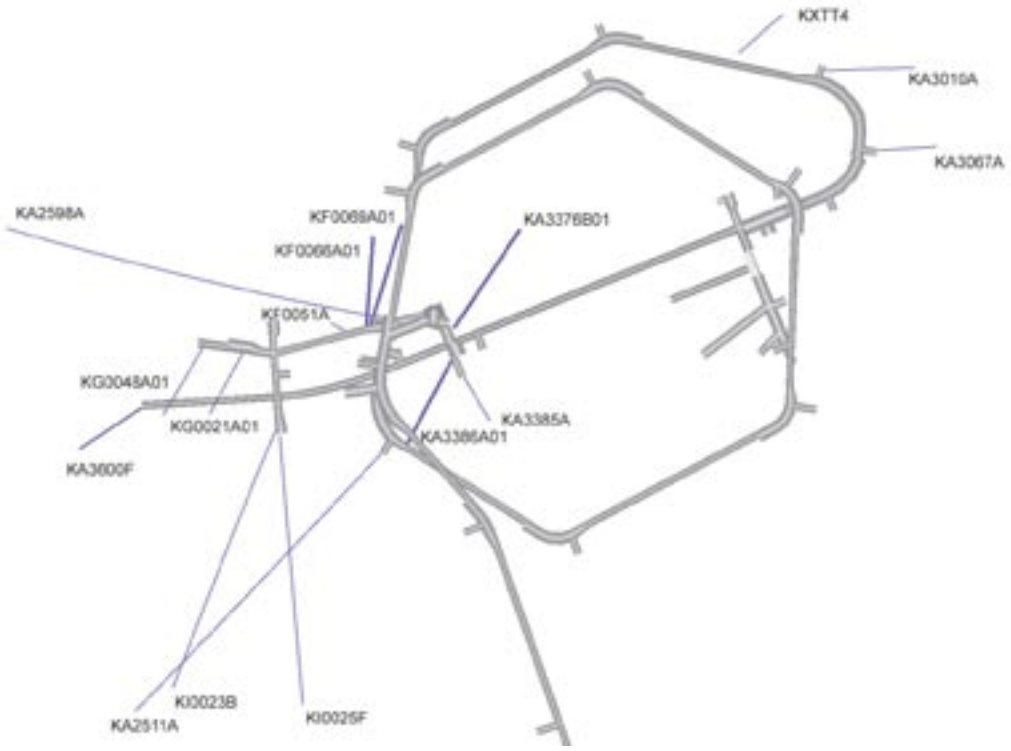

Figure 2-2. Core borehole KA3376B01 and core boreholes where pressure is monitored using HMS (not monitored for KF0066A01).

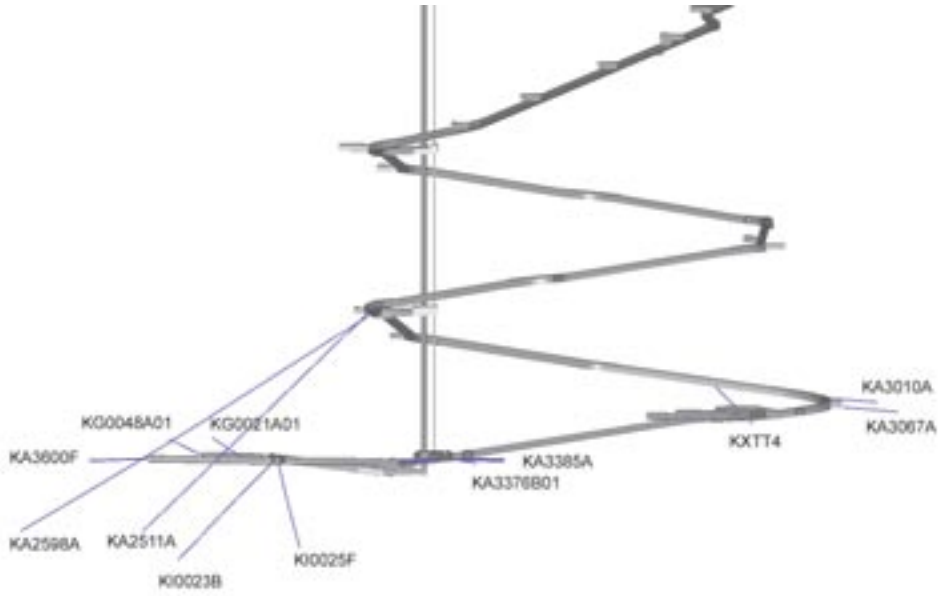

Figure 2-3. *Core borehole KA3376B01 and core boreholes where pressure is monitored using HMS (KA3386A01, KF0051A, KF0066A01 and KF0069A01 are not visible). Front, direction north.*

Posiva Flow Log /Rouhiainen, 2000/ is based on pulse transit time of a thermal pulse for small flows (0.1–10 mL/min) and thermal dilution rate for high flows (2–500 L/min). The method measures local inflows along the borehole, not the cumulative flow. The flow rate is measured in a test section (equal to test scale, L) limited by packers consisting of assemblies of soft rubber discs. The test section is moved in steps with step length dL. When the test scale, L, is equal to the step length dL, this is referred to as "Sequential flow logging" mode. "Overlapping flow logging" mode aims at determining the exact position along the borehole of fractures or fracture zones and the test scale (L) is larger than the step length (dL). Flow from a fracture is measured as long as the fracture stays between the packers. Besides the inflow, single point resistance is also measured and considered an important correlation parameter as it gives the exact position of flow anomalies. Posiva flow logging was performed in the core borehole /see Fransson, 2003/. Besides the Posiva flow logging, *inflow during drilling* was also measured every three meters for probe boreholes and grouting boreholes see Table 2-2.

A *pressure build-up test* is a transient test where pressure and flow are studied as a function of time. This gives a possibility to investigate the hydraulic properties further away from a borehole and e.g. see if the borehole is connected to larger, more conductive fractures which are not necessarily identified using flow logging. The pressure build-up test starts with a flow period and ends by a recovery period. Pressure build-up tests were performed in the core borehole /Fransson, 2003/, percussion drilled probe boreholes and one grouting borehole (G 15) that was viewed as a complementary probe borehole, see Table 2-2.

Water loss measurements are short duration tests. A water loss measurement is an injection test using constant pressure and assuming steady state conditions. These tests are also referred to as Lugeon tests /Kutzner, 1996/ and are evaluated by calculating a Lugeon value. This is determined by the volume of water that is injected in a borehole per meter and time unit (minutes) at a pressure of 10 bar. Water loss measurements were carried out in probe boreholes and in grouting boreholes of Fan 1:1. The methodology presented herein does not include water loss measurements; data was collected for later evaluation.

At Äspö Hard Rock Laboratory (Äspö HRL) several boreholes are connected to a *hydro monitoring system (HMS)* that continually monitor ground water pressure. Normally, this system registers the pressure once every second hour and a detailed scanning starts when the measured pressure change exceeds 2 kPa. In /Fransson, 2003/ pressure responses in several core boreholes, see Figure 2-2 and Figure 2-3 were analysed when evaluating drilling and testing of the core borehole (KA3376B01). KA3385A and KA2598A were in these investigations found to have the largest responses. Pressure data for the period 2003-04-01 to 2003-09-25 will be exemplified by boreholes KA3385A, KA2598A and KF0069A01 (Figure 2-2) located in the vicinity of the core borehole and future tunnel to give a picture of how the activities in Table 1-1 influence the pressure.

2.2.2 Evaluation of data

In brief, the results from borehole investigations along the APSE-tunnel are presented in terms of:

- Strike, dip and location of natural open fractures along core borehole KA3376B01.
- Inflow along borehole (core borehole, percussion drilled probe and grouting boreholes).
- Specific capacity and estimated hydraulic apertures (core borehole, percussion drilled probe- and grouting boreholes).
- Transmissivity (core borehole, percussion drilled probe boreholes).

Inflow measurements from Posiva Flow Log and drilling are used to identify location of conductive features. Further, the specific capacity, Q/dh, is estimated based on these inflows and the hydraulic head.

The transmissivity, T, is estimated from the recovery phase of a pressure build-up test using Jacob's method /Cooper and Jacob, 1946/. The recovery, s", is expressed as given below:

$$s'' = \frac{Q}{2\pi T}\frac{1}{2}\left(0.8091 + \ln\frac{T}{r^2 S}\cdot\left(\frac{t_{PB}\cdot t_P}{t_{PB}+t_P}\right)\right) = \frac{Q}{4\pi T}\left(0.8091 + \ln\frac{Tt_e}{r^2 S}\right) \qquad (2\text{-}1)$$

where r=radial distance, S=storage coefficient and Q=flow /e.g. Gustafson, 1986/. The adjusted time, t_e, is estimated from the time of injection or flow time, t_P, and the time since recovery started or the Pressure build-up time, t_{PB}. Initially, log-log plots of the recovery, s", and the adjusted time, t_e, are used to evaluate the flow dimension of tests. A slope of 1:1 indicates an effect of wellbore storage. The shape of curves also indicates if there is one-dimensional (1D) flow, radial or two-dimensional (2D) flow, or three-dimensional (3D) flow, /e.g. Carlsson and Gustafson, 1991/. /Doe and Geier, 1990/ further describe the spatial dimension for flow in hydraulic tests. Jacob's method consists of plotting the recovery, s", and the adjusted time, t_e, on a semi-logarithmic plot. The transmissivity is evaluated using the following equation:

$$T = \frac{0.183Q}{\Delta s''} \qquad (2\text{-}2)$$

where, Δs" is the slope of the recovery line on the plot of s" against t_e (change in s" during a decade, t_1 to $10t_1$).

The hydraulic aperture, b, was estimated using the "cubic-law" /e.g. de Marsily, 1986/:

$$T = \frac{\rho g b^3}{12\mu} \qquad (2\text{-}3)$$

which describes how the hydraulic aperture, b, between two plane-parallel plates are related to the transmissivity, T. Besides the aperture, the transmissivity is influenced by the density and viscosity of the fluid, ρ and μ, and the acceleration due to gravity, g.

The specific capacity (Q/dh) is assumed to give a description of the conductive feature in the immediate vicinity of the borehole. /Fransson, 2001/ indicates that the median specific capacity of several boreholes intersecting the same fracture is an approximation of the effective, cross fracture transmissivity. Therefore, the median specific capacity is assumed to be approximately equal to the transmissivity:

$$\frac{Q}{dh} \approx T = \frac{\rho g b^3}{12\mu} \qquad (2\text{-}4)$$

Further, the variation in specific capacity is assumed to give a picture of variations in aperture within a conductive feature.

2.2.3 Compilation and interpretation of data

Data presented in the previous sections are compiled into three different descriptions, Description 1–3, which are obtained at different stages of the project, see principal sketch in Figure 2-4. The figure shows the boreholes and the interpreted conductive features from above. If viewed along the three boreholes (one core drilled and two percussion drilled probe boreholes) they should be put in a triangle and not at the same height to obtain a three-dimensional model. Input data and main assumptions for each description are presented in Table 2-3.

To compile data and obtain a geometrical model, a three-dimensional CAD-based visualisation tool, RVS (Rock Visualisation System) is used. Input data are borehole coordinates, location and strike/dip of natural open fractures and location of conductive 3 m sections. From the resulting geometrical model possible location and strike /dip of conductive features are interpreted.

2.3 Grouting design

2.3.1 Design process

The design process uses numerical calculations. Calculations on grout spread and sealing effect are carried out for a theoretical pre-evaluation of possible results when applying different designs. Different solutions on grouting design are used as a basis for calculations and compared to the requirements on the grouting.

Calculation of the grouting result is based on the characterisation of hydraulic structures. The characterisation describes the hydraulic properties and orientation of the structures and a geometrical model is determined based on this information. The calculations concern the spread of grout in the fractures and how this affects the flow of water into the tunnel, i.e. the sealing effect. In the calculations the geometry of the fractures, the grouting technique and the properties of the grout are included.

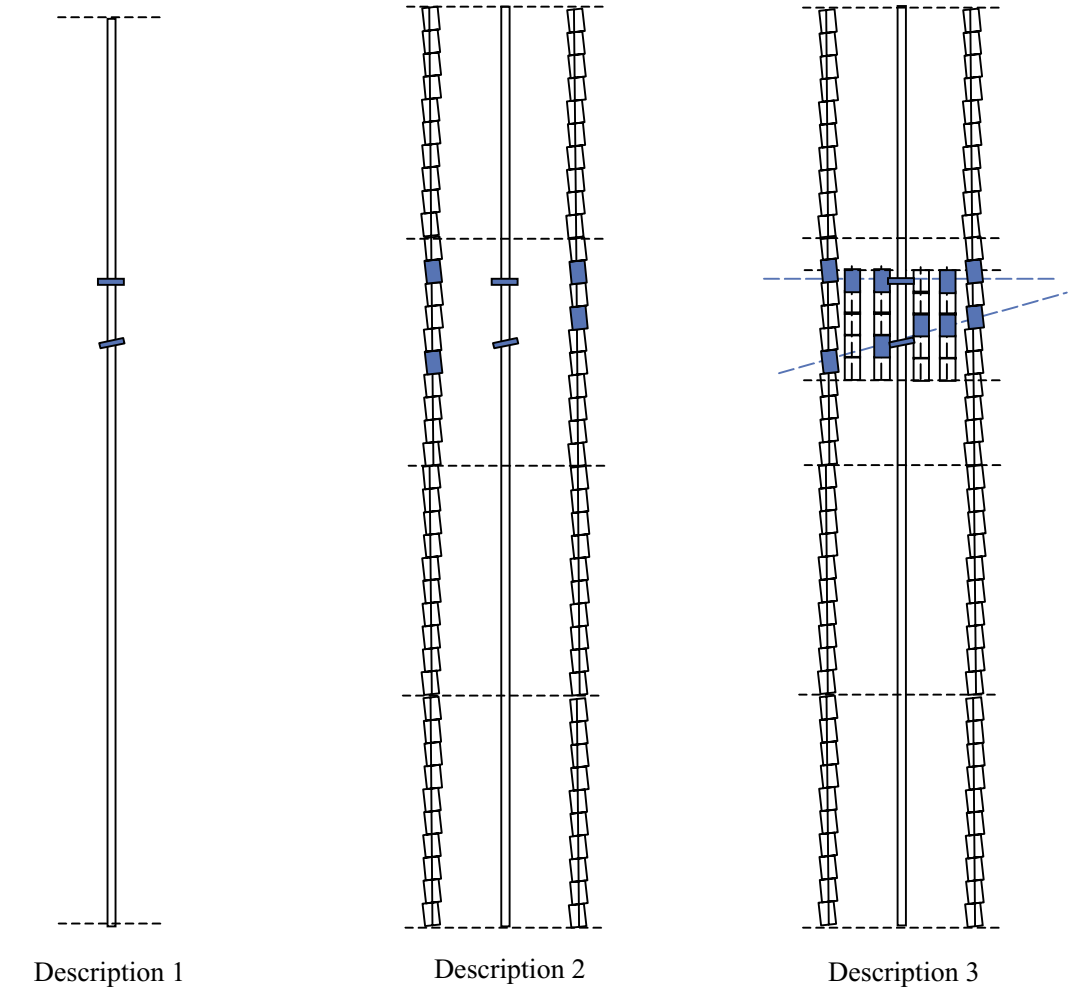

Figure 2-4. *Principal sketch of how the rock mass is described at the three different stages: Description 1 based on data from core borehole; Description 2 based on data from core borehole and two percussion drilled probe boreholes; and Description 3 based on data from core borehole and percussion drilled probe and grouting boreholes.*

Table 2-3 Input data and main assumptions/hypotheses for Descriptions 1-3.

Description	Input data	Main assumptions/hypotheses
General		1. Focus on describing conductive features based on natural inflow. 2. Focus on inflows >2 L/min (hydraulic aperture based on specific capacity b(Q/dh) ≈ 50 µm, smaller fractures assumed not to be groutable). 3. Inflow within a section is assumed to originate from one major fracture. 4. Specific capacity, Q/dh, describes "local" hydraulic properties and transmissivity describes "global" hydraulic properties.
Description 1	Core borehole Location, strike and dip of natural open fractures. Location of inflows along borehole Transmissivity	5. Locations of inflow (Posiva Flow Log) are coupled to the closest natural fracture(s) (BIPS, core mapping). Data from inflow logging, BIPS and core mapping are used for extrapolation to describe location, strike, dip and inflow of conductive features along the future tunnel.
Description 2	Above and probe boreholes Location of inflows along boreholes (3 m sections). Transmissivity	6. Variation in aperture within a conductive fracture is indicated by the local inflow to the core borehole and section inflows to probe boreholes intersecting this extrapolated conductive fracture (with inflow, location, strike and dip based on flow logging and BIPS, core mapping). 7. The median specific capacity is an approximation of the cross fracture transmissivity (at this stage specific capacities from the core borehole and one or two probe boreholes are used).
Description 3	Above and grouting boreholes Location of inflows along borehole (3 m sections).	8. Variation in aperture within a conductive fracture is indicated by the local inflow to the grouting boreholes intersecting the extrapolated conductive fracture (with inflow, location, strike and dip based on flow logging and BIPS, core mapping). 9. The median specific capacity is an approximation of the cross fracture transmissivity (at this stage specific capacities from the grouting boreholes are used). Total inflow of a borehole can be a "good-enough" approximation of a section or fracture inflow.

2.3.2 The geometry of the fractures

The characterisation presents the hydraulic apertures and the orientation of the structures as discussed above. The hydraulic apertures are by several authors /Hakami, 1995; Barton et al, 1985; Chen et al, 2000/ concluded to be considerably less than a physical mean aperture which in turn, is found to be governing for grouting /Hässler, 1991; Janson, 1998/. The physical aperture should also be considered as it is the crucial factor determining the possibility to penetrate into the fractures with a cement based grout /Eriksson, 2002/. To facilitate estimations of grout flow and grout take, the hydraulic apertures is for the design interpreted in terms of physical apertures. This interpretation is made using an expression presented by /Zimmerman and Bodvarsson, 1996/, see Equation 2-5. In Equation 2-5, b is the hydraulic aperture, $b_{average}$ the arithmetic mean aperture, σ_b the standard deviation in aperture and c fraction of contact area. An iterative solving procedure is used to obtain the arithmetic mean aperture for values on hydraulic aperture and amount of contact. The standard deviation in aperture is set in relation to the mean aperture, for instance to be half of the mean aperture.

$$b^3 = \left(b_{average}{}^3\right)\left[1-\frac{1.5\sigma_b^2}{\left(b_{average}\right)^2}\right](1-2c) \qquad (2\text{-}5)$$

Based on the statistical parameters on mean aperture and variation in aperture the geometry of the fractures is modelled for a log-normal distribution. The log-normal distribution is commonly used to describe the geometry of rock fracture aperture /e.g. Hakami, 1995/. The varying aperture field is represented by a number of conductive elements.

2.3.3 The grouting technique

In the modelling the technical performance of the grouting operation must be represented. This includes the number and placement of grouting holes, the grouting order, grouting pressure and flow and the refusal criterion, i.e. when the grouting operation is stopped. These aspects are included by means presented in /Eriksson, 2002/.

The most significant aspect is the number of grouting holes which based on result of previous calculations is important. The refusal criteria can be either a minimum flow criterion or a maximum volume criterion. The grouting order is set to follow a descending specific capacity in accordance with the practical performance.

This description is a simplified description of the grouting procedure. One aspect missing is the capacity of the pump, which can be assumed to have a certain impact on the result. Another issue is that the grouting is done with a piston pump with a varying pressure. In the calculation an even pressure is assumed and it is not known what impact on the result a varying pressure has.

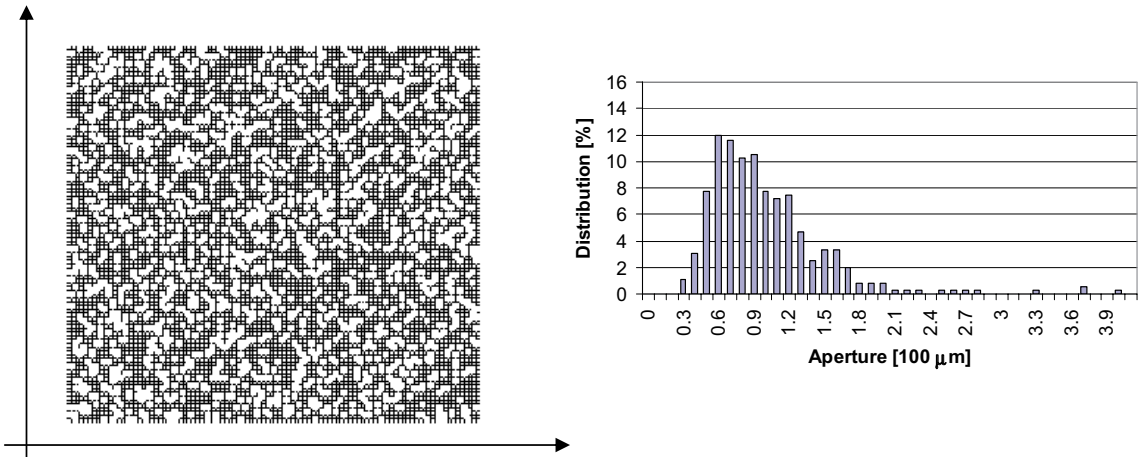

Figure 2-5. *Illustration of the fracture model in the calculation tool. To the left is a figure showing the fracture model with an orthogonal pattern of conductive elements where the white areas represent no flow positions (contact areas). To the right the diagram shows a distribution of the conductive elements within the fracture surface (contact areas excluded).*

2.3.4 Grout properties

The grout is characterised in terms of rheology, penetrability and bleed and the properties are described as time dependent.

The rheology is described with use of the Bingham model where two parameters, a yield value (τ_0) and a viscosity (μ_B), is used to describe the flow behaviour. The use of the Bingham model to describe the flow behaviour of grouts is recommended for instance by /Håkansson, 1993/. The Bingham model states a linear relation between the shear stress and the shear rate as illustrated in Figure 2-6 and that the yield value (τ_0) is found at the intercept with the y-axis and that the viscosity (μ_B) is the gradient of the linear relation. The Newtonian model for water is also shown in the figure.

Based on the rheological behaviour the flow equations are derived /Hässler, 1991/. The flow equations are based on flow in 1D elements with an opposing water pressure /Eriksson, 2002/.

The penetrability of cement based grouts is limited compared to Newtonian fluids and only apertures large enough can be penetrated with the suspension. To include this aspect in the calculations the grout is characterised with two parameters, a minimum (b_{min}) and a critical aperture ($b_{critical}$), defining an aperture interval where the grout will be filtered and not pass. The aperture size below which filtration occurs is given the notation ($b_{critical}$) and the aperture size below which no grout can pass is denoted as (b_{min}). Between these two values of aperture the grout will be filtered, as illustrated in Figure 2-7. If the aperture is larger than $b_{critical}$ no filtration occurs and if the aperture is smaller than b_{min} no grout can pass. In front of the constriction a filter cake forms if the aperture is smaller than $b_{critical}$, which is represented in Figure 2-7 by black shading. Further details of this are given in /Eriksson, 2002/.

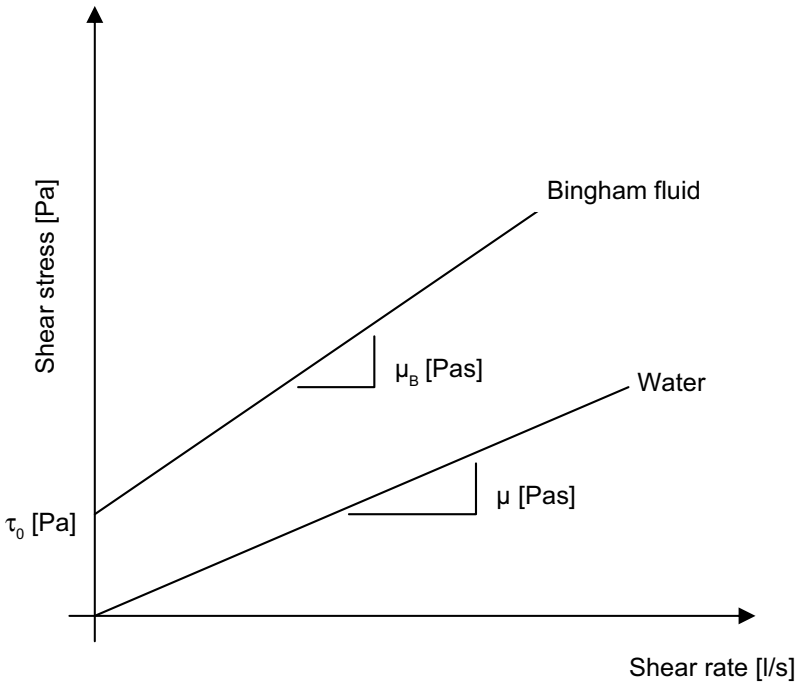

Figure 2-6. *Illustration of the flow models for suspensions (Bingham flow model) and for water (Newtonian flow model).*

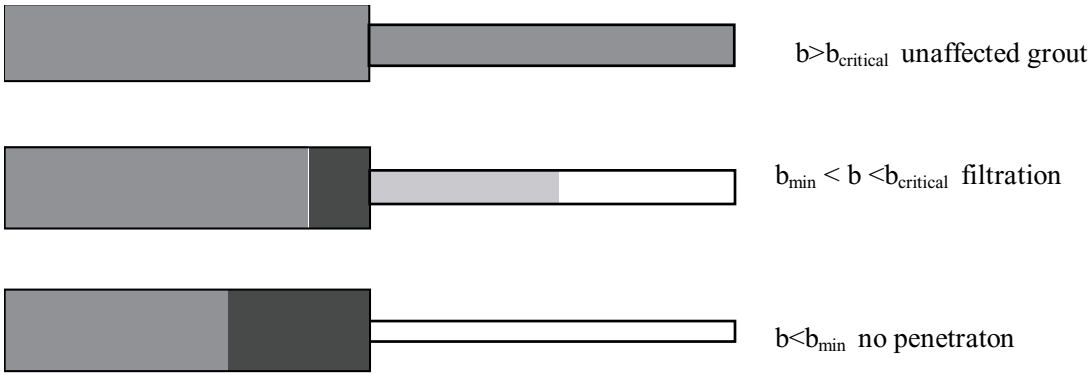

Figure 2-7. *A conceptual model of how to view the filtration process during grouting /Eriksson, 2002/. The median gray represents grout of initial quality. The black shading in front of the constriction represents a thickened grout which blocks further flow (filter cake). The light gray represents a grout that has been filtered thus having a reduced density.*

Bleed refers to the separation of water and solid in the grout, and results in a volume of water on top of the grout. This volume is potentially giving a resulting higher conductivity in a grouted fracture compared to a completely filled fracture. The bleed is included in the model so that the aperture of a grouted element in the calculation is given a resulting aperture in relation to the bleed, i.e. 10% bleed gives a resulting aperture of 0.1 times the initial aperture /Eriksson, 2002/.

2.3.5 Calculation procedure

In the calculation procedure, calculations on inflow and grouting are made according to the flow chart in Figure 2-8. In each loop new realisations on geometrical input data are made based on Equation 2-5.

2.3.6 Presentation of calculated result

The results of the calculations are presented in terms of calculated grout take, grouting time and sealing effect. An estimation of inflow based on the calculated results is also presented even though the calculation tool is not developed for the purpose of calculating inflow, see /Eriksson, 2002/.

Each identified fracture is calculated based on its geometrical data according to Figure 2-8. The grouting result is calculated using Monte-Carlo simulations to estimate a span of possible results as shown in the right hand side of Figure 2-9. The results are mainly presented as the median calculated values of the calculated full distribution, but the range in results is also presented.

The grout take and the grouting time are presented as the amount of grout injected to the rock and the total time used for the injection respectively. The presented grout take and time for grouting is excluding the grout and time used for filling the holes. The sealing effect is the calculated reduction in calculated inflow as result of the grouting.

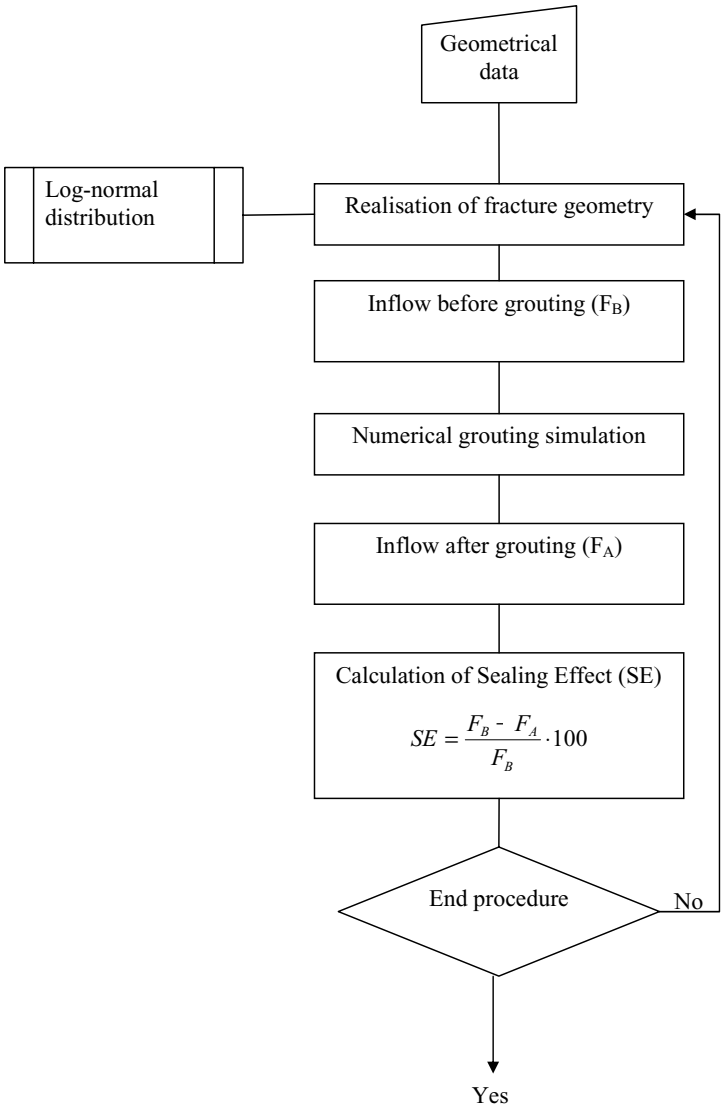

Figure 2-8. *Illustration of the calculation procedure.*

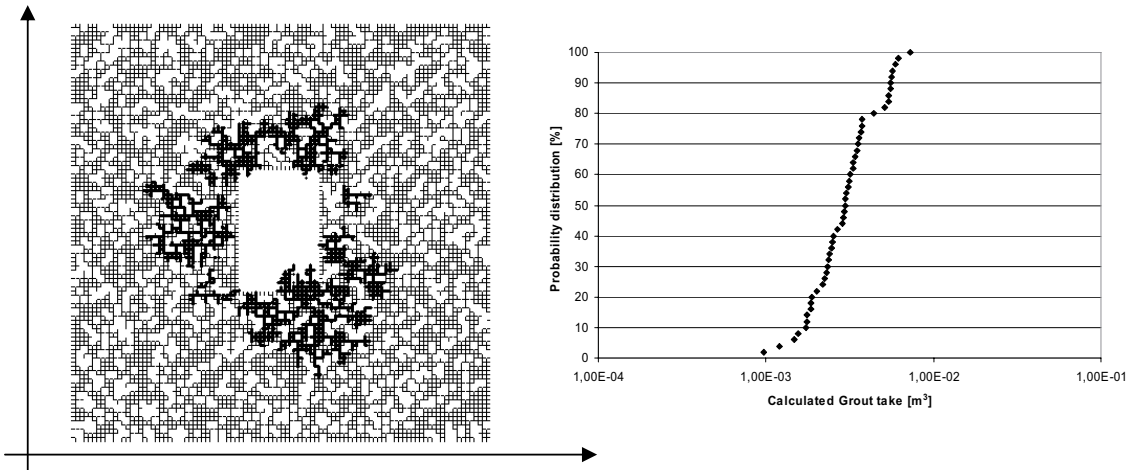

Figure 2-9. *An example of the result of a calculation. The left figure shows a realisation of a fracture grouting. The right diagram shows the distribution of calculated grout take based on a number of realisations on input data.*

3 Results

3.1 Pre-investigation of grout properties

Pre-investigation of grouts was performed to achieve and find properties on grouts suitable for the grouting. The measurements were performed as recommended in /Friedrich and Vorschulze, 2002/ with three measurements on each property. Measurements on rheology was performed using a rotational viscometer /Håkansson, 1993/, the penetrability using the penetrability meter /Eriksson and Stille, 2003/ and bleed according to standard (SS 13 75 31) and using a small cylinder as recommended by /Eriksson et al, 1999/.

Grout properties for two grouts, Grout A and Grout B, were determined. The properties were examined firstly in the laboratory of KTH and secondly at site mixed with the equipment to be used. For a third grout, Grout C, the properties were never determined since it was only to be used as final stop grout.

In Table 3-1 the properties and composition of grouts A–C are listed.

3.2 Characterisation based on core borehole KA3376B01: Description 1

3.2.1 Inflow along borehole

Figure 3-1 presents accumulated inflow measured during drilling and accumulated inflow calculated from Posiva Flow Log (see Table 3-3). The upper measurement limit for Posiva Flow Log is approximately 5 L/min, which explains the difference between these measurements and the result from inflow during drilling.

Table 3-1. Properties of the three examined grouts valid for t<3600sec.

Property		Grout A UF 16, w/c 2.0 0.9% HPM	B UF 16, w/c 1.0 0.9% HPM	C UF 16, w/c 0.8 0.9% HPM
Rheology	Yield value [Pa]	$0.296 \cdot e^{0.0004t}$	$1.5 \cdot e^{0.0004t}$	–
	Viscosity [Pa]	$0.0056 \cdot e^{0.0004t}$	$0.017 \cdot e^{0.0004t}$	–
Penetrability	b_{min} [µm]	37	41	–
	$b_{critical}$ [µm]	$0.0032t+60$	$0.0032t+75$	–
Density	[kg/m^3]	1290	1480	–
Bleed	[%]	15	5	–

Inflows exceeding 5 L/min have been estimated based on inflow during drilling (see Table 3-2). Observe that there is a difference in up to 0.6 m between the location for inflow during drilling and the location identified by Posiva Flow Log. A location based on Posiva Flow Log is assumed to be the better of the two. The total inflow based on Posiva Flow Log and inflow during drilling are 45.9 L/min and 80 L/min respectively. The inflow to the conductive part at approximately 50–57 m based on Posiva Flow Log is 27.4 L/min and based on measurements during drilling, 59 L/min. Using inflows during drilling for the conductive part results in a total inflow for the borehole of 77.5 L/min.

3.2.2 BIPS and core mapping

Strike, dip and location of natural open fractures along the core borehole based on BIPS and core mapping are presented in Appendix D.

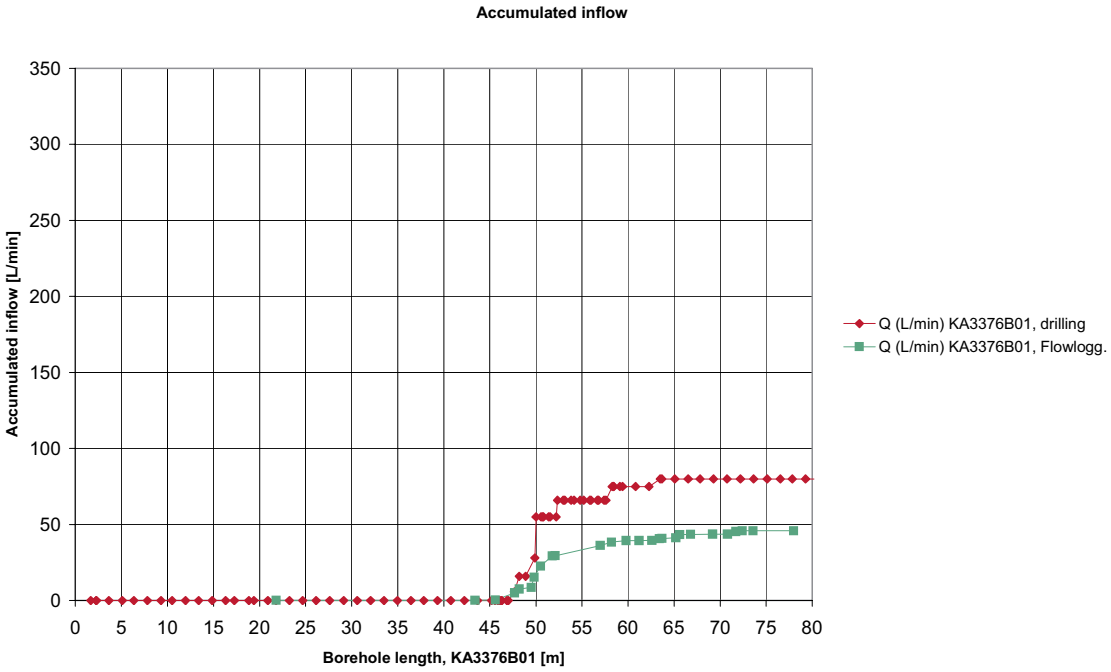

Figure 3-1. *Inflow along core borehole KA3376B01. Upper measurement limit for Posiva Flow Log is approximately 5 L/min, explaining the difference between these measurements and inflow during drilling.*

Table 3-2. Inflows based on Posiva Flow Log compared to inflow during drilling, core borehole KA3376B01. As the maximum measurable inflow with PFL is 5 L/min, the inflow rates in the more conductive parts have to be adjusted based on inflow during drilling.

Borehole	Borehole depth, PFL [m]	Inflow, PFL [L/min]	Borehole depth, drilling [m]	Inflow during drilling [L/min]
	49.8	6.7	48.9–49.9	28–16=12
	50.5	7.3	49.9–50.0	55–28=27
	51.8	6.7	52.2–52.3	66–55=11
	57.0	6.7	57.6–58.3	75–66=9
Sum:		27.4		59
45.9 (total inflow Posiva flow logging)–27.4+59=77.5 L/min, total inflow during drilling: 80 L/min				

3.2.3 Specific capacity and estimated hydraulic aperture based on inflow

Natural inflows were identified at 25 locations along the core borehole. Most of them were below 2 L/min (corresponding to fractures expected to be less than 50 µm and not to be groutable, see Table 2-3). Upper measurement limit for Posiva Flow Log is approximately 5 L/min. Larger inflows are estimated based on inflow during drilling (see difference between measurements in Table 3-2 and Figure 3-1). Hydraulic apertures were estimated for a density and viscosity of the fluid of ρ=1000 kg/m^3 and μ=1.3E–3 Pa s respectively, and an acceleration due to gravity, g=9.8 m/s^2. Two different hydraulic heads are used, the actual depth 450 m and 343 m, which was registered during the pressure build-up test. As shown below, the difference in hydraulic aperture for the two different hydraulic heads is fairly small.

3.2.4 Transmissivity

Test data and evaluated specific capacity and transmissivity for the core borehole are presented in Table 3-4 and Table 3-5. Graphs for the evaluation of the tests are shown in Appendix E.

Table 3-3. Inflow, specific capacity and estimated hydraulic apertures based on Posiva flow logging and inflow during drilling. Inflows >2 L/min are written in bold.

Inflow number	Borehole depth [m] PFL	Inflow [L/min] PFL and Drilling	Q/dh [m^2/s] dh: 450 m	b(Q/dh) [µm]	Q/dh [m^2/s] dh: 343 m	b(Q/dh) [µm]
1	21.8	0.11	4.2E–09	19	5.5E–09	21
2	43.4	0.02	8.0E–10	11	1.1E–09	12
3	45.6	0.23	8.6E–09	24	1.1E–08	26
4	**47.7**	**4.67**	**1.7E–07**	**65**	**2.3E–07**	**71**
5	**48.2**	**2.50**	**9.3E–08**	**53**	**1.2E–07**	**58**
6	49.5	1.17	4.3E–08	41	5.7E–08	45
7	**49.8**	**12.00***	**4.4E–07**	**89**	**5.8E–07**	**98**
8	**50.5**	**27.00***	**1.0E–06**	**117**	**1.3E–06**	**128**
9	**51.8**	**11.00***	**4.1E–07**	**87**	**5.3E–07**	**95**
10	52.1	0.20	7.4E–09	23	9.7E–09	25
11	**57**	**9.00***	**3.3E–07**	**81**	**4.4E–07**	**89**
12	**58.2**	**2.23**	**8.3E–08**	**51**	**1.1E–07**	**56**
13	59.8	0.90	3.3E–08	38	4.4E–08	41
14	61.2	0.03	1.2E–09	13	1.6E–09	14
15	62.6	0.16	6.0E–09	21	7.9E–09	23
16	63.4	1.13	4.2E–08	41	5.5E–08	44
17	63.7	0.12	4.3E–09	19	5.7E–09	21
18	65.2	0.50	1.9E–08	31	2.4E–08	34
19	**65.6**	**2.10**	**7.8E–08**	**50**	**1.0E–07**	**55**
20	66.8	0.15	5.6E–09	21	7.3E–09	23
21	69.2	0.05	1.7E–09	14	2.3E–09	15
22	70.8	0.02	8.6E–10	11	1.1E–09	12
23	71.7	1.75	6.5E–08	47	8.5E–08	51
24	72.4	0.48	1.8E–08	31	2.3E–08	33
25	73.6	0.02	5.7E–10	10	7.5E–10	11
	Sum:	77.55	2.9E–06		3.8E–06	

* Upper measurement limit for Posiva Flow Log is approximately 5 L/min. Larger inflows are estimated based on inflow during drilling (see difference between measurements in Figure 3-1).

Table 3-4. Test data for pressure build-up test, core borehole KA3376B01.

Borehole	Test section, sec up [m]	Test section, sec low [m]	Hydraulic head [m]	Flow [L/min]	Flow period [hours]	Recovery period [hours]
KA3376B01	~2.5	80.19	~343	96.3	~24	~24

Table 3-5. Specific capacity and transmissivity for core borehole KA3376B01.

Borehole	Test section, sec up [m]	Test section, sec low [m]	Specific capacity [m^2/s]	Transmissivity [m^2/s]
KA3376B01	~2–2.5	80.19	4.7E–6	1.5E–5

Table 3-6. Evaluated geometrical properties of the singular rock fractures based on the hydraulic apertures and Equation 2-5.

	Inflow number	b [μm]	$b_{average}$ [μm]	σ_b [μm]	c [%]
Fan 1	4	71	98	49	20
	5	58	80	40	20
	7	98	134	68	20
	8	128	177	89	20
	9	95	132	66	20
Fan 2	11	89	123	62	20
	12	56	77	39	20
	19	55	76	38	20

3.2.5 Initial results Description 1

Inflow logging of the core borehole KA3376B01 identified eight locations of inflow exceeding 2 L/min. These were found between approximately 45–66 m along the core borehole. Estimated hydraulic apertures vary between 55–128 μm. At this stage, these apertures were assumed to be the median hydraulic apertures describing eight different fractures. The specific capacity estimated for the entire borehole is lower than the transmissivity, which based on the assumption that the specific capacity gives a local description, would indicate a more conductive feature further away from the borehole.

3.3 Prediction 1 based on Description 1

The first prediction was made based on the information obtained from the core drilled investigation hole.

3.3.1 Interpreted geometry of the fractures

The interpretation of fracture properties was is this stage made based on the information obtained from the core drilled hole. Only fractures with a hydraulic aperture >50 μm were included. The variation in aperture, i.e. the standard deviation of the log-normal distribution, was assumed to be equal to half the arithmetic mean aperture based on common descriptions of fracture properties in the literature, see e.g. /Lanaro, 2001/. It was also assumed that 20% contact area was present. Based on these, the standard

deviation in aperture (σ_b) and the amount of contact (c), and the hydraulic aperture (b) the characteristic value of the physical aperture ($b_{average}$) was calculated using Equation 2-1.

3.3.2 Grouting design

The preliminary design for grouting was optimised for grouting small fractures, fractures with apertures on the limit to what is possible to grout using cement-based grout. Therefore, a grout with low-viscosity and a good penetrability, a dense hole pattern and a low minimum flow criteria was designed in accordance with the findings in /Eriksson, 2002/. The grouting pressure was set to 2 MPa above ground water pressure which can be considered to be a commonly used grouting pressure. Below is presented data of the grouting design.

- 21 bore holes, 16 m long.
- Minimum flow 0.2 liter/min.
- Grouting pressure 2 MPa above ground water pressure.
- Maximum hole distance 2 m.
- Bore hole radius 0.032 m.
- Grouting to be started with Grout A and after ~100 litres the grout to be changed to Grout B. Again, after ~50 litres the grouting to be continued with Grout C. After grouting ~50 litres of this grout, grouting to be stopped.

3.3.3 Predicted grouting result

The calculated results of each fracture are presented in Table 3-7.

Based on the above given calculated values the following prediction of the grouting result was made:

Fan 1

In Fan 1 fractures the expected result is:

- Total grouted volume excluding filling of the holes 497 litres.
- Grouting time excluding filling of the holes 569 min.
- Sealing effect 99%.
- Inflow 1 l/min.

Fan 2

In Fan 2 the expected result was:

- Total grouted volume excluding filling of the holes 152 litres.
- Grouting time excluding filling of the holes 435 min.
- Sealing effect 97%.
- Inflow 1 l/min.

Table 3-7. Calculated median grout volume, grouting time and sealing effect for Fan 1 and 2.

	Inflow number	Median grouted volume [l]	Median grouted time [min]	Median sealing effect [%]
Fan 1	4	19	54	99
	5	7	17	97
	7	104	320	99
	8	257	569	99
	9	104	315	99
Fan 2	11	134	435	99
	12	9	22	91
	19	9	22	91

3.4 Characterisation based on core borehole and percussion drilled probe boreholes: Description 2

3.4.1 Inflow along borehole

Figure 3-2 presents a compilation of accumulated inflows along core- and probe boreholes. Inflows along probe boreholes were generally measured for 3 m sections, see Table 3-8 and Appendix F. Locations along the core borehole are approximate since differences in orientation of boreholes are not considered. Increase in inflow is seen at approximately the same location for the core borehole and the probe boreholes SQ0049B and SQ0049C. The inflows to these probe boreholes were up to three times the inflow of the core borehole. The intention was to fill the core borehole with grout at low pressure (to minimize the risk of spreading the grout) before drilling the probe boreholes. However, inflows to the tunnel during excavation indicated that the filling was not complete and therefore one cannot exclude that the core borehole may have acted as a connection between intersecting fractures. The first probe borehole of each pair was closed during drilling of the second probe borehole. Grouting was performed in Fan 1, before continuing to excavate and then SQ0059 G15 and the other grouting boreholes in Fan 2 were drilled. Further, Fan 2 was grouted before drilling SQ0059 S_C1 and SQ0059 S_B2.

3.4.2 Specific capacity and estimated hydraulic aperture based on inflow

Inflows are measured during drilling and generally for 3 m sections, see Table 3-8, Table 3-9 and Table 3-10. The specific capacity is estimated for a hydraulic head of 343 m (same as for the pressure build-up test in the core borehole). For all probe boreholes, inflows exceeding 2 L/min were only found for two sections of SQ0049B, three sections of SQ0049C and three sections of G15 (grouting borehole in which a pressure build-up test was also performed). Hydraulic apertures were estimated for a density and viscosity of the fluid of ρ=1000 kg/m^3 and μ=1.3E–3 Pa s respectively, and an acceleration due to gravity, g=9.8 m/s^2.

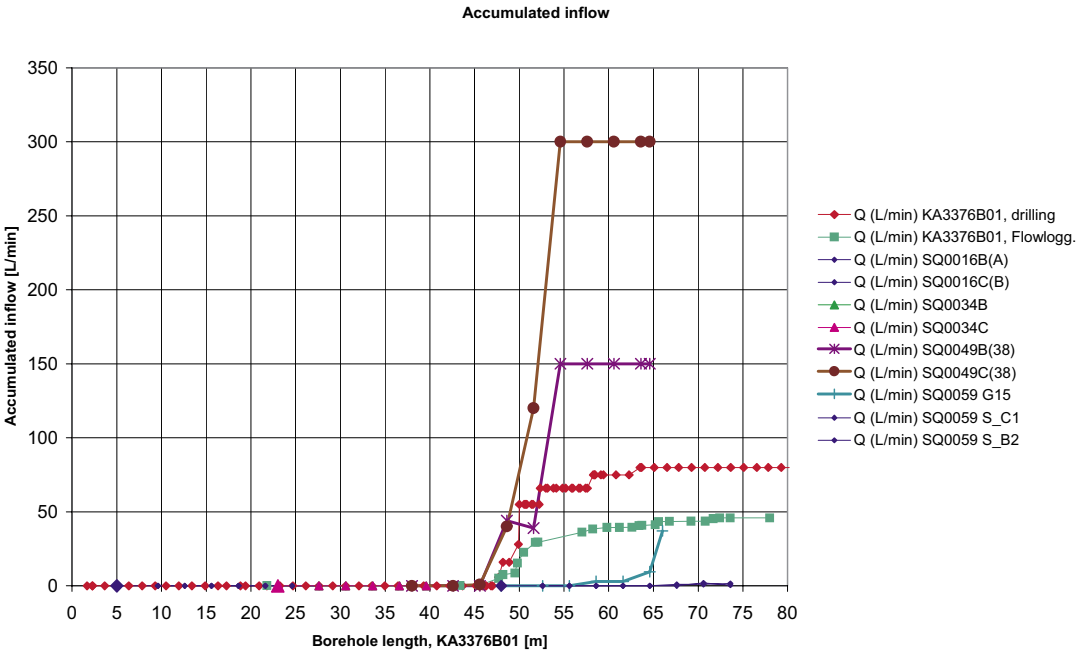

Figure 3-2. *Compilation of data: inflow along core- and probe boreholes. Location along borehole is approximate, differences in orientation of boreholes are not considered. Initially utilised names of probe boreholes are written within parentheses.*

Table 3-8. Inflow, specific capacity and estimated hydraulic apertures based on inflow during drilling, SQ0049B. Inflows >2 L/min are written in bold and are used for the geometrical model (RVS).

Section no	Section	Length [m]	dQ [L/min]	dQ [m^3/s]	Q/dh [m^2/s] dh: 343 m	b(Q/dh) [μm]
	0–4.6	4.6	0	0	0	0
	4.6–7.6	3	0	0	0	0
B1	**7.6–10.6**	**3**	**45**	**7.50E–04**	**2.19E–06**	**151**
	10.6–13.6	3	0	0	0	0
B2	**13.6–16.6**	**3**	**105**	**1.75E–03**	**5.10E–06**	**201**
	16.6–19.6	3	0	0	0	0
	19.6–22.6	3	0	0	0	0
	22.6–25.6	3	0	0	0	0
	25.6–26.6	1	0	0	0	0

Table 3-9. Inflow, specific capacity and estimated hydraulic apertures based on inflow during drilling, SQ0049C. Inflows >2 L/min are written in bold and are used for the geometrical model (RVS).

Section no	Section	Length [m]	dQ [L/min]	dQ [m³/s]	Q/dh [m²/s] dh: 343 m	b(Q/dh) [μm]
	0–4.6	4.6	0	0	0	0
	4.6–7.6	3	0.9	1.50E–05	4.37E–08	41
C1	**7.6–10.6**	**3**	**39.1**	**6.52E–04**	**1.90E–06**	**145**
C2	**10.6–13.6**	**3**	**80**	**1.33E–03**	**3.89E–06**	**184**
C3	**13.6–16.6**	**3**	**180**	**3.00E–03**	**8.75E–06**	**240**
	16.6–19.6	3	0	0	0	0
	19.6–22.6	3	0	0	0	0
	22.6–25.6	3	0	0	0	0
	25.6–26.6	1	0	0	0	0

Table 3-10. Inflow, specific capacity and estimated hydraulic apertures based on inflow during drilling, G15. Inflows >2 L/min are written in bold and are used for the geometrical model (RVS).

Section no	Section	Length [m]	dQ [L/min]	dQ [m³/s]	Q/dh [m²/s] dh: 343 m	b(Q/dh) [μm]
	0–4.6	4.6	0	0	0	0
	4.6–7.6	3	0	0	0	0
G15_1	**7.6–10.6**	**3**	**3**	**5.00E–05**	**1.46E–07**	**61**
	10.6–13.6	3	0	0	0	0
G15_2	**13.6–16.6**	**3**	**6.6**	**1.10E–04**	**3.21E–07**	**80**
G15_3	**16.6–18.0**	**1.4**	**27.6**	**4.60E–04**	**1.34E–06**	**129**

3.4.3 Transmissivity

Test data and evaluated specific capacity and transmissivity for the core borehole are presented in Table 3-11 and Table 3-12. Graphs for the evaluation of the tests are shown in Appendix E. According to these graphs, the pressure in probe boreholes SQ0016B, SQ0016C and SQ0034C has not recovered. For probe boreholes SQ0034B, SQ0049B, SQ0049C and G15 (SQ0059) the pressure recovers to approximately 340 m, which is close to the pressure registered for the core borehole. For some of the boreholes the test equipment limited the inflow and therefore the inflow from drilling was used to estimate specific capacities.

3.4.4 Initial results Description 2

Major inflows for the percussion drilled probe boreholes were found at approximately 45–66 m. This is in agreement with the results from the core borehole. Inflows exceeding 2 L/min were found in three of the probe boreholes (SQ0049B, SQ0049C and SQ0059_G15). SQ0049B had two sections with an inflow exceeding 2 L/min and the other two boreholes had three sections. Inflows correspond to estimated hydraulic apertures between 60–240 μm.

Table 3-11 Test data for pressure build-up tests in percussion drilled probe boreholes.

Borehole	Test section, sec up [m]	Test section, sec low [m]	Hydraulic head [m]	Flow [L/min] PBT (drilling)	Flow period [hours]	Recovery period [hours]
1: SQ0016B	0.55	22.6	Not recov.	0.06/(0.045)	~1	~1
1: SQ0016C	0.50	22.6	Not recov.	0.09/(0.1)	~1	~1
2: SQ0034C	0.85	19.6	Not recov.	0.02/(0.025)	~1	~1
2: SQ0034B	0.85	19.6	~340	0.73/(0.825)	~1	~1
3: SQ0049B	1.0	26.6	~340	33*/(150)	~1	~1
3: SQ0049C	0.65	26.6	~340	33*/(300)	~1	~1
4: SQ0059G15	–	18.0	~340	28*/(37)	~1	~7
4: SQ0059S_C1	0	25.6	–	–/(1.5)	No test	No test
4: SQ0059S_B2	0	25.6	–	–/(0.5–2)	No test	No test

*limitation of flow due to hoses used for the PBT.

Table 3-12 Specific capacity and transmissivity for percussion drilled probe boreholes.

Borehole	Test section, sec up [m]	Test section, sec low [m]	Specific capacity [m^2/s], dh: 343 m	Transmissivity [m^2/s]
1: SQ0016B	0.55	22.6	2.9E–9	2.4E–8
1: SQ0016C	0.50	22.6	4.4E–9	2.7E–8
2: SQ0034C	0.85	19.6	9.7E–10	–
2: SQ0034B	0.85	19.6	3.5E–8	–
3: SQ0049B	1.0	26.6	7.3E–6*	1.3E–5
3: SQ0049C	0.65	26.6	1.5E–5*	1.3E–5
4: SQ0059G15	–	18.0	1.8E–6	1.1E–6
4: SQ0059S_C1	0	25.6	7.8E–8**	No test
4: SQ0059S_B2	0	25.6	2.4E–8**	No test

* limitation of flow due to hoses used for the PBT, inflow during drilling are used for calculations

**Flow from drilling, PBT not performed.

For Description 1, inflows identified by flow logging were assumed to represent the median hydraulic apertures of fractures. To get a further developed description, the approximate location of probe boreholes along the core borehole is used. Further, the probe boreholes are assumed to be parallel and fractures perpendicular to the core borehole and the future tunnel. This results in all inflows at 7.6–10.6 m describing the variation within one fracture (B1 and C1, Table 3-8 and Table 3-9), inflows at 10.6–13.6 m describing the second fracture (C2) and all inflows at 13.6–16.6 m describing the third fracture (B2 and C3). Inflows number 4, 8 and 9 from the core borehole are found at 47.7, 50.5 and 51.8 m. The approximate location of sections 7.6–10.6 m along the core borehole is 45.6–48.6 m (49–11+7.6=45.6 m). Sections 10.6–13.6 m and 13.6–16.6 m are found at approximately 48.6–51.6 m and 51.6–54.6 m. Under the assumptions above, inflow number 4 and inflows B1 and C1 may originate from the same fracture. The same applies for inflow number 8 (together with C2) and inflow number 9 (together with B2 and C3). By extrapolating like this, new data was obtained which was assumed to describe a variation within that fracture. Inflows number 4, 8 and 9 from the core borehole resulted in new data and median hydraulic apertures of 145, 128 and 201 μm respectively. Assumed median hydraulic apertures of the other five fractures (inflows) were not changed.

3.5 Prediction 2 based on Description 2

The second prediction was made based on the information obtained from the probe holes. The inflow data is found in Appendix F.

3.5.1 Interpreted geometry of the fractures

The interpretation of fracture properties based on the information obtained from the probe holes gave a different range of apertures than the earlier interpretation for Fan 1. Three features (4, 8 and 9) were given a new interpretation with geometrical statistical data whilst the interpretation of the others was kept as in Prediction 1. The calculation for Fan 1 was calculated with a new design and with the new fracture statistics.

3.5.2 Grouting design

Fan 1

After evaluation of the probe holes a different design on the grouting of Fan 1 was decided. Three different designs were evaluated through calculations and the one found most suitable was recommended to be used. The decision analysis used for the selection of design is presented in Appendix G.

In the chosen design the grouting of the first fan was decided to be performed using two grouting rounds. The first grouting was to be performed as follows:

- 11 bore holes, 16 m long.
- Minimum flow 1.0 liter/min.
- Grouting pressure 1 MPa above ground water pressure.
- Bore hole radius 0.032 m.
- The grouting to be started with Grout B and continued until 150 litre is grouted, if refusal based on the flow criterion is not obtained. After this change to Grout C and max 50 additional litres to be grouted. After this the grouting is to be stopped.
- The grouting to be performed in a descending order based on the specific capacity.

Table 3-13. Evaluated geometrical properties of the singular rock fractures based on the hydraulic apertures and Equation 2-5.

	Inflow number	b [μm]	$b_{average}$ [μm]	σ_b [μm]	c [%]
Fan 1	4	145	185	67	20
	5	58	80	40	20
	7	98	134	68	20
	8	128	157	39	20
	9	201	264	111	20
Fan 2	11	89	123	62	20
	12	56	77	39	20
	19	55	76	38	20

The second grouting round was to be performed as follows:

- 20 bore holes, 16 m long.
- Minimum flow 1.0 liter/min.
- Grouting pressure 2 MPa above ground water pressure.
- Bore hole radius 0.032 m.
- The grouting to be started with Grout A and continued until 100 litre is grouted, if refusal based on the flow criterion is not obtained. After this change to Grout B and max 50 additional litres to be grouted. After this the grouting to be stopped.
- The grouting to be performed in a descending order based on the specific capacity.

Fan 2

No difference in the interpretation of Fan 2 arose from the information of the probe holes. Therefore the preliminary design was kept.

3.5.3 Predicted grouting result

The calculated results of Fan 1 are presented in Table 3-14 and Table 3-15 and of Fan 2 in Table 3-7.

Fan 1

Grouting round 1

Table 3-14. Calculated median grout volume, grouting time and sealing effect for grouting round 1 of Fan 1.

Inflow number	Median grouted volume [l]	Median grouted time [min]	Median sealing effect [%]
4	112.5	326.1	100
5	1,8	4.9	11
7	26.7	75,8	79
8	63.1	186,8	100
9	329.4	727.7	100

Based on the above given calculated values the following prediction of the grouting result was made:

In Fan 1 grouting round 1 the expected result was:

- Total grouted volume excluding filling of the holes 630 litres.
- Grouting time excluding filling of the holes 728 min.
- Sealing effect 97%.
- Inflow 0.4 l/min.

Grouting round 2

Table 3-15. Calculated median grout volume, grouting time and sealing effect for grouting round 2 of Fan 1.

Inflow number	Median grouted volume [l]	Median grouted time [min]	Median sealing effect [%]
4*	–	–	–
5	11.1	27.1	71
7	0.3	4.4	0
8*	–	–	–
9*	–	–	–

* Can not be regrouted in the model since the fracture was totally sealed in the first grouting round.

In Fan 1 grouting round 2 the expected result was:

- Total grouted volume excluding filling of the holes 11 litres.
- Grouting time excluding filling of the holes 27 min.
- Sealing effect 62%.
- Inflow 0.1 l/min.

Fan 2

Same as in prediction 1, see Section 3.3.3.

3.6 Characterisation based on core borehole, percussion drilled probe boreholes and grouting boreholes: Description 3

3.6.1 Inflow along borehole

Figure 3-3 presents a compilation of accumulated inflows along core and probe boreholes as well as the location of Fan 1 and Fan 2. Accumulated inflows for Fans 1:1, 1:2 and 2 are shown in Figure 3-4, Figure 3-5 and Figure 3-6 respectively. Inflows along the grouting boreholes were, as for the probe boreholes, generally measured for 3 m sections, see Appendix H. Locations of the grouting boreholes along the core borehole are approximate since differences in orientation of boreholes are not considered. The intention was to fill the core borehole with grout at low pressure (to minimize the risk of spreading the grout) before drilling the probe boreholes. However, inflows to the tunnel during excavation indicated that the filling was not complete and therefore one cannot exclude that the core borehole may have acted as a connection between intersecting fractures. The first probe borehole of each pair was closed during drilling of the second probe borehole. Probe boreholes SQ0049B and SQ0049C were not filled with grout prior to the drilling and grouting of Fan 1:1. Grouting was performed in Fan 1, before continuing to excavate and then SQ0059 G15 and the other grouting boreholes in Fan 2 were drilled. Further, Fan 2 was grouted before drilling SQ0059 S_C1 and SQ0059 S_B2. For each of the first four to five boreholes in grouting Fan 1:1, the borehole was drilled and then the packer was closed before drilling the next borehole. For later grouting boreholes, two boreholes were generally drilled simultaneously resulting in two boreholes being open at the same time. Often, these were drilled on the opposite sides of the grouting fan.

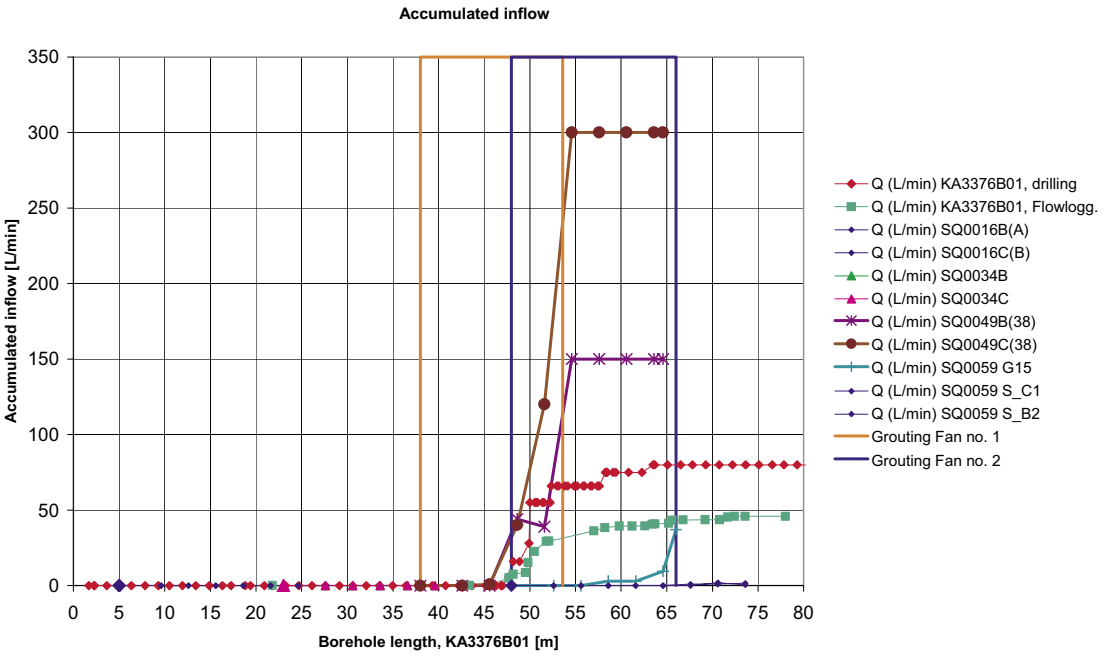

Figure 3-3. *Compilation of data: inflow along borehole for core- and probe boreholes. Location along borehole is approximate, differences in orientation of boreholes are not considered. Inflow data for Grouting Fans 1 and 2 are presented below. Initially utilised names of probe boreholes are written within parentheses.*

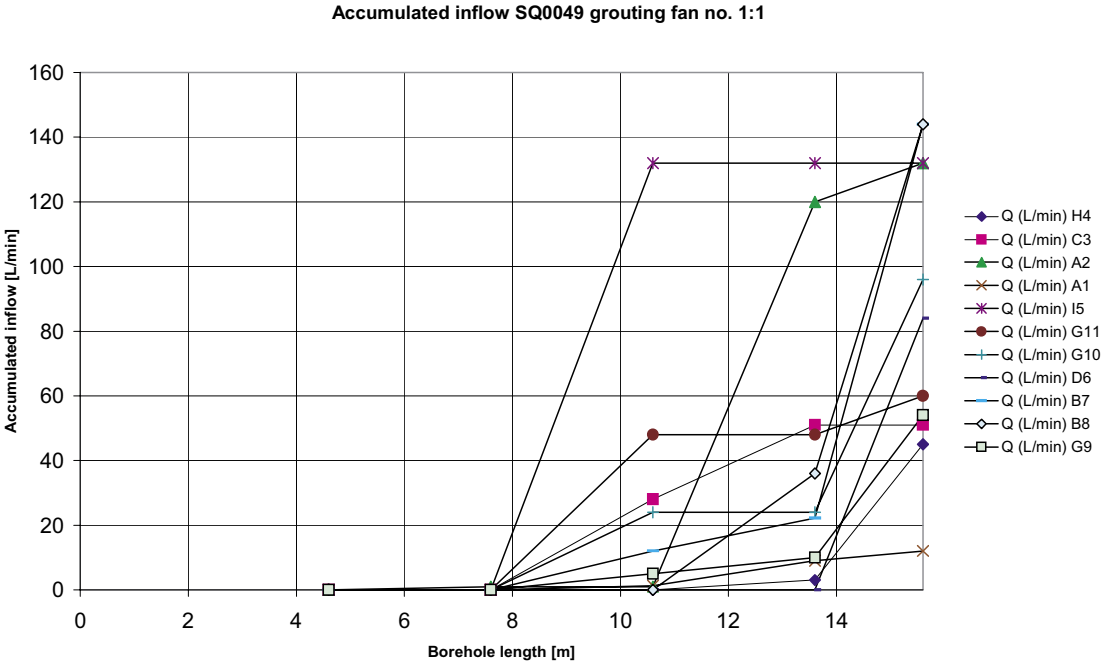

Figure 3-4. *Compilation of data: inflow along borehole for grouting boreholes, Fan 1:1. Differences in orientation of boreholes are not considered. A larger increase in inflow is seen at 8–10 m (approximately 49–11+8=46 m along the core borehole, Figure 3-3).*

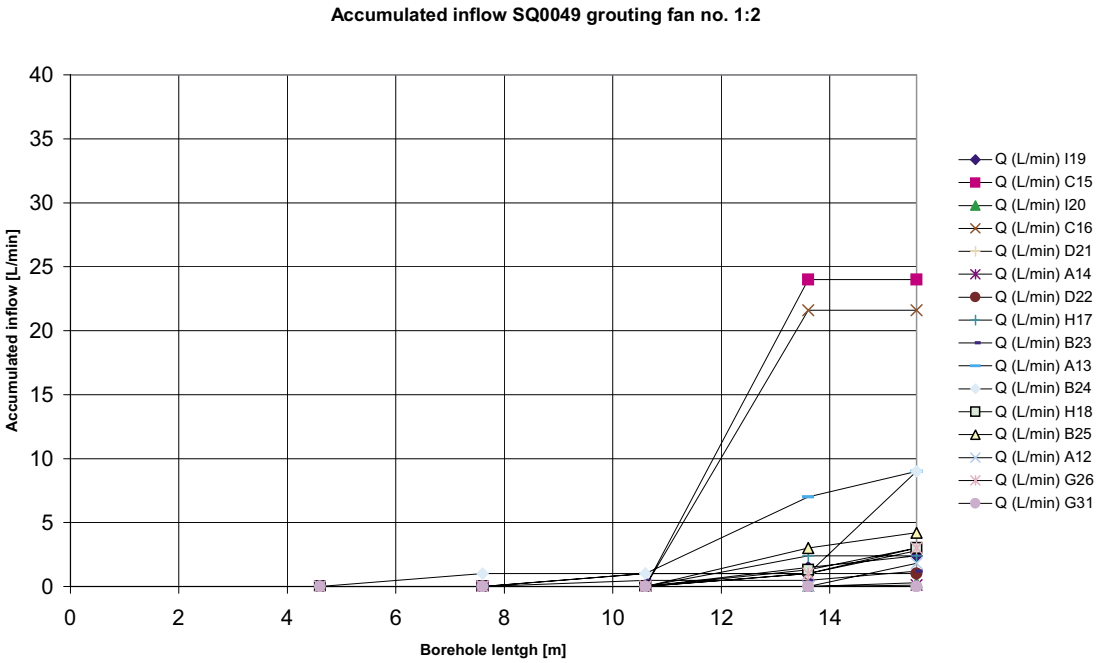

Figure 3-5. *Compilation of data: inflow along borehole for grouting boreholes, Fan 1:2. Differences in orientation of boreholes are not considered. A larger increase in inflow is seen at 10–14 m (approximately 49–11+10=48 m along the core borehole, Figure 3-3).*

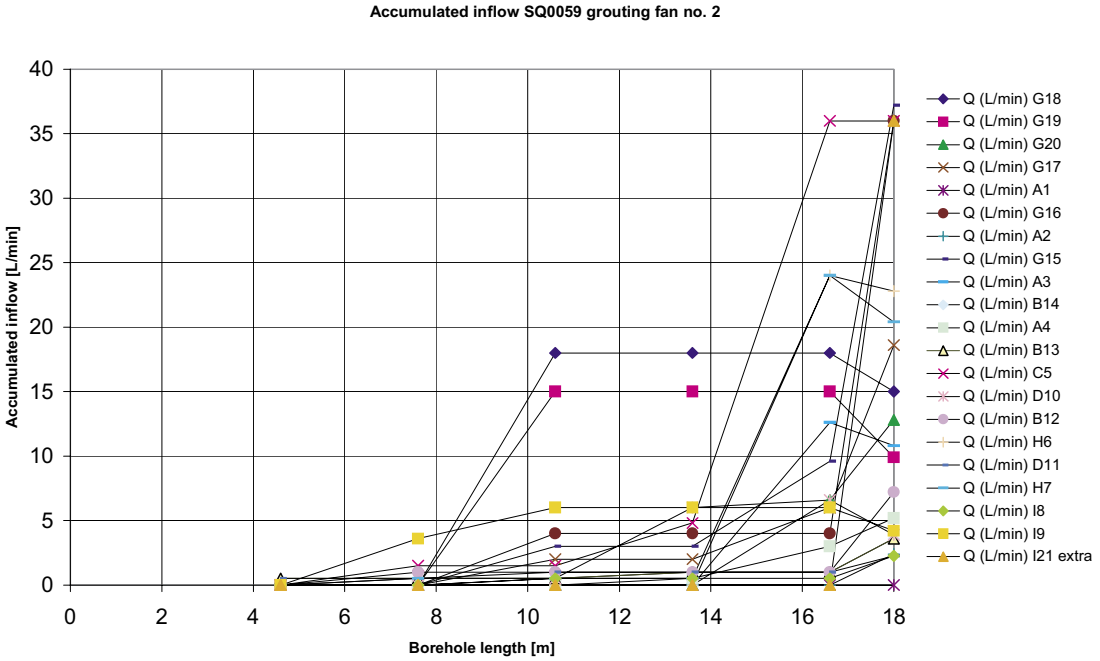

Figure 3-6. *Compilation of data: inflow along borehole for grouting boreholes, Fan 2. Differences in orientation of boreholes are not considered. A larger increase in inflow is seen at 8–10 m (approximately 59–11+8=56 m along the core borehole, Figure 3-3).*

Figure 3-4 shows an increase in inflow at 8–10 m, which would correspond to approximately 46 m along the core borehole. This is in agreement with the increase seen at 45–46 m for both core- and probe boreholes (Figure 3-3). Similar results are seen when comparing Figure 3-6 with increasing inflow at e.g. 8–10 m and 16–18 m. This would correspond to the slight increase at 56 m and the larger one at 64 m (Figure 3-3).

The four control boreholes drilled after grouting of Fan 1:2 all had total inflows below 1 L/min (approximate values were 0.3, 0.05, 0.3 and 0.3 L/min). These boreholes were shorter (length 13.6 m) than the grouting boreholes.

The four control boreholes drilled after grouting of Fan 2 all had total inflows below 1 L/min (approximate values were 0.7, 0.4, 0.4 and 0.3 L/min). These boreholes were shorter (length 16.6 m) than the grouting boreholes. Two additional boreholes (SQ0059S_C1 and SQ0059S_B2) were also drilled. The length was 25.6 m and total inflows were approximately 1.6 and 0.5 L/min.

3.6.2 Specific capacity and estimated hydraulic aperture based on inflow

Inflows, Q, instead of specific capacity are used below to compare Fan 1:1, Fan 1:2 and Fan 2:1. Appendix H presents inflow for all boreholes and sections as well as estimated hydraulic apertures. The specific capacity is obtained when dividing inflow by difference in hydraulic head, dh. The median specific capacity, Q/dh (for dh=340 m) for the different fans are included in Appendix H. Figure 3-7 and Figure 3-8 present frequency histograms and box-and-whisker plots of inflows (log10Q) for the fans. Figure 3-7 compares the inflow to the grouting boreholes in Fan 1:1 and Fan 1:2. The median inflow when grouting Fan 1:1 goes from 84 L/min (Q/dh: 4.1E–6 m^2/s) to 3 L/min (1.4E–7 m^2/s). Inflows for the four control boreholes after grouting of Fan 1:2 were all below 1 L/min. However, difficulties to measure small inflows generally make the exact values uncertain.

In Figure 3-8, inflows to the grouting boreholes in Fan 1:2 and Fan 2:1 are shown. Fan 1:2 had a median inflow of 3 L/min (1.4E–7 m^2/s) and Fan 2:1 had a median inflow of 10 L/min (4.8E–7 m^2/s). Inflows for the four control boreholes after grouting of Fan 2 were all below 1 L/min. However, difficulties to measure small inflows generally make the exact values uncertain. Fan 1:2 has a high frequency of small inflows compared to Fan 2:1. This may be due to the grouting of Fan 1:1 partly sealing the fractures, resulting in some tight boreholes.

One of the assumptions for this work (see Table 2-3) is that inflow within a section is assumed to originate from one major fracture. In Figure 3-9, Figure 3-10 and Figure 3-11, the largest total inflow to a section, Qmax, is divided by the total inflow to that borehole, Qtot. This was made for all grouting boreholes within each fan and data are presented in frequency histograms. Figure 3-9, Figure 3-10 and Figure 3-11 all show that at least 40–50%, but commonly a larger fraction of the total inflow originates from one section of the borehole.

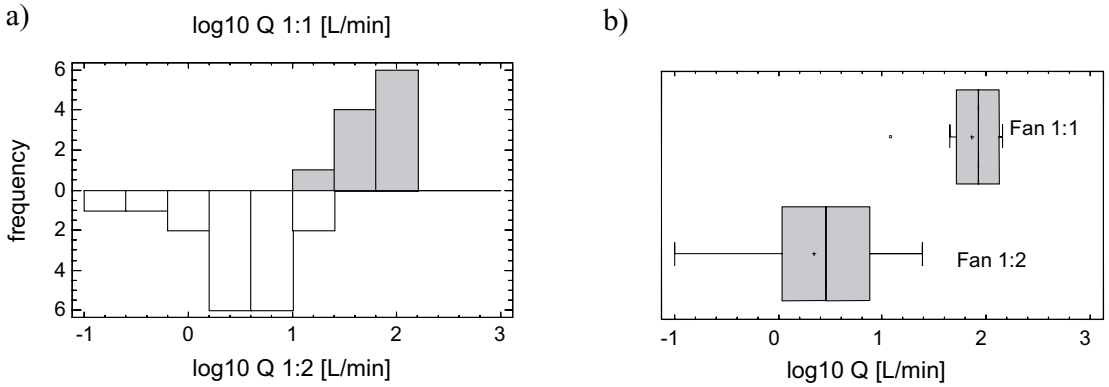

Figure 3-7. *a) Frequency histograms and b) box-and-whisker plots of inflows (log10 Q) in holes for grouting of Fan 1:1 and in holes for grouting of Fan 1:2. (Log10 Q=0 is 1 L/min, Log10 Q=0.5 is 3 L/min, Log10 Q=2 is 100 L/min).*

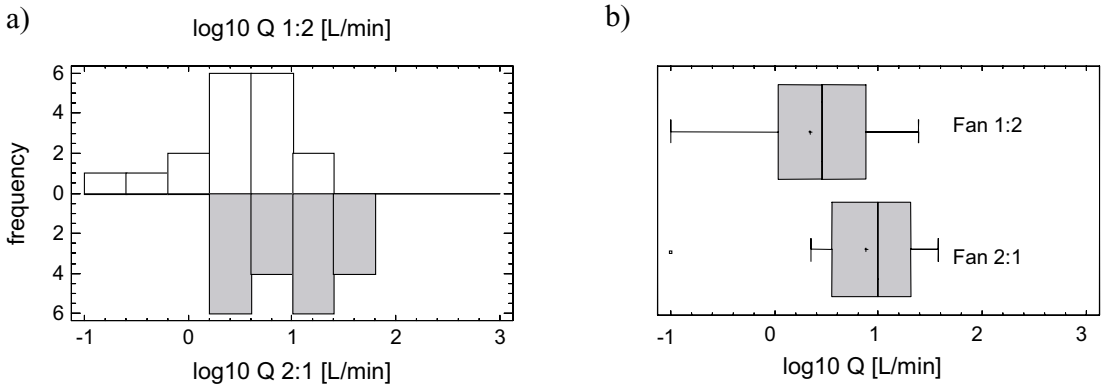

Figure 3-8. *a) Frequency histograms and b) box-and-whisker plots of inflow (log10 Q) in holes for grouting of Fan 1:2 and in holes for grouting of Fan 2:1. (Log10 Q=0 is 1 L/min, Log10 Q=0.5 is 3 L/min, Log10 Q=1 is 10 L/min).*

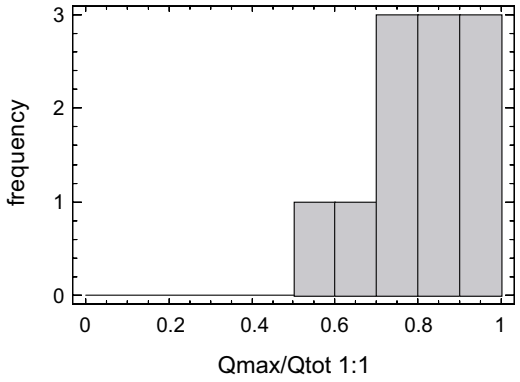

Figure 3-9. *Frequency histogram of Qmax/Qtot for Fan 1:1 (11 boreholes).*

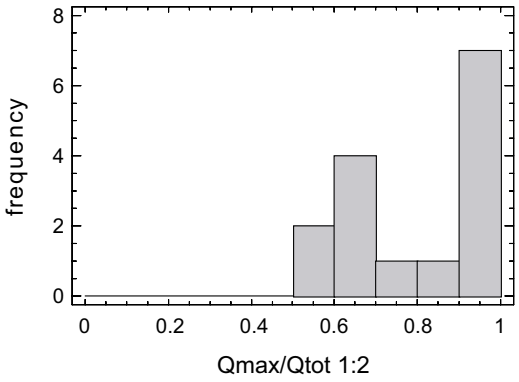

Figure 3-10. *Frequency histogram of Qmax/Qtot for Fan 1:2 (15 out of a total of 21 boreholes, 6 boreholes had no/low inflow or only full length measurements).*

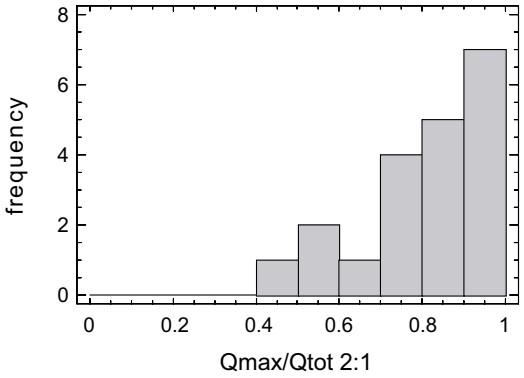

Figure 3-11. *Frequency histogram of Qmax/Qtot for Fan 2:1 (20 out of a total of 21 boreholes, 1 borehole had only a full length measurement).*

3.6.3 Initial results Description 3

An increase in inflow for the grouting boreholes was found at approximately 45–46 m along the core borehole. This is in agreement with the results from the core and probe boreholes. As an initial assumption, boreholes are assumed to be parallel and fractures are assumed to be perpendicular to the tunnel. The description focuses on inflow exceeding 2 L/min and assumes one major inflow in each section. For Fan 1 the result would be in all three fractures where all inflows at 7.6–10.6 m describe the variation within one fracture, all inflows at 10.6–13.6 m describe the second fracture and all inflows at 13.6–15.6 m describe the third fracture. Data are presented in Appendix H. The median inflow and hydraulic aperture for all boreholes and each section are assumed to give a general description of the cross-fracture properties.

3.7 Prediction 3 based on Description 3

The third prediction was made based on the information obtained from the grouting holes. The inflow data is found in Appendix H.

3.7.1 Interpreted geometry of the fractures

Information from the inflow of water in the grouting holes gave additional information for a new statistical description of the fracture geometries. The interpretation of the statistical description is simplified by assuming that all water in a borehole section of three meters emanates from one fracture.

The interpretation was made by letting the zero values correspond to contact areas and the median value and standard deviation between the non zero values to correspond to the hydraulic aperture and standard deviation in aperture**.** For Fan 1 this is presented in Table 3-16.

For Fan 2 however, it was not possible to use this method to evaluate a physical aperture and a standard deviation since the amount of contact becomes too high. In Table 3-17 the results after assuming an amount of contact of 40% for Fan 2 are given. These values are used in the calculations.

3.7.2 Grouting design

See section 3.5.2 for design of Fan 1 and section 3.3.2 for design on Fan 2.

3.7.3 Predicted grouting result

The calculated results of Fan 1:1 are presented in Table 3-18 and of Fan 2 in Table 3-21.

Table 3-16. Evaluated geometrical properties for one fracture representing the flow in a three meters bore hole section based on Equation 2-5 in Fan 1.

	Section number	b [μm]	$b_{average}$ [μm]	σ_b [μm]	c [%]
Fan 1:1	1	0	0	0	90
	2	43	43	0	91
	3	123	214	98	36
	4	92	150	53	36
	5	150	186	65	18

Table 3-17. Evaluated geometrical properties for one fracture representing the flow in a three meters bore hole section based on Equation 2-5 in Fan 2.

	Section number	b [μm]	$b_{average}$ [μm]	σ_b [μm]	c [%]
Fan 2	1	34	58	0	40
	2	38	81	46	40
	3	54	108	54	40
	4	34	67	32	40
	5	90	162	48	40
	6	68	151	90	40

Fan 1

Grouting round 1

Table 3-18. Calculated median grout volume, grouting time and sealing effect for grouting round 1.

Section number	Median grouted volume [l]	Median grouted time [min]	Median sealing effect [%]
1	0	0	0
2	0	0	0
3	68	333	100
4	20	110	1
5	133	641	100

Based on the above given calculated values the following prediction of the grouting result is made:

- Total grouted volume excluding filling of the holes 221 litres.
- Grouting time excluding filling of the holes 641 min.
- Sealing effect 97%.

Grouting round 2

The fracture properties for simulation of grouting round 2 are presented in Table 3-19. These values of fracture properties are obtained from the result of the numerical grouting simulation presented in Table 3-18, hence not on inflow in the bore holes.

Table 3-19. Evaluated geometrical properties for the second round of grouting based on the result in the numerical simulation of Grouting round 1.

	Section number	b [μm]	$b_{average}$ [μm]	σ_b [μm]	c [%]
Fan 1:2	1	0	0	0	90
	2	43	43	0	91
	3	32	64	32	36
	4	57	114	57	36
	5	0	0	0	18

Table 3-20. Calculated median grout volume, grouting time and sealing effect for grouting round 2.

Section number	Median grouted volume [l]	Median grouted time [min]	Median sealing effect [%]
1	0	0	0
2	0	0	0
3	2	18	23
4	44	430	99
5	0	0	0

Based on the above given calculated values the following prediction of the grouting result is made:

- Total grouted volume excluding filling of the holes 46 litres.
- Grouting time excluding filling of the holes 430 min.
- Sealing effect 92%.

The total calculated result for Fan 1

Based on the above given calculated values the following prediction of the grouting result is made:

- Total grouted volume excluding filling of the holes 267 litres.
- Grouting time excluding filling of the holes 1071 min.
- Sealing effect 99.6%.
- Inflow 0.1 l/min.

Fan 2

Table 3-21 Calculated median grout volume, grouting time and sealing effect for grouting round 1.

Inflow number	Median grouted volume [l]	Median grouted time [min]	Median sealing effect [%]
1	2	11	20
2	6	27	83
3	21	110	99
4	3	11	29
5	165	898	100
6	94	451	100

Based on the above given calculated values the following prediction of the grouting result is made:

- Total grouted volume excluding filling of the holes 291 litres.
- Grouting time excluding filling of the holes 898 min.
- Sealing effect 95%.
- Inflow 0.1 l/min.

3.8 Grouting result

The outcome of the practical grouting operation is presented as grout take, grouting time and evaluated sealing effect. The values concerning grout take and grouting time are the values measured with the grouting equipment. In Appendix J these measured values are presented in more detail. The evaluated sealing effect is based on the measurement of inflow from the grouting holes and control holes. In Appendix C positions for probe, grouting and control holes are shown. In Appendix H and J respectively, the measured values on inflow in grouting holes and in control holes are presented.

In Fan 1:1, a total of 1633 litres of grout including filling of the holes and hoses was injected. Excluding filling of the holes and hoses a volume of approximately 863 litres was injected. Nine of the eleven grouting holes were grouted with grout C as stop grout and two with grout B. The grouting time, i.e. the time for pumping including filling of the holes was 196 minutes. If it is assumed that filling the holes takes approximately 3 minutes per hole the actual grouting time is around 160 minutes. The sealing effect evaluated as the decrease in median flow from the grouting holes in Fan 1:1 to the mean flow in grouting holes in Fan 1:2 was 97%.

In Fan 1:2, a total of 2537 litres of grout including filling of the holes and hoses was injected. Excluding filling of the holes and hoses a volume of approximately 1137 litres was injected. In six cases the grouting was stopped with grout A, in ten cases with grout B and in four cases with grout C. The grouting time, i.e. the time for pumping including filling of the holes was 854 minutes. If it is assumed that filling the holes takes approximately 3 minutes per hole the actual grouting time is around 800 minutes. The sealing effect evaluated as the decrease in median flow from the grouting holes to the median flow in control holes was 97%.

In total the grouting in Fan 1 was performed using 4170 litres of grout with a grouting time of 1050 minutes pumping time. The total sealing effect was 99.9% evaluated from the inflow in the grouting holes and the control holes.

In Fan 2, a total of 2456 litres of grout including filling of the holes and hoses was injected. Excluding filling of the holes and hoses a volume of approximately 1470 litres was injected. In all grouting holes the grouting was finished with grout C due to a change in design compared to the two other grouting rounds. Holes with less than 4 litres/min of inflow were directly grouted with grout C and the rest was ended with grout C. The grouting time, i.e. the time for pumping including filling of the holes was 480 minutes. If it is assumed that filling the holes takes approximately 3 minutes per hole the actual grouting time is around 420 minutes. The sealing effect evaluated as the decrease in median flow from the grouting holes to the mean flow in control holes was 95%.

Table 3-22 Summary of measured and evaluated grouting result.

Fan	Grout take [l] Including hole filling/ excluding hole filing	Grouting time [min] Including hole filling/ excluding hole filing	Sealing effect [%]
1:1	1633/863	196/160	97
1:2	2537/1137	854/800	97
2:1	2456/1470	480/420	95

3.9 Pressure responses (HMS) during drilling, testing and grouting

The *hydro monitoring system (HMS)* at Äspö continually monitors ground water pressure in several boreholes. Normally, this system registers the pressure once every second hour and a detailed scanning starts when the measured pressure change exceeds 2 kPa. As an example, pressure data for boreholes KA3385A, KA2598A and KF0069A01 are presented in Figure 3-12. The boreholes are located in the vicinity of the core borehole and future tunnel to give a picture of how the activities in Table influence the pressure. In /Fransson, 2003/ pressure responses in several core boreholes, see Figure 2-2 and Figure 2-3 were analysed when evaluating drilling and testing of the core borehole (KA3376B01). KA3385A and KA2598A were in these investigations found to have the largest responses.

As an example, pressure build-up tests in probe boreholes SQ0049B and SQ0049C can clearly be seen in boreholes KA3385A and KA2598A. The effect when grouting Fan 1:1 and Fan 1:2 is smaller.

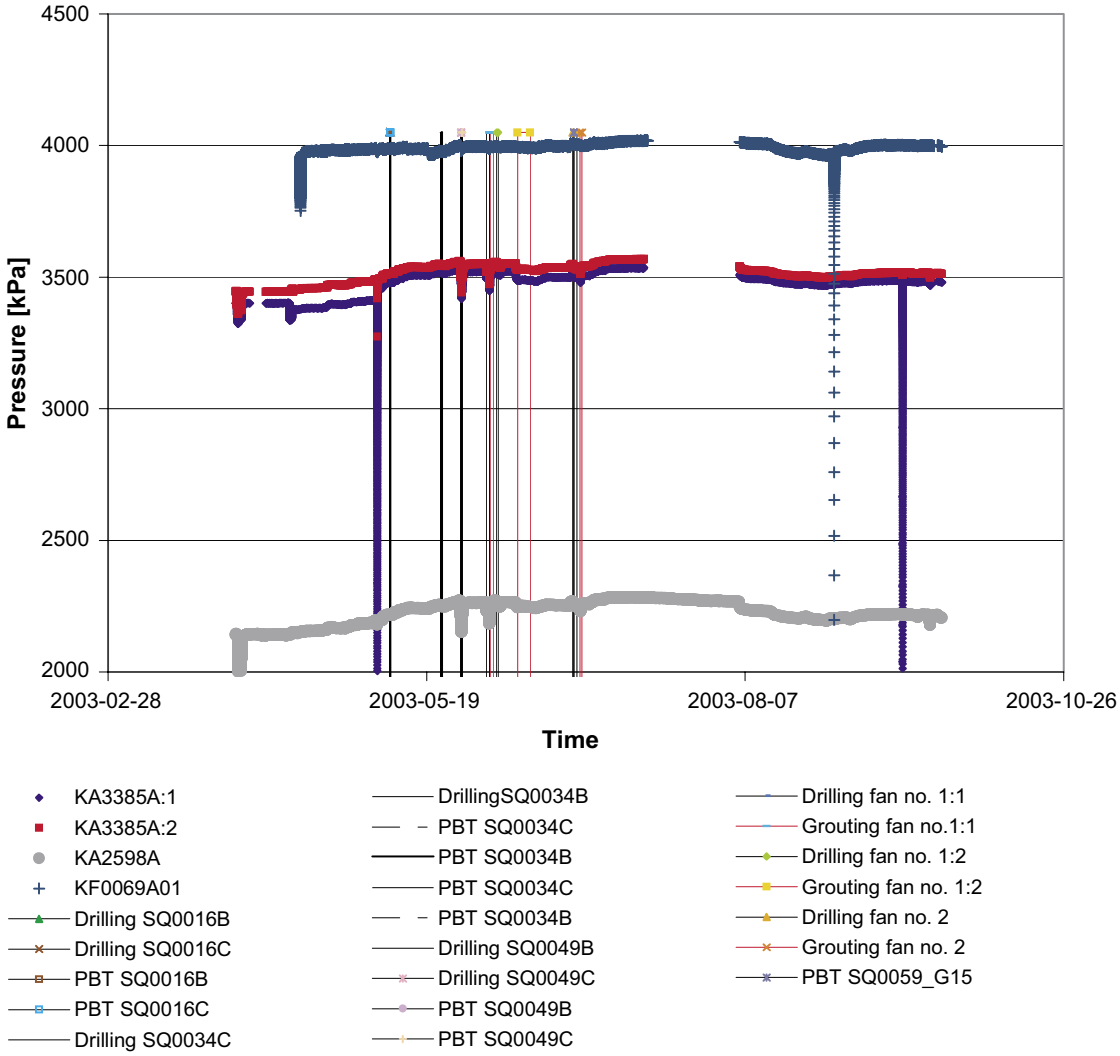

Figure 3-12. *Pressure responses for KA3385A, KA2598A and KF0069A01 located in the vicinity of the tunnel (see Figure 2-2) during drilling testing and grouting. Data registered by the Hydro Monitoring System (HMS).*

4 Discussion

4.1 Evaluation of methodology

4.1.1 Hydrogeological characterisation

Description 1

Main assumptions and hypotheses for this work are presented in Table 2-3. The general assumption for the entire hydrogeological characterisation is that the conductive fractures in the rock mass can be identified and described based on natural inflow. Further, descriptions will focus on inflows >2 L/min since the prevailing pressure results in an estimated hydraulic aperture of approximately 50 μm and smaller fractures are considered difficult to seal with cement based grouts. For description and design purposes, inflow within a section (here generally 3 m) is assumed to originate from one major fracture. In previous studies /Fransson, 1999, 2001/, inflow or specific capacity is assumed to describe "local" hydraulic properties, whereas transmissivity evaluated from pressure build-up tests or recovery tests describes "global" hydraulic properties. This is also assumed and investigated in this study.

Throughout this work locations of larger inflow (Posiva Flow Log) are coupled to the closest natural open fracture(s) based on BIPS and core mapping. Data from inflow logging, BIPS and core mapping are used for extrapolation to describe location, strike, dip and inflow of possible conductive features along the future tunnel.

Figure 4-1 presents a compilation of data from flow logging and geological mapping of core borehole KA3376B01. Location, strike and dip originate from BIPS and core logging. Horizontal red lines numbered from 1–25 indicate inflows and location of conductive features based on Posiva Flow Log. The smallest of these inflows is approximately 0.02 L/min. The APSE-tunnel is approximately parallel to the core borehole, which is found at the level of the floor of the tunnel and at a distance of approximately two meters to the left in the beginning of the tunnel and approximately three meters in the end of the tunnel. Figures are made using a three-dimensional CAD-based visualisation tool, Rock Visualisation System (RVS) and beside data above, coordinates of boreholes are used to make the images. The largest inflows are found for inflow numbers 7, 8, 9 and 11 (>5 L/min). Inflows >2 L/min are found for inflows 4, 5, 12 and 19.

For inflow number 7 found at 49.8 m along the core borehole, no natural fracture was identified. For inflow number 8 (50.5 m, Q: 27 L/min) a natural fracture is identified at 50.42 m. For inflow number 9 (51.8 m, Q: 11 L/min) two or three fractures are found (two are close to perpendicular and one sub-parallel). The closest is found at 51.78 m. In the vicinity of inflow number 11 (57 m, Q: 9 L/min) two fractures are identified, the closest has the same location. For inflows 8, 9 and 11 the closest fractures are close to perpendicular to the borehole (strike 120–135° and dip 70–85°). Fracture fillings are in these cases calcite and chlorite.

Inflow number 4 (47.7 m, Q: 4.7 L/min) has three fractures in close vicinity, two parallel and one sub-parallel to the borehole. A sub-parallel fracture is also identified close to inflow number 5 (48.2 m, Q: 2.5 L/min). The fracture close to inflow number 12 (58.2 m, Q: 2.2 L/min) is less steep than the most transmissive fractures but has approximately the same strike. Finally, around inflow number 19 (65.6 m), three fractures of varying strikes and dips are seen. Here as well, the most important fracture fillings are calcite and chlorite.

Figure 4-1. *Description 1: compilation of data for core borehole KA3376B01. Location, strike and dip from BIPS and core logging. Horizontal red lines numbered from 1–25 indicate location of conductive features based on Posiva Flow Log. The smallest of these inflows is approximately 0.02 L/min.*

According to Description 1 above, both local and total inflows were <2 L/min until 47.7 m. The largest inflows (>5 L/min) were found between 50–57 m. Could new information obtained from probe boreholes confirm this description?

Description 2

The general assumptions for the study presented for Description 1 are made also for Description 2. The principles for extrapolation of possible conductive fractures are also the same. Additional assumptions and hypotheses presented in Table 2-3 are firstly that the variation in aperture within a conductive fracture is indicated by the local inflow to the core borehole and section inflows to probe boreholes intersecting a possible extrapolated conductive fracture. Further, the median specific capacity is assumed to be an approximation of the cross fracture transmissivity (at this stage specific capacities from the core borehole and one or two probe boreholes are used).

Figure 4-2 presents Description 2 compiling data from core borehole KA3376B01 and probe boreholes SQ0049B, SQ0049C and SQ0059_G15. Here, coordinates along the boreholes are used for the RVS-model to get an image that is as correct as possible considering borehole and fracture orientation. As shown in the figure, probe boreholes were not straight, which influences where they intersect a fracture. Sections referred to as C1 and B1 are the first sections having inflows exceeding 2 L/min. Relating the location of these cylinders to the core borehole length, an increase in inflows is seen at approximately 46–49 m, which is in agreement with information obtained from the core borehole. This is also in agreement with the somewhat simpler and straightforward description in Figure 3-2 showing inflow along borehole for core- and probe boreholes. In Figure 3-2, location along the borehole is approximate and differences in orientation of boreholes are not considered.

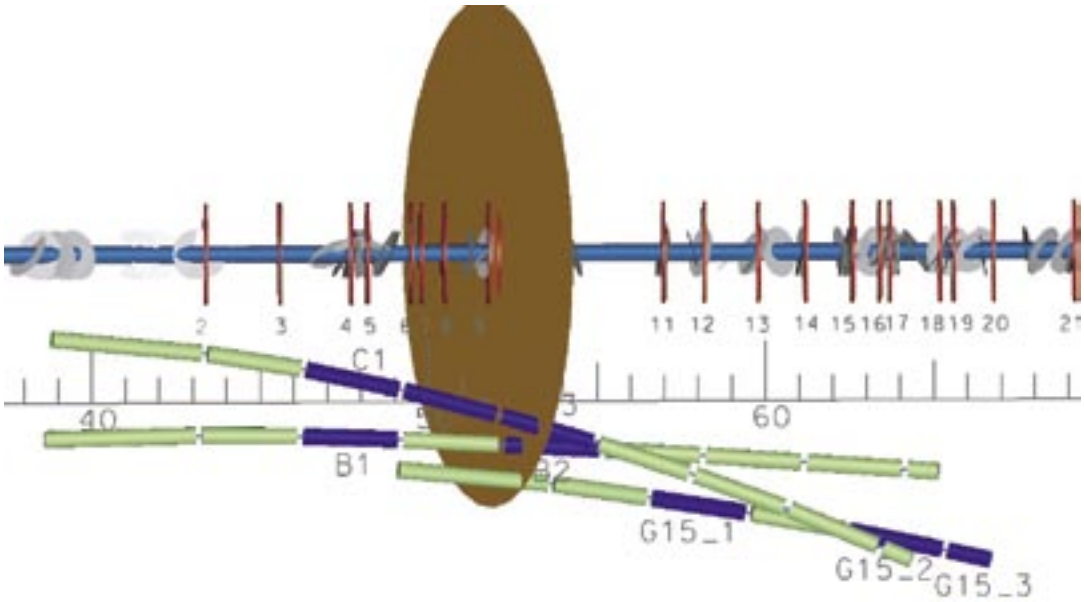

Figure 4-2. *Description 2: compilation of data from core borehole KA3376B01 and probe boreholes SQ0049B, SQ0049C and SQ0059_G15 including an extrapolated fracture based on inflow no 9. Vertical red lines numbered from 1–21 indicate locations of conductive features based on Posiva Flow Log. Grey discs show strike and dip of natural fractures. The blue cylinders along the probe boreholes represent a section (generally 3 m) having an inflow during drilling which is >2 L/min (green <2 L/min). The brown disc shown in the figure represents inflow no 9 along the core borehole and the disc is given the strike and dip of the fracture found closest to the location of inflow (from BIPS and core logging).*

Figure 4-2 shows an extrapolated fracture based on inflow number 9. Probe boreholes SQ0049B and SQ0049C intersect this fracture at cylinders B2 and C3. For Description 1, inflows to the core borehole and estimated hydraulic apertures were assumed to describe the fractures. Here, additional data are obtained through B2 and C3 and the median inflow of number 9, B2 and C3 is assumed to give an improved description, see Table 4-1. It is also assumed that this new data give a first indication of the variation in aperture within the possible fractures. Inflows number 4 and 8 are treated similarly.

Borehole SQ0059_G15 was drilled after grouting of Fan 1 (found at approximately 38–54 m). As shown, the first cylinder of the borehole has an inflow <2 L/min (green), indicating that a locally small aperture was intersected or that the larger inflows to the previous probe boreholes were sealed off.

By extrapolating strike and dip, probe boreholes intersected what can possibly be the structures with inflows >2 L/min identified by the core borehole (7, 8, 9 and 11 >5 L/min and 4, 5, 12 and 19 >2 L/min). Table 4-1 presents a compilation of inflow data from the core and the probe boreholes (section inflows for SQ0049B, SQ0049C and G15) for these structures except for inflows number 5 and 7. These were not included since only a sub-parallel fracture (possibly not intersecting the probe boreholes) was identified close to inflow number 5 (48.2 m). For inflow number 7 found at 49.8 m along the core borehole, no natural open fracture was identified. A possible explanation could be that a fracture considered to be sealed when logging the core actually conducts water. All major inflows identified by probe boreholes are intersected by extrapolated structures from the core borehole except for G15_3, which might be outside the main investigated area. Fractures related to inflows number 11, 12 and 19 are beside borehole G15 intersected by SQ0049B and SQ0049C. Due to the large inflows along these boreholes, smaller inflows at the inner part of the boreholes may not be seen. In this case we assume these inflows are smaller than the identified and use the smaller of the two apertures to obtain a median hydraulic aperture. The description below is in agreement with the somewhat simpler initial Description 2 in the results section.

Table 4-1. Inflow number, location of fracture, intersected sections of probe boreholes, (SQ0049B, SQ0049C and G15, grouting borehole where a pressure build-up test was performed) corresponding inflows, estimated hydraulic apertures and median hydraulic apertures.

Inflow no/location of fracture (BIPS, core borehole)	Intersected sections of probe boreholes SQ0049B: B1–2 SQ0049C: C1–3 G15: G15_1–2	Inflows [L/min]	Estimated hydraulic apertures [µm]	Median hydraulic aperture [µm]
4/47.66 m	4/B1/C1	5/45/40	71/151/145	145
8/50.42 m	8/–/C2	27/–/80	128/–/184	128
9/51.78 m	9/B2/C3	11 /150/180	95/201/240	201
11/57.0 m or 12 / 58.09 m	11/G15_1 12/G15_1	9/3 2.2/3	89/61 56/61	61* 56*
19/65.48 m	19/G15_2	2.1/6.6	55/80	55*

* Extrapolated fractures also intersected by SQ0049B and SQ0049C, which are assumed to have lower inflows.

Having in mind the assumption that the median specific capacity (or median hydraulic aperture) is an approximation of the cross fracture transmissivity (or the corresponding effective hydraulic aperture, see /Fransson, 2001/). The largest difference in inflows from the core- and probe boreholes is found at what is assumed to be a fracture at inflow number 9 (at approximately 52 m). This inflow was 11 L/min and for probe boreholes at the same location along the borehole, 3 m section inflows were 150 and 180 L/min.

Possible reasons for this may be that the core and probe boreholes are not intersecting the same fracture or that the fracture has comparatively small apertures in the vicinity of the core borehole. This is indicated by the large transmissivity of the core borehole (T:1.5E–5 m^2/s). Assuming the transmissivity is an approximation of the specific capacity, T≈Q/dh and dh 340 m, the inflow, Q, would be approximately 300 L/min. Both probe boreholes (SQ0049C and SQ0049B) have the transmissivity, T:1.3E–5 m^2/s, which is in better agreement with their total borehole inflows during drilling of 300 and 150 L/min respectively (if T≈Q/dh and dh 340 m, inflow, Q is approximately 270 L/min). This confirms the usefulness of transient, time-dependent tests and shows that only local, assumed steady-state testing in one borehole may not be enough to be properly prepared.

In Figure 4-3 and Figure 4-4, normal probability plots of inflows (log10 Q) from Posiva flow logging and from section inflows during drilling of probe boreholes SQ0016B, SQ0016C, SQ0034B, SQ0034C, SQ0049B and SQ0049C are shown. Posiva Flow Log manages to measure small inflows, which was not possible for the inflow measurements that were performed during drilling. As presented in Figure 4-4, 80% of the sections of the probe boreholes had inflows below 1 L/min and for this analysis they where assumed to have an inflow of 0.1 L/min (Log10 Q=–1 is 0.1 L/min). A line having the same median value and the same slope can be fitted to the two distributions. A comparison between inflow data from Posiva Flow Log and inflow during drilling (subdivided into inflows for 3 m sections) show good agreement as well. Consequently it seems like data from the core borehole and the probe boreholes follow the same distributions. Further, this result indicates that there are few conductive fractures along these boreholes since similar distributions are obtained for detailed and 3 m section measurements. For grouting purposes, we are only likely to seal fractures having inflows exceeding 2 L/min. Therefore, for this test location, the 3 m section measurements give both valuable and useful information.

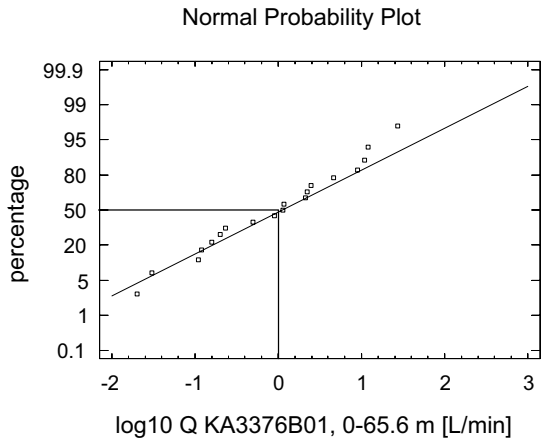

Figure 4-3. *Normal probability plot of inflows (log10 Q) based on Posiva Flow Log and inflow during drilling (0–65.6 m).*

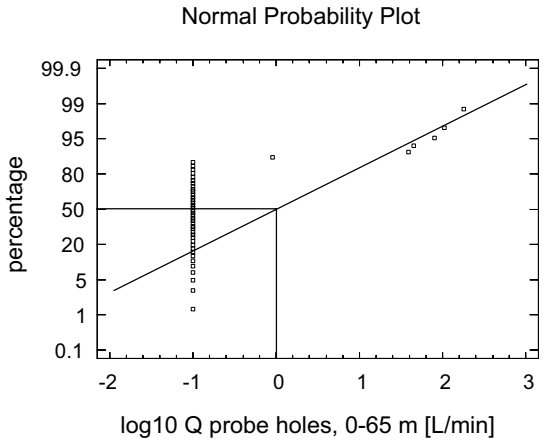

Figure 4-4. *Normal probability plot of inflows (log10 Q) based on section inflows during drilling of probe boreholes SQ0016B, SQ0016C, SQ0034B, SQ0034C, SQ0049B and SQ0049C (0–65 m).*

Description 3

The general assumptions for the study presented for Descriptions 1–2 are also made for Description 3 (Table 2-3). The principles for extrapolation of possible conductive fractures are also the same. Additional assumptions and hypotheses presented in Table 2-3 are that the variation in aperture within a conductive fracture is indicated by the local inflow to the grouting boreholes intersecting a possible extrapolated conductive fracture. Further, the median specific capacity is an approximation of the cross fracture transmissivity (at this stage specific capacities from the grouting boreholes are used). One hypothesis to be studied for the grouting boreholes is if the total inflow to a borehole seems to be a "good-enough" approximation of a section (and possibly fracture) inflow.

Figure 4-5 shows the extrapolated fracture based on inflow number 9, compilation of data from core borehole KA3376B01 and grouting boreholes for Fan 1:1. Included is also data from the tunnel mapping where conductive fractures are presented in blue. The probe boreholes are within or behind the tunnel and therefore hidden, these boreholes are seen in Figure 4-6. In Figure 4-6, the image is seen from above and rotated so that the possible fracture of inflow no 9 is seen in parallel in order to be able to identify all intersections. Appendix K presents similar images like Figure 4-5 and Figure 4-6 for the sections of the grouting fans. Further, a comparison between results based on borehole data and tunnel mapping is also presented.

Assumptions presented in Table 2-3 connected to Description 3 are that the median specific capacity is an approximation of the cross fracture transmissivity (at this stage specific capacities from the grouting boreholes are used). Further, total inflow of a borehole can be a "good-enough" approximation of a section or fracture inflow. In Figure 4-7, Figure 4-8 and Figure 4-9 total inflows of grouting boreholes in Fan 1:1, 2:1 and 1:2 are shown.

An initial observation is that data seem to follow a log-normal distribution. The dashed lines in Figure 4-7 and Figure 4-8 represent inflows estimated from the transmissivities of probe boreholes SQ0049B and SQ0049C (along Fan 1) and grouting borehole G15. The inflows were estimated assuming that $T \approx Q/dh$ and using a difference in hydraulic head, dh of 343 m (from pressure build-up test). For Figure 4-7 this inflow is as pointed out earlier larger than all inflows, whereas for Figure 4-8 the inflow is within the interval even though a complete match to the median value is not found. The probe boreholes being longer than the grouting boreholes may explain the larger disagreement for Fan 1:1. As seen in Figure 4-5 and Figure 4-6 these figures indicate that few of the grouting boreholes are actually intersecting the extrapolated structure. The tunnel mapping indicates another possible explanation since a trace of a conductive fracture is seen in the roof of the tunnel at this location. This fracture could possibly be intersected by few of the grouting boreholes or the probe boreholes only.

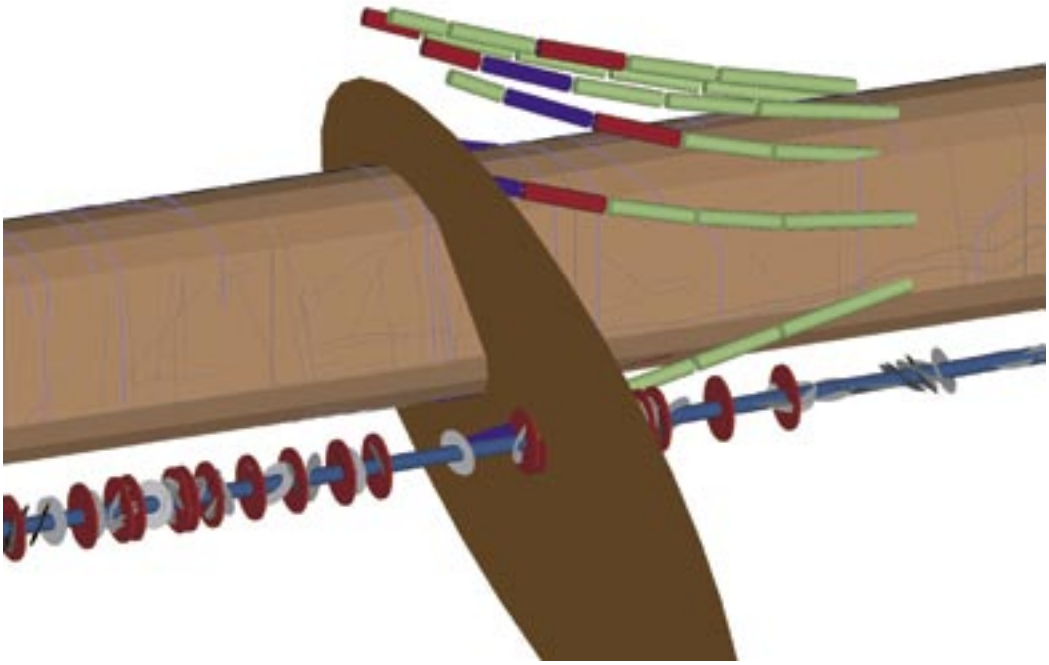

Figure 4-5. *Description 3: compilation of data from core borehole KA3376B01, grouting boreholes for Fan 1:1. Included is also data from the tunnel mapping where conductive fractures are presented in blue. Red discs along the core borehole indicate locations of conductive features based on Posiva Flow Log. Grey discs show strike and dip of natural fractures. The blue cylinders along the probe boreholes represent a section (generally 3 m) having an inflow during drilling which is >2 L/min (red: largest inflow and green: <2 L/min). The brown disc shown in the figure represents inflow no 9 along the core borehole and is given the strike and dip of the fracture found closest to the location of inflow (from BIPS and core logging). Only grouting boreholes having a section inflow >2 L/min are included.*

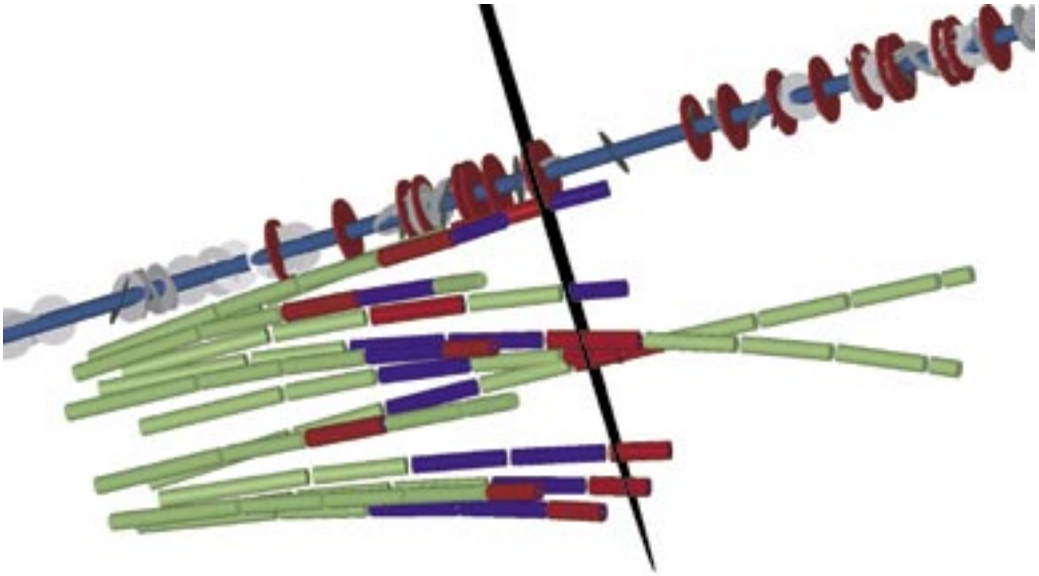

Figure 4-6. *Description 3: compilation of data from core borehole KA3376B01, probe boreholes SQ0049B, SQ0049C and grouting boreholes for Fan 1:1. Red discs along the core borehole indicate locations of conductive features based on Posiva Flow Log. Grey discs show strike and dip of natural fractures. The blue cylinders along the probe boreholes represent a section (generally 3 m) having an inflow during drilling which is >2 L/min (red: largest inflow and green: <2 L/min). The image is seen from above and rotated so that the possible fracture of inflow no 9 is seen in parallel in order to be able to identify all intersections.*

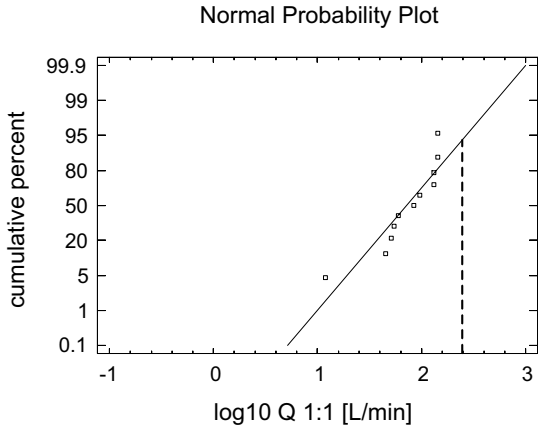

Figure 4-7. *Normal probability plot (log10 Q) of total inflow of grouting boreholes, Fan 1:1, and inflow estimated from the transmissivities (pressure build-up tests) of probe boreholes SQ0049B and SQ0049C (dashed line). T(SQ0049B and SQ0049C): 1.3E–5 m²/s. T≈Q/dh, dh:343, Q≈1.3E–5 m²/s*343m*60s*1000 L≈267.5 L/min, log10 Q≈2.4.*

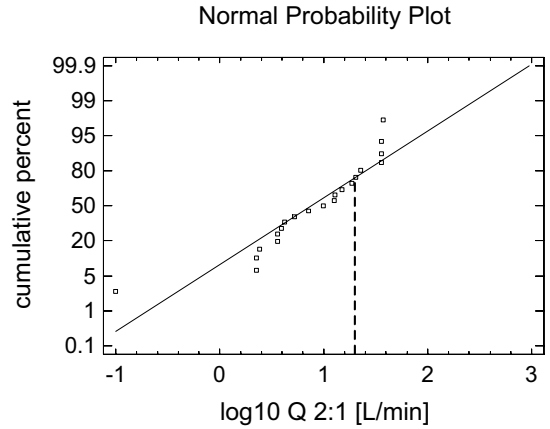

Figure 4-8. *Normal probability plot (log10 Q) of total inflow of grouting boreholes, Fan 2:1 and inflow estimated from the transmissivity (pressure build-up test) of probe borehole SQ0059 G15 (dashed line). T(SQ0059 G15): 1.1E–6 m²/s. T≈Q/dh, dh:343, Q≈1.1E–6 m²/s*343m*60s*1000 L≈22.6 L/min, log10 Q≈1.35.*

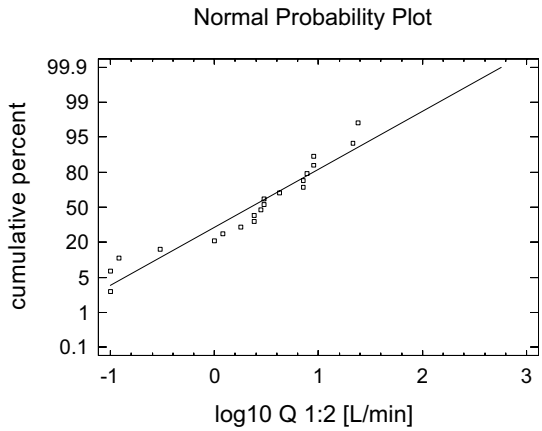

Figure 4-9. *Normal probability plot (log10 Q) of total inflow of grouting boreholes, Fan 1:2.*

The assumption of a total inflow to a borehole being a "good-enough" approximation of a section or fracture inflow is partly analysed and presented in frequency histograms in Figure 3-9, Figure 3-10 and Figure 3-11. All figures show that at least 40–50%, but commonly a larger fraction of the total inflow originates from one section of the borehole. Further, Table 4-2 shows that the median specific capacity and median hydraulic apertures based on total inflows, Qtot and the sections with maximum inflows, Qtot give fairly small differences. Using maximum section inflow will however underestimate the fraction of low inflows. Fan 1:2 has the largest fraction of boreholes with inflow <2 L/min, which may be explained by the sealing resulting from grouting of Fan 1:1.

To describe possible fractures intersecting the tunnel, Table 4-3 is based on the assumption that the grouting boreholes are parallel and fractures are perpendicular to the tunnel. For Table 4-4 grouting borehole data and the fractures are extrapolated from the core borehole compiling data in RVS. The tables presents median inflow, fraction of the intersecting boreholes with inflow <2 L/min, estimated median specific capacity and median hydraulic apertures. Inflows in sections 7.6–10.6m (Fan 1), 10.6–13.6m (Fan 1), 13.6–15.6m (Fan 1) in Table 4-3 corresponds well to inflows no 4, 8 and 9 in Table 4-4. For Fan 2, data from section inflows and extrapolated fractures cannot be that easily linked. For Table 4-4, only 5 of the 11 boreholes intersect the fracture based on inflow no 9.

To further evaluate the assumption that total inflow to a borehole is a "good-enough" approximation of a section or fracture inflow, the median hydraulic aperture, 187 µm, based on full length inflows Qtot for Fan 1:1 could be compared to the corresponding median hydraulic aperture for maximum section inflows (not considering orientation of boreholes and fractures) Qmax, 177 µm (Table 4-2) and the median hydraulic apertures, 148 µm and 150 µm, for the fracture based on section 13.6–15.6m (Fan 1, Table 4-3) and inflow no 9 (Table 4-4). If an acceptable design and prognosis could be made based on total inflow, section measurements may not be necessary. The smaller median apertures for inflows into sections 7.6–10.6m (Fan 1), 10.6–13.6m (Fan 1) or inflows no 4 and 8 are possibly what needed to be sealed by Fan 1:2.

Description 3 as well as Descriptions 1 and 2 show an increase in inflow at approximately 46–49 m, with the largest increase in the vicinity of the extrapolated fracture no 9. Focusing on conductive features based on natural inflow exceeding 2 L/min and extrapolating strike and dip of these features have been useful and consistent throughout the field test giving similar descriptions, particularly concerning expected positions for larger inflows.

Table 4-2. Fan number, median inflow, fraction of boreholes with inflow <2 L/min, median specific capacity and median hydraulic apertures based on total inflow, Qtot and section with maximum inflow, Qmax. Inflow data are presented in Appendix H.

Fan		Median inflow [L/min]	Fraction of boreholes with inflow <2 L/min	Median specific capacity [m²/s]	Median hydraulic aperture [µm]
1:1	Qtot:	84	0/11=0	4.1E–6	187
	Qmax	72		3.5E–6	177
1:2	Qtot:	2.9	7/20=0.35	1.4E–7	61
	Qmax	1.8		8.7E–8	52*
2:1	Qtot:	9.9	1/21=0.05	4.8E–7	91
	Qmax	6.6		3.2E–7	80

*16 of 20 boreholes had section measurements

Table 4-3. Grouting borehole data: Sections along grouting boreholes, fraction of boreholes with inflow <2 L/min, estimated median specific capacity and median hydraulic apertures. Sections and corresponding inflows are presented in Appendix H.

Sections along grouting boreholes	Median inflow [L/min] >2 L/min	Fraction of boreholes with inflow <2 L/min	Median specific capacity [m^2/s]	Median hydraulic aperture [μm]
7.6–10.6m (Fan 1)	5	0.45	2.4E–7	73
10.6–13.6m (Fan 1)	5	0.36	2.4E–7	73
13.6–15.6m (Fan 1)	42	0.18	2.0E–6	148
16.6–18m (Fan 2)	1.8	0.52	8.7E–8	51

Table 4-4 Grouting borehole data: inflow number and location of fracture along core borehole, fraction of boreholes with inflow <2 L/min, estimated median specific capacity and median hydraulic apertures. Intersected grouting boreholes, sections and corresponding inflows are presented in Appendix L.

Inflow no/location of fracture (BIPS, core borehole)	Median inflow [L/min]	Fraction of boreholes with inflow <2 L/min	Median specific capacity [m^2/s]	Median hydraulic aperture [μm]
4/47.66 m (Fan 1)	5	0.45	2.4E–7	73
8/50.42 m (Fan 1)	5	0.36	2.4E–7	73
9/51.78 m (Fan 1)	44	5 of 11 intersected	2.1E–6	150
11/57.0 m (Fan 2)	0	0.9	0	0
12 / 58.09 m (Fan 2)	0.25	0.67	1.2E–8	27
19/65.48 m (Fan 2)	0	0.76	0	0

4.1.2 Grouting design and prediction of result

Based on the descriptions of the fractures, prediction of result and choice of design was made.

The spread of grout in the fractures depends on several aspects relating to the properties of the grout, the fracture geometry and the technique. In /Eriksson, 2002/, a modelling approach was presented to facilitate prediction of grout spread and sealing effect for design of grouting works and this approach was used in this study.

In Section 3 in this report the predicted results of grout take, grouting time and sealing effect were presented based on estimations of fracture properties from inflow in the boreholes. Calculations were first made based on the inflow in the core drilled investigation hole, secondly with information from the probe holes and finally with information about inflow in the grouting holes.

As discussed in the previous section, it was found that the inflow was largely affected by the local aperture and that large variations in inflow appeared. This was especially obvious after the drilling of probe holes for the first fan where large quantities of water appeared.

The grouting design was based on the description obtained from analysis of the core drilled investigation hole. The information from this hole indicated that both Fan 1 and Fan 2 would consist of small aperture sized fractures. For instance, in Fan 1, the first estimation of the fractures was that the apertures would be limited to around 100 μm. Apertures in the vicinity of 100 μm and smaller requires, according to /Eriksson, 2002/, special technique for a good grouting result. Therefore, a design suitable for grouting this situation was presented.

After drilling the probe holes it was found that some of the fractures had an aperture larger than 100 µm. This information gave reason to re-evaluate the design for the grouting of Fan 1. It was found that using the initial design would mean that considerable grouting volumes and grouting time would be required. An alternative design with two rounds was found to facilitate an equally good sealing result but with use of much smaller volumes of grout. Based on this finding the grouting design was changed. It is concluded that the information obtained concerning the fracture properties and the calculations made, could motivate a change in design. In Fan 1:2 and Fan 2 the expected situation was encountered and change of designs was therefore not needed.

Generally the calculations predicted much smaller volumes of grout to be used than the outcome. The grouting time was also poorly predicted with the calculations. However, the sealing effect from the grouting was well predicted in the calculations.

Based on the work with design and prediction of grouting result that was carried out based on the initial characterisation, some conclusions can be drawn.

- It is found that the early description of fracture properties based on the core drilled hole was valuable in that an early design could be prepared.
- The information obtained from the probe holes could confirm or reject the expected situation and the design.
- It is found that the predicted volumes were considerably smaller than the obtained.
- It is found that the predicted grouting times were deviating from the obtained, but not as systematically as the grouting volumes.
- The calculated sealing effects were very close to the obtained in Fan 1:1 and Fan 2. In Fan 1:2 a moderate difference was seen.

The general conclusion is that the calculations, despite inaccurate results regarding some aspects, were valuable for development of different designs and for objective evaluations.

For further optimisation of grouting design, there may be reasons to try to increase the accuracy in the calculations.

In general there may also be several reasons for a low accuracy in the prediction of grout take and time. For instance

- Model inaccuracy.
- Inadequate description of the rock.
- Real grout properties not in accordance with properties used in the calculations.
- Real pressures not in accordance with pressures used in the calculations.
- Bad interpretation of fracture geometry.
- Poorly filled investigation hole and probe holes.
- Deformation of the rock when grouting.

Among these, the interpretation of fracture geometry is earlier recognised as a problematic area. The interpretation of fracture geometry was made using the expression presented by /Zimmerman and Bodvarsson, 1996/, see Equation 2-5. This expression is useful since it defines a physical aperture based on a hydraulic aperture. The expression gives a relation of around 1.5–1.8 of physical to hydraulic aperture depending on the

particular case. This is considerably less compared to relations given by several other authors and it may therefore be questioned if the use of Equation 2-5 was suitable in this situation. For instance, /Janson, 1998/ found in laboratory tests the grout take to be more sensitive than the hydraulic aperture to variations in physical aperture. In the laboratory test the prediction of penetration length of the grout was successful but the grouted volume was underestimated the due to the unnoticed porosity. In /Winberg et al, 2000/, the total porosity was concluded to be around 10–30 times the volume obtained from the hydraulic aperture. The current study lacked in accuracy in prediction of grouting volume and time, which in agreement with the references above, indicates the importance of an adequate fracture interpretation.

4.2 What was achieved

One of the aims with the grouting experiment was to investigate what can be achieved with the best available technology, material and knowledge under the current conditions, i.e. a relatively tight rock mass at great depth. As input to this question the result in this experiment, in terms of what was achieved, is valuable.

The experiment was in the first fan made with focus on sealing the rock mass as tight as possible. Still, it was made using regular equipment and commercial grouts. In the second fan, modifications in the design were made to speed up production since the work was behind schedule. These modifications were however limited and the same pressures and grouts as originally planned were used and thus a comparison between the results is possible.

The rock in the position of the first fan was initially more permeable than what may be considered tight rock. The rock mass conductivity (K) based on the flow in the bore holes was estimated to around $2.7 \cdot 10^{-7}$ m/s. Tight rock is by SKB considered to correspond to the conductivity $1 \cdot 10^{-8}$ m/s /Andersson et al, 2000/. The first of the two grouting rounds in Fan 1 aimed at lowering the conductivity by sealing the larger fractures with small volumes of grout under a low pressure. This strategy was successful and the sealing effect based on the reduction in inflow in the bore holes is evaluated to 97%, to a resulting conductivity of $9.5 \cdot 10^{-9}$ m/s. The conductivity is evaluated as the median bore hole specific capacity (used as estimate of fracture transmissivity) divided by the hole length, according to Equation 4-1. Practically, this grouting round was also successful. Only 11 grouting holes were used and the average grouting time around 18 minutes per hole.

$$K = \frac{T}{L} \cong \frac{\hat{Q}}{dh} / L \qquad \text{(Equation 4-1)}$$

In the second round of grouting in Fan 1 the aim was a final sealing of the rock using a design optimised for tight rock. In this case a larger number of grouting holes (20 holes) and a low flow criterion were used. The result of the grouting was successful, another 97% sealing effect and a resulting conductivity of $3.3 \cdot 10^{-10}$ m/s was achieved. From a resource point of view this grouting round was time consuming and required a mean grouting time of 42 minutes per hole.

The second fan was, as mentioned before, somewhat modified to speed up production. It was expected that this grouting should not result in a result as good as in Fan 1, but that still a good sealing result would be obtained. The grouting of Fan 2 resulted in a sealing effect of around 95% and a conductivity of around $1.9 \cdot 10^{-9}$ m/s. This was achieved with a mean grouting time per hole of around 24 minutes.

Figure 4-10 shows the conductivity in the rock mass of the two fans before and after grouting.

A measurement of the resulting inflow over the 20 m tunnel that was grouted gives an estimated inflow of 1 l/min. Using Equation 4-2 /Thiem, 1906/ and assuming that $[\ln R_0/r_w+\zeta]/2\pi$ can be approximated with 1, the conductivity over this part of the tunnel is around $2.5\cdot10^{-9}$ m/s. Based on the investigations in the bore holes it is reasonable that this inflow emanates from the second fan where approximately the same conductivity was found.

$$K = \frac{Q \cdot \left(\ln \frac{R_0}{r_t} + \xi \right)}{hL2\pi} \cong \frac{Q}{hL} \qquad \text{(Equation 4-2)}$$

4.3 Practical aspects

In this section some practical aspects of the work will be discussed. The content of the section mainly emanates from a meeting held after the completion of the work with most of the involved persons participating.

It should be noted that this section both discuss practical aspects on the research part of the work and the production part of the work. These are not easily separated in the project.

One aspect of the work was that the extent of measurements was considerable. Measurements were both performed to characterise the rock mass and for control of grout properties.

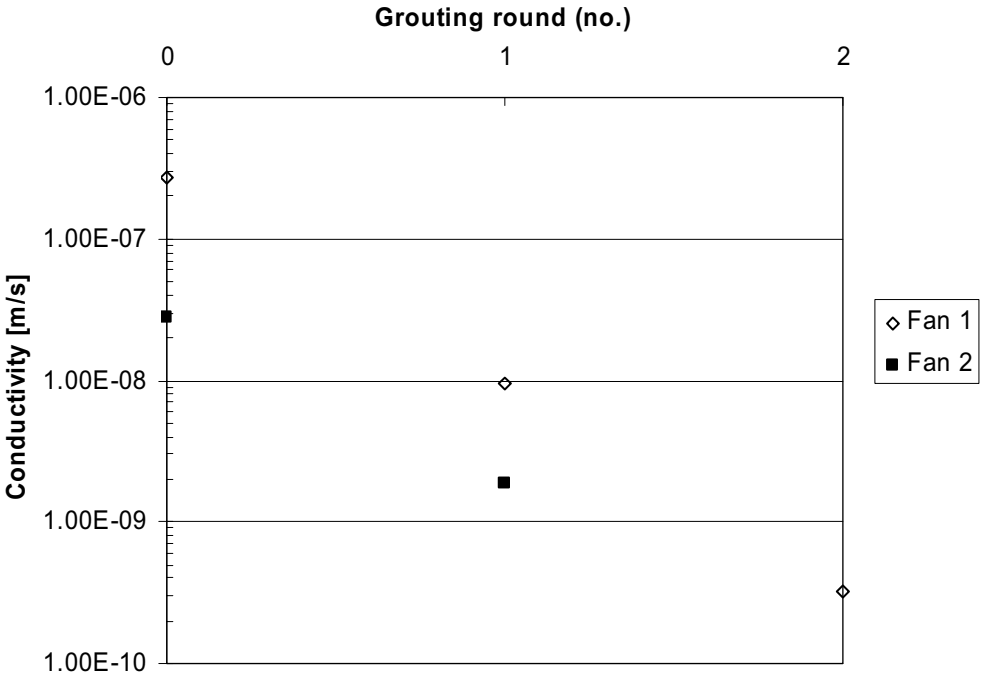

Figure 4-10. *Evaluated conductivity in Fan 1 and 2 before and after grouting. Grouting round no 0 refers to the measured inflow in the grouting holes before grouting. Grouting no 1 refers to the measured inflow in the grouting holes for Fan 1:2 and the control holes for Fan 2. Grouting round no 3 refers to the measured inflow in the control holes in Fan 1.*

The measurements were both part of the research program and part of the methodology, i.e. part of the actual production.

From a production point of view it was considered a burden to do the measurements. Measurements for the characterisation program were practically in conflict with the predominant desire to advance the tunnel front. It was disturbing since it was

- time consuming to stabilise pressure for the pressure build up tests,
- time consuming to measure inflow every third meter during drilling and difficult to put the drill in position again,
- difficult to measure small leakages in the inflow measurement.

It was also found that

- one person extra would be required to take minutes of measured values.

However, it was for instance noticed that some special devices for the measurements, for instance a funnel that facilitate measurement of inflow with the drill in the hole, could easily have been developed.

Measurements of grout properties were in the same way time consuming for the production since the grouting was not allowed to start before the grout was accepted. The measurements as such were easily performed. It was considered that if the grouting could start before the measurements were finished, they would not be time consuming. Also, it was found that regular personal could manage to do the measurements without additional help.

The experience was also that it was practically difficult to seal investigation, probe and grouting holes. The investigation hole and the probe holes would have required special techniques to be adequately sealed before grouting. In this case an input to the problem was that the research program did not want any grout spread from the sealing of these holes but that all sealing should be done in the grouting operation. Concerning the grouting holes it was found difficult to seal the boreholes when the grouting was finished with a high w/c grout with bleed. In these cases it would be valuable to exchange the grout to a low w/c grout in the borehole.

The grouting operation was considered overall adequate but it was difficult to grout with the low flow required by the design and it was questioned whether the pumping equipment was suitable for such a low flow. Further, the time-aspect of the low flow-criterion was annoying. The grouting in Fan 1:2 was experienced extra long but was complicated since only a single shift of personnel was used, i.e. the fan could not be finished in one sequence.

Overall, the grouting methodology, i.e. the whole process, was considered to be functional but the measurements were extensive. Special equipment was required due to the high pressure situation working several hundreds of meters below the water table.

In the project several other issues were important, for instance communication. The grouting aspects were discussed with the work force in a meeting prior to the performance and this was experienced as valuable by all involved. During operations, there were also a number of suggestions and questions to be answered concerning the execution that were not covered by the technical descriptions. One example was grouting order considering connected holes and other recently acquired experiences and observations. If more grouting should have been done, follow up meetings would have been valuable for motivation and communication.

5 Conclusions and suggestions

Conclusions regarding the hydrogeological characterisation are related to the assumptions and hypotheses presented in Table 2-3. Based on this field study the following is concluded for the characterisation.

Descriptions 1–3 all identify the same locations along the core borehole for the first larger inflow (>2 L/min) at approximately 46–49 m and the largest inflow at approximately 50–55 m. This is true both for the simpler description not considering orientation of boreholes and fractures and for the description based on the RVS-compilations (Rock Visualisation System). All major inflows identified by probe boreholes are intersected by extrapolated structures from the core borehole except for the inner conductive section of the probe borehole in Fan 2, which might be outside the main investigated area. The agreement between data from boreholes and tunnel mapping after excavation is also good (see Appendix K). Further, detailed testing using Posiva Flow Log (test section: L: 1 m, moved in steps with step length dL: 0.1 m) and inflow during drilling (generally 3 m sections) results in similar distributions of inflow. This indicates that there are few conductive fractures.

- Focusing on conductive features based on natural inflow exceeding 2 L/min and extrapolating strike and dip of these features have been useful and consistent throughout the field test giving similar descriptions, particularly on where the larger inflows can be expected.
- Using cement-based grouts and being under the prevailing pressure we were focusing on sealing fractures larger than 50 µm, i.e. fractures with inflows larger than 2 L/min. Therefore, for this test site, the 3 m section measurements gave both valuable and useful information.

Possible reasons for the large variation in inflows from the core- and probe boreholes ("local" properties of inflow number 9: 11 L/min, and probe boreholes SQ0049C and SQ0049B: 150 and 180 L/min) may be that the core and probe boreholes are not intersecting the same fracture or that the fracture has comparatively small apertures in the vicinity of the core borehole. The large transmissivity ("global" properties) of the core borehole (Inflow: 80 L/min and T:1.5E–5 m^2/s) indicates that the latter could be the explanation. Assuming that T=1.5E–5 ≈Q/dh and dh 340 m, the inflow, Q, would be approximately 300 L/min. Both probe boreholes above have the transmissivity T:1.3E–5 m^2/s, which is in better agreement with their total borehole inflows during drilling of 300 and 150 L/min respectively (if T≈Q/dh and dh 340 m, inflow, Q is approximately 270 L/min). Also when comparing inflow based on transmissivity of the probe boreholes to inflows of grouting boreholes, probe boreholes SQ0049C and SQ0049B have larger inflows than all boreholes in the corresponding Fan 1. For probe borehole SQ0059_G15 investigating the area of Fan 2, the inflow is within the interval even though a complete match to the median value is not found. The probe boreholes being longer than the grouting boreholes may explain the larger disagreement for Fan 1:1.

- The above confirm the usefulness of transient, time-dependent tests and shows that only local, assumed steady-state testing in one or few boreholes may not be enough to be properly prepared. Further, the median specific capacity seems to give an idea about the cross-fracture transmissivity.

The assumption of a total inflow of a borehole being a “good-enough” approximation of a section or fracture inflow is partly analysed and presented in frequency histograms showing that at least 40–50%, but commonly a larger fraction of the total inflow at this site originates from one section (generally 3 m) of the grouting boreholes. For this field study, borehole data from all boreholes within a grouting fan have also been presented in terms of: (1) full length inflows; (2) maximum section inflows (not considering orientation of boreholes and fractures) and (3) section inflows (assuming that boreholes are parallel with several perpendicular fractures). For Fan 1:1, the median of full-length inflows (1) is 84 L/min (187 µm), the median for maximum section inflows (2) is 72 L/min (177 µm) and the largest median section inflow (Fan 1:1, section 13.6–15.6 m) (3) is 42 L/min (148 µm). For the extrapolated fracture no 9, the median inflow is 44 L/min (150 µm).

- If the differences between section and full-length inflows for a particular site are acceptable considering e.g. a maximum inflow criterion or needed detail in grouting design, full-length tests could be used for design and predictions. However for a design having to consider fractures with small apertures and inflows, a detailed investigation is useful.

It is also concluded that the theoretical description of the grouting has been valuable as a design approach. Different alternative approaches for the grouting could be evaluated with the calculation tool and motivate choice of design. The accuracy in the prediction of grout take and grouting time lacks in some cases and is more accurate in some. The calculated sealing effect was however found acceptably accurate, giving reasons to suggest using calculations as a means to design grouting method.

A further evaluation of possible explanations for the deviation between calculated and measured grout take is found important. The most important work is judged to be further development of the interpretation of fracture geometries and of the modelling approach. To further evaluate the result, some tasks appear as especially interesting:

- Core drill and possibly measure grouted apertures in the fractures.
- Back calculate for different apertures and see if fitting values can be found.
- It is concluded that the result of the grouting operation is a more or less completely dry part of the tunnel. From the evaluation based on the boreholes the sealing effect in the first fan is 99.9 % and in the second fan 95%. Based on the inflow in the control hole the resulting conductivity in Fan 1 is $3.3 \cdot 10^{-10}$ m/s and 1.9 10^{-9} m/s in Fan 2. After the construction of the tunnel an inflow of approximately 1 l/min is noticed over the grouted tunnel part, estimated to $2.5 \cdot 10^{-9}$ m/s. Based on the control holes for the two grouting fans, it was found that the conductivity in the first fan was approximately 1/10 of the second. Theoretically, the inflow thus mainly emanates from the second fan.

It is found that conductivities considerably lower than “rule of thumbs” or commonly mentioned limits for cement grouting can be achieved with a proper design, execution and workmanship. In this particular case some main aspects is considered to be

- The quality of the mixed grout.
- The low refusal criterion.
- The practical execution with a proper mixing and quality control of the grout.

The last point is mentioned since it is considered important with a good organisation, capable of communicating important issues to the workmanship. If the execution of the work lacks, the result will not be successful.

References

Andersson J, Ström A, Svemar C, Almén K-E, Ericsson LO, 2000. Vilka krav ställer djupförvaret på berget? Geovetenskapliga lämplighetsindikatorer och kriterier för lokalisering och platsutvärdering. SKB R-00-15, Svensk Kärnbränslehantering AB. (In Swedish).

Barton N, Bandis S, Bakhtar K, 1985. Strength, deformation and conductivity coupling of rock joints. International Journal of Rock Mechanics & Mining Sciences, Geomechanical Abstracts 22(3), pp 121 –140.

Carlsson L, Gustafson G, 1991. Provpumpning som geohydrologisk undersöknings-metodik Application of pumping test analysis for geohydrological investigations. R66:1991, Byggforskningsrådet, Stockholm. (In Swedish).

Carlsten C, Stråhle A, 2000. Borehole radar and BIPS investigations in boreholes at the Boda area. TR-01-02, Swedish Nuclear Fuel and Waste Management Co.

Carlsten C, Stråhle A, Ludvigson J-E, 2001. Conductive fracture mapping, A study on the correlation between borehole-TV and radar images and difference flow logging results in borehole KLX02. R-01-48.

Chen Z, Narayan SP, Yang Z, Rahman SS, 2000. An Experimental Investigation of Hydraulic Behaviour of Fractures and Joints in Granitic Rock. International Journal of Rock Mechanics & Mining Sciences 37, pp 1061–1071.

Cooper HH, Jacob CE, 1946. A generalized graphical method for evaluating formation constants and summarizing well-field history. American geophysical union transactions 27, pp 256–534.

Doe TW, Geier JE, 1990. Stripa project, Interpretation of Fracture System Geometry Using Well Test Data. Technical Report 91-03, Swedish Nuclear Fuel and Waste Management Co.

Eriksson M, Dalmalm T, Brantberger M, Stille H, 1999. Separations- och filtrerings-stabilitet hos cementbaserade injekteringsmedel: En litteratur- och laborationsstudie. Rapport 3065. Division of Soil and Rock Mechanics, Department of Civil and Environmental Engineering, Royal Institute of Technology, Stockholm, Sweden. (In Swedish).

Eriksson M, 2002. Prediction of Grout Spread and Sealing Effect – A Probabilistic Method. Ph D Thesis, Division of Soil and Rock Mechanics, Royal Institute of Technology, Stockholm, Sweden.

Eriksson M, Stille H, 2003. A Method for Measuring and Evaluating the Penetrability of Grouts. Proc Grouting and Ground Treatment Conference, New Orleans 2003, pp 1326–1337.

Fransson Å, 1999. Grouting predictions based on hydraulic tests of short duration. Analytical, numerical and experimental approaches. Chalmers University of Technology, Department of Geology, Göteborg.

Fransson Å, 2001. Characterisation of a fractured rock mass for a grouting field test. Tunnelling and Underground Space Technology, Vol. 16, pp. 331–339.

Fransson Å, 2003. Äspö Pillar Stability Experiment Core boreholes KF0066A01, KF0069A01, KA3386A01 and KA3376B01: Hydrogeological characterisation and pressure responses during drilling and testing. International Progress Report, IPR-03-06. Svensk Kärnbränslehantering AB.

Friedrich M, Vorschulze C, 2002. Investigation of variations in rheology and penetrability of cement-based grout – with application on prediction of grouting works. Master Thesis 02/09, Division of Soil and Rock Mechanics, Royal Institute of Technology, Stockholm.

Gustafson G, 1986. Geohydrologiska förundersökningar i berg. Bakgrund – metodik – användning. BeFo 84:1/86, Stiftelsen Bergteknisk Forskning, Stockholm. (In Swedish).

Hakami E, 1995. Aperture Distribution of Rock Fractures. Ph D Thesis, Division of Engineering Geology, Royal Institute of Technology, Stockholm.

Håkansson U, 1993. Rheology of Fresh Cement-Based Grout. Doctoral Thesis Division of Soil and Rock Mechanics, Department of Civil and Environmental Engineering, Royal Institute of Technology, Stockholm.

Hässler L, 1991. Grouting of Rock – Simulation and Classification. Doctoral Thesis Division of Soil and Rock Mechanics, Department of Civil and Environmental Engineering, Royal Institute of Technology, Stockholm.

Janson T, 1998. Calculation Models for Estimation of Grout Take in Hard Jointed Rock. Doctoral Thesis 1018, Division of Soil and Rock Mechanics, Department of Civil and Environmental Engineering, Royal Institute of Technology, Stockholm.

Kutzner C, 1996.Grouting of rock and soil. AA Balkema, Rotterdam.

Lanaro F, 2001. Geometry, Mechanics and Transmissivity of Rock Fractures. Doctoral Thesis, Division of Engineering Geology, Department of Civil and Environmental Engineering, Royal Institute of Technology, Stockholm, Sweden.

de Marsily G, 1986. Quantitative Hydrogeology. Groundwater Hydrology for Engineers. Academic Press, Inc, San Diego.

Rouhiainen P, 2000. Äspö Hard Rock Laboratory Difference flow measurements in borehole KLX02 at Laxemar. International Progress Report IPR-01-06. Swedish Nuclear Fuel and Waste Management Co.

Thiem G, 1906. Hydrologische Metoden. Leipzig: Gebhardt.

Winberg A, Andersson P, Hermansson J, Byegård J, Cvetkovic V, Birgersson L, 2000. Final report of the first stage of the tracer retention understanding experiments. TR-00-07, SKB, Stockholm.

Zimmerman RW, Bodvardsson GS, 1996. Hydraulic conductivity of Rock Fractures. Transport in Porous Media, Vol. 23, pp 1–30.

Appendix A

References to data collected during investigation and production

Activity	Location/borehole	Date	Data
HMS	See HMS/SICADA	2003-04-01 – 2003-09-25	HMS Äspö, SICADA
Drilling (acc. inflow)	SQ0016B	2003-05-09, 14:50 – 2003-05-09, 15:26	Appendix F
Drilling (acc. inflow)	SQ0016C	2003-05-09, 17:28 – 2003-05-09, 18:09	Appendix F
Pressure build-up test	SQ0016B	2003-05-09, 19:45 – 2003-05-09, 20:45	Appendix E
Pressure build-up test	SQ0016C	2003-05-09, 21:45 – 2003-05-09, 22:45	Appendix E
Drilling (acc. inflow)	SQ0034C	2003-05-22, 09:15 – 2003-05-22, 09:43	Appendix F
Drilling (acc. inflow)	SQ0034B	2003-05-22, 11:41 – 2003-05-22, 12:08	Appendix F
Pressure build-up test	SQ0034C	2003-05-22, 16:43 – 2003-05-22, 17:43	Appendix E
Pressure build-up test	SQ0034B	2003-05-22, 18:43 – 2003-05-22, 19:43	Appendix E
Drilling (acc. inflow)	SQ0049B	2003-05-27, 12:15 – 2003-05-27, 13:08	Appendix F
Drilling (acc. inflow)	SQ0049C	2003-05-27, 15:30 – 2003-05-27, 16:18	Appendix F
Pressure build-up test	SQ0049B	2003-05-27, 18:21 – 2003-05-27, 19:21	Appendix E
Pressure build-up test	SQ0049C	2003-05-27, 20:51 – 2003-05-27, 21:51	Appendix E
Drilling (acc. inflow)	Fan no 1:1 (0049)	2003-06-02, 23:00 – 2003-06-03, 18:01	Appendix H
Water loss measurements	Fan no 1:1 (0049)	2003-06-03	Appendix B
Grouting	Fan no 1:1 (0049)	2003-06-03, 21:50 – 2003-06-04, 16:52	Appendix J
Drilling (acc. inflow)	Fan no 1:2 (0049)	2003-06-05, 14:52 – 2003-06-05, 21:59	Appendix H
Grouting	Fan no 1:2 (0049)	2003-06-10, 19:39 – 2003-06-13, 23:30	Appendix J
Drilling (acc. inflow)	Fan no 2 (0059)	2003-06-24, 15:40 – 2003-06-25, 17:02	Appendix H
Pressure build-up test	G15 (0059)	2003-06-24, 22:45 – 2003-06-24, 23:45	Appendix E
Grouting	Fan no 2 (0059)	2003-06-26, 12:49 – 2003-06-27, 00:44	Appendix J
Drilling (acc. inflow)	SQ0059 S_C1	2003-06-27, 20:00 – 2003-06-27, 20:35	Appendix F
Drilling (acc. inflow)	SQ0059 S_B2	2003-06-27, 20:07 – 2003-06-27, 21:07	Appendix F

Appendix B

Water loss measurements

Borehole no	Inflow natural (litre)	Borehole length (m)	Waterloss Length (m)	Time (min)	Final pressure (MPa)	Volume (L)	Flow, V/t (L/min)	Lugeon value
Percussion drilled probe boreholes								
2003-05-10								
SQ0016B	0.05	22.5	21.9	2	0.5	0.8	0.4	0.04
SQ0016C	0.09	22.5	21.8	2	0.5	0.42	0.2	0.02
2003-05-22								
SQ0034C	0.2	19	18.4	1	1.2	0	0	0
SQ0034B	1	19	18.4	1	0.9	0	0	0
Fan 1:1								
2003-06-03								
A1	7.2	15.6	15	1	0.5	11	11	1.5
A2	132	15.6	15	1	0.2	35	35	11.7
C3	45	15.6	15	1	0.15	28	28	12.5
H4	45	15.6	15	1	0.2	29	29	9.7
I5	132	15.6	15	1	0.15	45	45	20.0
D6	84	15.6	15	1	0.4	56	56	9.3
B7	144	15.6	15	1	0.2	52	52	17.3
B8	144	15.6	15	1	0.35	56	56	10.7
G9	60	15.6	15	1	0.65	40	40	4.1
G10	96	15.6	15	1	0.5	44	44	5.9
G11	60	15.6	15	1	0.65	42	42	4.3

No water loss measurements were performed for the other percussion drilled probe boreholes or grouting boreholes. Slight deviations are seen between these data and inflow measurements presented in Appendix F and Appendix H. This is due to different persons measuring and documenting the data.

Appendix C

Positions of probe holes, grouting holes and control holes

Probe holes SQ0049B and SQ0049C

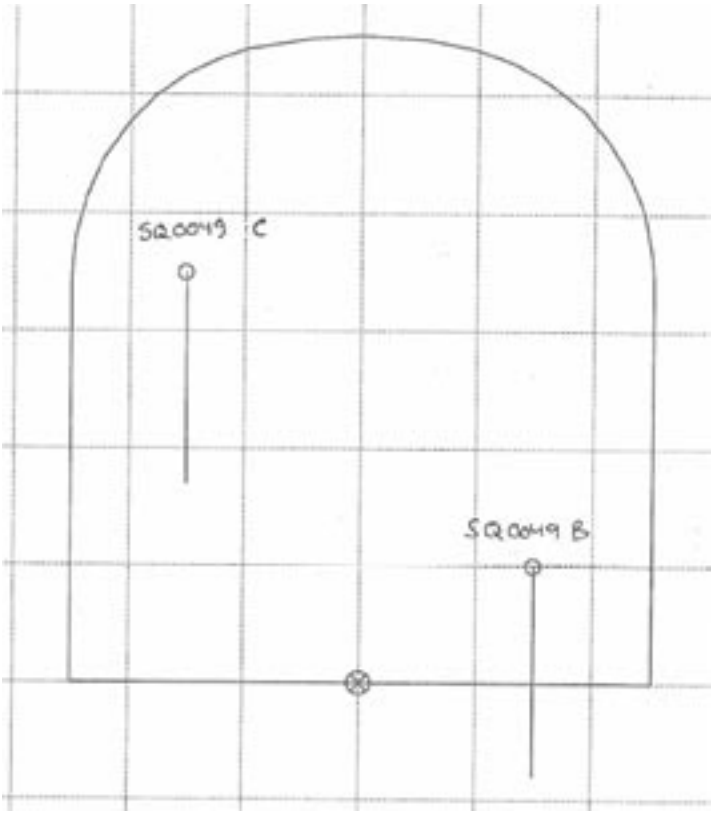

Grouting holes in Fan 1:1

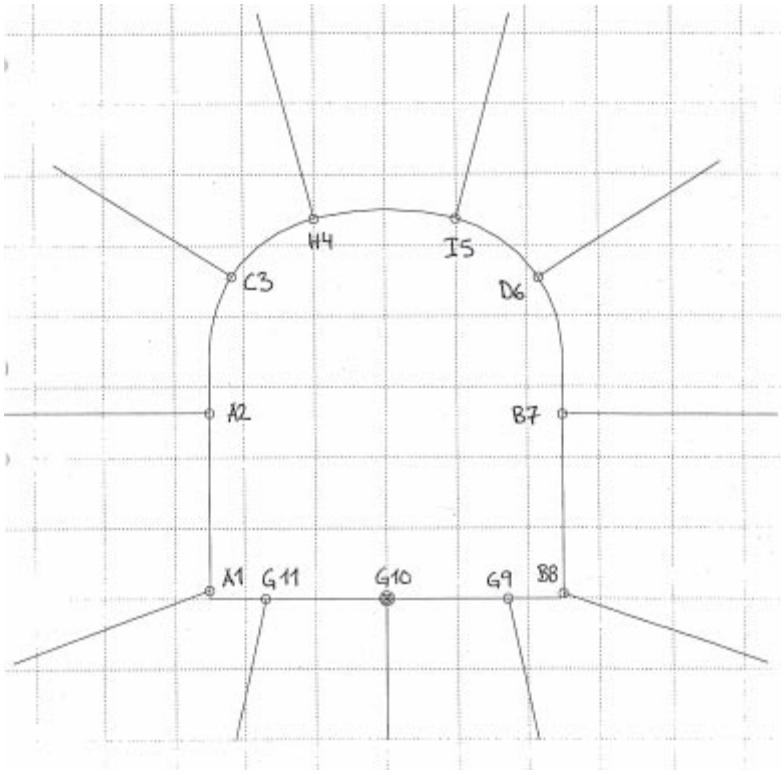

Grouting holes in Fan 1:2

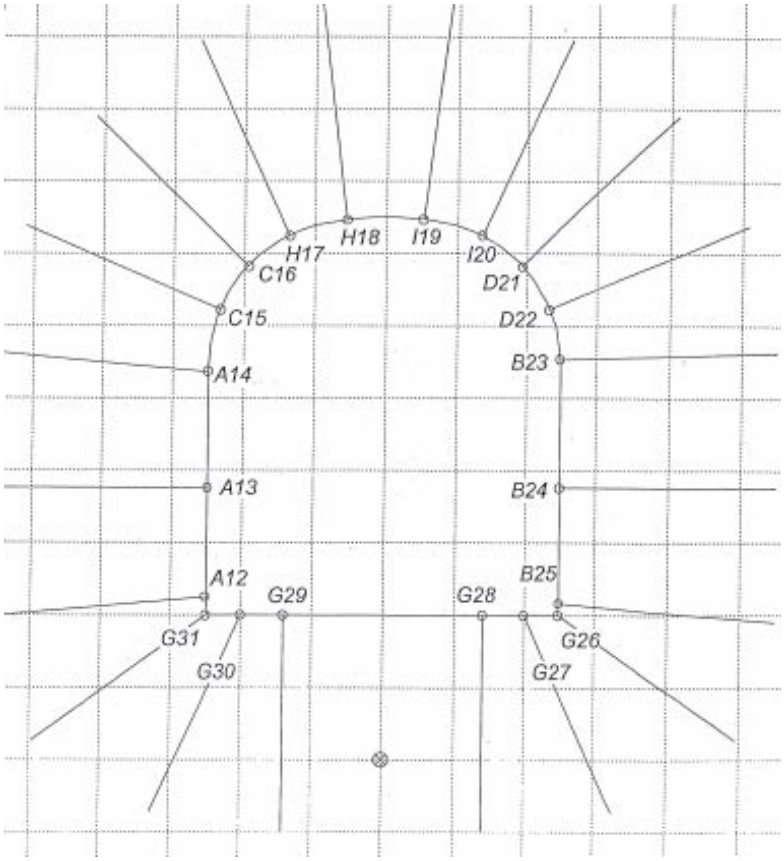

Grouting holes in Fan 2

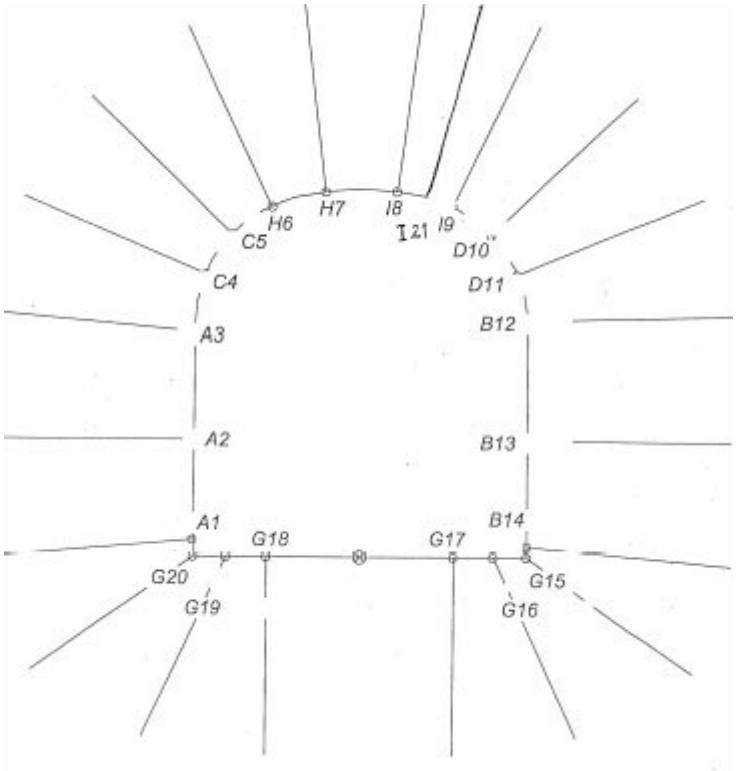

Position of control holes in Fan 1 and 2

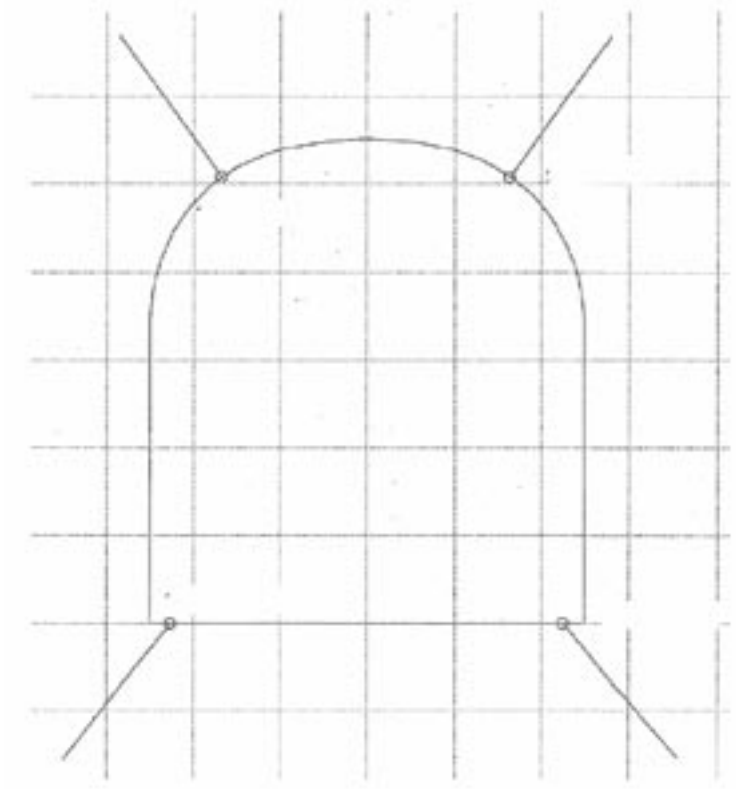

Compilation of orientation, location and inflows of natural fractures

Appendix D

Strike, dip and location of natural fractures along the core borehole (based on BIPS and core mapping) and inflows from Posiva Flow Log. Possible fractures with inflows >5 L/min (grey colour) and >2 L/min (black line). Natural fracture (inflow number 7) at 49.8 m is missing.

PFL No	Length (m)	Idcode	From Length (m)	To Length (m)	Variable	Fill 1	Fill 2	Fill 3	Fill 4	Roughness	Surface	Alteration	Strike (degrees)	Dip (degrees)	Width (mm)	Aperture (mm)	Confidence	Alpha (degrees)	Beta (degrees)	Calcomment
		KA3376B01	41.31	41.31	Natural Fracture	Calcite				Irregular	Rough	Slightly Altered	93.0	12.2	1.0	0.0	Certain	77.8	183.0	Dip/Strike Calculated
		KA3376B01	41.91	41.91	Natural Fracture	Calcite				Irregular	Rough	Slightly Altered	278.0	10.7	1.0	0.0	Certain	79.3	8.0	Dip/Strike Calculated
		KA3376B01	43.11	43.11	Natural Fracture	Chlorite				Irregular	Rough	Fresh	301.0	23.1	1.0	0.0	Certain	66.9	31.0	Dip/Strike Calculated
		KA3376B01	43.17	43.17	Natural Fracture	Calcite				Irregular	Rough	Moderately Altered	272.0	7.5	1.0	0.0	Probable	82.5	2.0	Dip/Strike Calculated
		KA3376B01	43.21	43.21	Natural Fracture	Calcite				Irregular	Rough	Moderately Altered	264.0	19.2	1.0	0.0	Certain	70.8	354.0	Dip/Strike Calculated
		KA3376B01	43.24	43.24	Natural Fracture	Calcite				Irregular	Rough	Moderately Altered	209.0	22.7	1.0	0.0	Certain	67.3	299.0	Dip/Strike Calculated
		KA3376B01	43.27	43.27	Natural Fracture	Calcite				Irregular	Rough	Moderately Altered	228.0	19.1	1.0	0.0	Certain	70.9	318.0	Dip/Strike Calculated
		KA3376B01	43.41	43.41	Natural Fracture	Calcite	Chlorite			Irregular	Rough	Moderately Altered	271.0	10.4	1.0	0.0	Probable	79.6	1.0	Dip/Strike Calculated
		KA3376B01	43.47	43.47	Natural Fracture	Calcite	Chlorite			Irregular	Rough	Moderately Altered	271.0	6.5	1.0	0.0	Probable	83.5	1.0	Dip/Strike Calculated
		KA3376B01	43.52	43.52	Natural Fracture	Calcite	Chlorite			Irregular	Rough	Slightly Altered	113.0	8.3	1.0	0.0	Probable	81.7	203.0	Dip/Strike Calculated
		KA3376B01	43.66	43.66	Natural Fracture	Calcite				Planar	Rough	Slightly Altered	279.0	2.0	1.0	0.0	Probable	88.0	9.0	Dip/Strike Calculated
		KA3376B01	43.95	43.95	Natural Fracture	Calcite				Undulating	Rough	Slightly Altered	89.0	4.5	1.0	0.0	Probable	85.5	179.0	Dip/Strike Calculated
		KA3376B01	43.96	43.96	Natural Fracture	Calcite				Undulating	Rough	Slightly Altered	89.0	3.6	1.0	0.0	Probable	86.4	179.0	Dip/Strike Calculated
		KA3376B01	47.19	47.19	Natural Fracture	Calcite	Chlorite			Planar	Rough	Slightly Altered	9.4	64.5	1.0	0.0	Certain	31.7	239.0	Dip/Strike Calculated
		KA3376B01	47.60	47.60	Natural Fracture	Chlorite	Calcite			Irregular	Rough	Moderately Altered	149.4	82.4	2.0	2.0	Certain	74.6	296.0	Dip/Strike Calculated
		KA3376B01	47.66	47.66	Natural Fracture	Chlorite	Calcite			Irregular	Rough	Highly Altered	138.0	82.7	1.0	1.0	Certain	83.1	339.0	Dip/Strike Calculated
4	47.7 m	KA3376B01	47.74	47.74	Natural Fracture	Chlorite	Calcite			Irregular	Rough	Moderately Altered	135.3	82.8	1.0	0.0	Certain	83.7	2.0	Dip/Strike Calculated
		KA3376B01	47.85	47.85	Natural Fracture	Chlorite	Calcite			Irregular	Rough	Moderately Altered	19.2	51.3	1.0	1.0	Certain	19.6	228.0	Dip/Strike Calculated
		KA3376B01	48.05	48.05	Natural Fracture	Chlorite				Irregular	Rough	Moderately Altered	316.3	75.6	1.0	0.0	Certain	74.7	183.0	Dip/Strike Calculated
		KA3376B01	48.09	48.09	Natural Fracture	Chlorite	Calcite			Irregular	Rough	Moderately Altered	299.7	74.5	1.0	0.0	Certain	67.4	137.0	Dip/Strike Calculated
5	48.2 m	KA3376B01	48.27	48.27	Natural Fracture	Chlorite	Calcite	Pyrite		Irregular	Rough	Moderately Altered	33.6	64.6	1.0	0.0	Certain	10.3	244.0	Dip/Strike Calculated
		KA3376B01	48.35	48.35	Natural Fracture	Chlorite	Calcite			Undulating	Rough	Moderately Altered	297.7	88.1	1.0	0.0	Certain	72.0	99.0	Dip/Strike Calculated
		KA3376B01	48.72	48.72	Natural Fracture	Chlorite	Calcite	Pyrite		Irregular	Rough	Moderately Altered	328.0	79.0	1.0	1.0	Certain	72.8	226.0	Dip/Strike Calculated
		KA3376B01	48.83	48.83	Natural Fracture	Chlorite	Calcite			Undulating	Rough	Moderately Altered	148.6	81.7	1.0	0.0	Certain	75.0	300.0	Dip/Strike Calculated
8	50.5 m	KA3376B01	50.42	50.42	Natural Fracture	Calcite	Chlorite			Undulating	Rough	Moderately Altered	125.7	85.8	1.0	1.0	Certain	79.7	71.0	Dip/Strike Calculated
		KA3376B01	51.20	51.20	Natural Fracture	Calcite	Chlorite			Undulating	Rough	Moderately Altered	132.4	79.6	2.0	1.0	Certain	80.0	18.0	Dip/Strike Calculated
		KA3376B01	51.69	51.69	Natural Fracture	Calcite				Irregular	Rough	Moderately Altered	129.6	69.3	2.0	2.0	Certain	69.4	16.0	Dip/Strike Calculated
9	51.8 m	KA3376B01	51.78	51.78	Natural Fracture	Calcite	Chlorite			Irregular	Rough	Moderately Altered	123.2	70.4	1.0	1.0	Certain	67.8	32.0	Dip/Strike Calculated
		KA3376B01	51.99	51.99	Natural Fracture	Chlorite	Calcite			Irregular	Rough	Slightly Altered	4.1	75.3	1.0	0.0	Certain	39.5	250.0	Dip/Strike Calculated
		KA3376B01	54.32	54.32	Natural Fracture	Chlorite	Calcite			Irregular	Rough	Slightly Altered	105.4	80.5	1.0	0.0	Certain	58.8	73.0	Dip/Strike Calculated
		KA3376B01	56.92	56.92	Natural Fracture	Calcite	Chlorite			Undulating	Rough	Moderately Altered	136.5	82.8	2.0	2.0	Certain	83.7	0.0	Dip/Strike Calculated
11	57.0 m	KA3376B01	57.00	57.00	Natural Fracture	Calcite	Chlorite			Undulating	Rough	Moderately Altered	130.7	78.4	1.0	1.0	Certain	78.3	24.0	Dip/Strike Calculated
		KA3376B01	57.87	57.87	Natural Fracture	Calcite	Chlorite			Irregular	Rough	Slightly Altered	109.3	67.9	1.0	0.0	Certain	63.8	87.0	Dip/Strike Calculated
12	58.2 m	KA3376B01	58.09	58.09	Natural Fracture	Calcite	Chlorite			Irregular	Rough	Moderately Altered	135.5	65.7	2.0	2.0	Certain	66.6	0.0	Dip/Strike Calculated
		KA3376B01	59.14	59.14	Natural Fracture	Calcite				Irregular	Rough	Slightly Altered	169.7	89.3	1.0	0.0	Certain	55.8	270.0	Dip/Strike Calculated
		KA3376B01	59.66	59.66	Natural Fracture	Calcite	Chlorite			Undulating	Rough	Moderately Altered	149.7	63.6	1.0	0.0	Certain	61.1	333.0	Dip/Strike Calculated
		KA3376B01	59.69	59.69	Natural Fracture	Chlorite	Calcite			Undulating	Rough	Moderately Altered	163.5	77.8	1.0	1.0	Certain	68.9	303.0	Dip/Strike Calculated
		KA3376B01	60.42	60.42	Natural Fracture	Chlorite				Irregular	Rough	Slightly Altered	292.1	48.7	1.0	0.0	Certain	42.8	156.0	Dip/Strike Calculated
		KA3376B01	61.67	61.67	Natural Fracture	Chlorite	Calcite			Planar	Rough	Moderately Altered	134.5	85.3	1.0	1.0	Certain	86.1	15.0	Dip/Strike Calculated
		KA3376B01	61.10	61.10	Natural Fracture	Chlorite	Calcite			Irregular	Rough	Moderately Altered	124.6	76.0	1.0	0.0	Certain	73.0	39.0	Dip/Strike Calculated
		KA3376B01	62.23	62.23	Natural Fracture	Chlorite	Calcite			Undulating	Rough	Moderately Altered	116.0	74.6	1.0	0.0	Certain	65.9	52.0	Dip/Strike Calculated
		KA3376B01	62.36	62.36	Natural Fracture	Calcite	Chlorite			Undulating	Rough	Moderately Altered	316.8	83.3	1.0	0.0	Certain	82.3	190.0	Dip/Strike Calculated
		KA3376B01	62.60	62.60	Natural Fracture	Chlorite	Epidote	Calcite		Planar	Rough	Moderately Altered	313.5	82.1	1.0	0.0	Certain	81.0	167.0	Dip/Strike Calculated
		KA3376B01	62.67	62.67	Natural Fracture	Chlorite				Undulating	Rough	Moderately Altered	313.3	80.4	1.0	0.0	Certain	79.3	168.0	Dip/Strike Calculated
		KA3376B01	63.20	63.20	Natural Fracture	Epidote				Planar	Rough	Moderately Altered	355.8	45.5	1.0	0.0	Certain	32.2	213.0	Dip/Strike Calculated
		KA3376B01	63.23	63.23	Natural Fracture	Calcite	Chlorite			Irregular	Rough	Moderately Altered	321.6	56.8	1.0	1.0	Certain	55.4	189.0	Dip/Strike Calculated
		KA3376B01	63.25	63.25	Natural Fracture	Calcite				Irregular	Rough	Moderately Altered	311.1	49.3	1.0	1.0	Certain	48.2	175.0	Dip/Strike Calculated
		KA3376B01	63.47	63.47	Natural Fracture	Epidote	Calcite	Chlorite		Irregular	Rough	Moderately Altered	135.5	81.5	2.0	0.0	Certain	82.4	0.0	Dip/Strike Calculated
		KA3376B01	63.51	63.51	Natural Fracture	Calcite	Chlorite			Undulating	Rough	Moderately Altered	136.1	77.5	1.0	0.0	Certain	78.4	357.0	Dip/Strike Calculated
		KA3376B01	63.54	63.54	Natural Fracture	Chlorite	Calcite			Undulating	Rough	Moderately Altered	317.5	88.2	1.0	0.0	Certain	86.6	217.0	Dip/Strike Calculated
		KA3376B01	63.61	63.61	Natural Fracture	Chlorite				Undulating	Rough	Moderately Altered	353.0	70.6	1.0	0.0	Certain	48.0	239.0	Dip/Strike Calculated
		KA3376B01	63.64	63.64	Natural Fracture	Chlorite	Calcite			Irregular	Rough	Moderately Altered	349.7	86.8	1.0	0.0	Certain	55.6	263.0	Dip/Strike Calculated
		KA3376B01	63.75	63.75	Natural Fracture	Chlorite	Calcite			Irregular	Rough	Moderately Altered	357.1	79.9	1.0	0.0	Certain	47.2	254.0	Dip/Strike Calculated
		KA3376B01	63.76	63.76	Natural Fracture	Chlorite	Calcite			Irregular	Rough	Moderately Altered	107.3	80.5	1.0	0.0	Certain	60.7	72.0	Dip/Strike Calculated
		KA3376B01	63.79	63.79	Natural Fracture	Chlorite	Calcite			Irregular	Rough	Moderately Altered	123.2	71.7	2.0	0.0	Certain	68.8	34.0	Dip/Strike Calculated
		KA3376B01	64.51	64.51	Natural Fracture	Calcite				Undulating	Rough	Moderately Altered	272.3	78.8	1.0	0.0	Certain	45.4	107.0	Dip/Strike Calculated
		KA3376B01	65.15	65.15	Natural Fracture	Calcite	Chlorite			Undulating	Rough	Highly Altered	160.3	82.3	2.0	2.0	Certain	64.4	286.0	Dip/Strike Calculated
		KA3376B01	65.30	65.30	Natural Fracture	Chlorite	Calcite			Irregular	Rough	Moderately Altered	315.5	48.7	1.0	1.0	Certain	47.8	180.0	Dip/Strike Calculated
		KA3376B01	65.35	65.35	Natural Fracture	Calcite				Planar	Rough	Moderately Altered	326.2	80.0	1.0	0.0	Certain	74.8	224.0	Dip/Strike Calculated
		KA3376B01	65.49	65.49	Natural Fracture	Calcite	Chlorite			Undulating	Rough	Moderately Altered	141.5	86.2	1.0	1.0	Certain	83.3	296.0	Dip/Strike Calculated
19	65.6 m	KA3376B01	65.51	65.51	Natural Fracture	Chlorite	Calcite			Undulating	Rough	Moderately Altered	318.7	43.8	1.0	0.0	Certain	42.8	183.0	Dip/Strike Calculated
		KA3376B01	65.66	65.66	Natural Fracture	Calcite	Chlorite			Undulating	Rough	Moderately Altered	358.4	80.3	2.0	2.0	Certain	46.0	295.0	Dip/Strike Calculated
		KA3376B01	66.24	66.24	Natural Fracture	Calcite				Planar	Rough	Slightly Altered	342.9	49.6	1.0	0.0	Probable	41.7	209.0	Dip/Strike Calculated
		KA3376B01	66.47	66.47	Natural Fracture	Calcite				Irregular	Rough	Slightly Altered	297.0	87.3	1.0	0.0	Certain	71.2	101.0	Dip/Strike Calculated

Appendix E

Graphs: Hydraulic tests

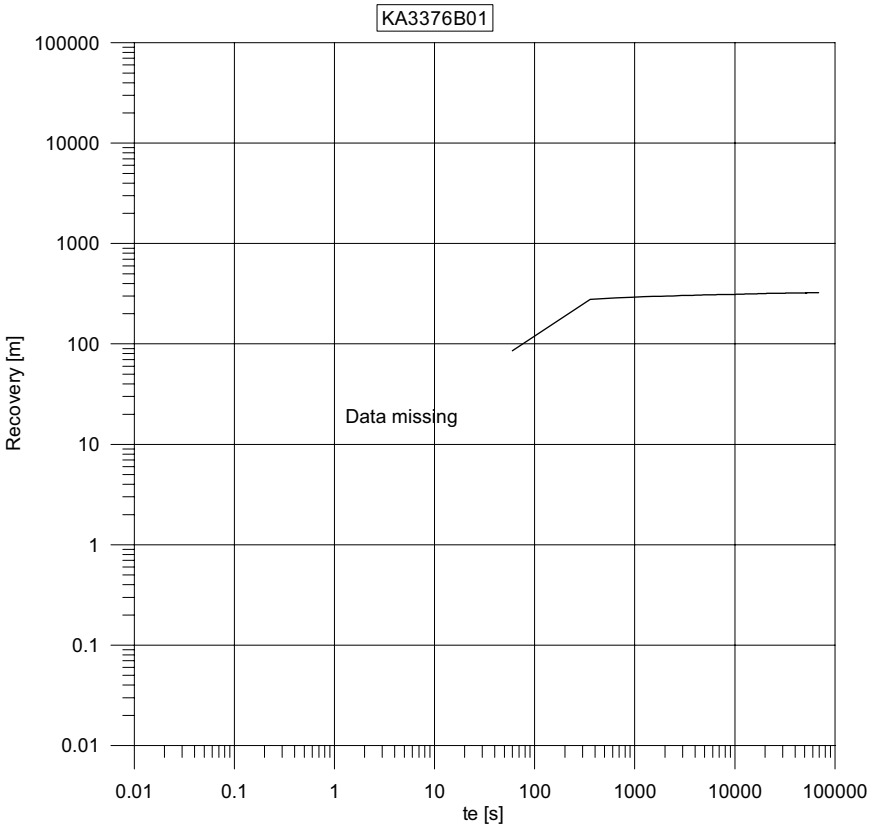

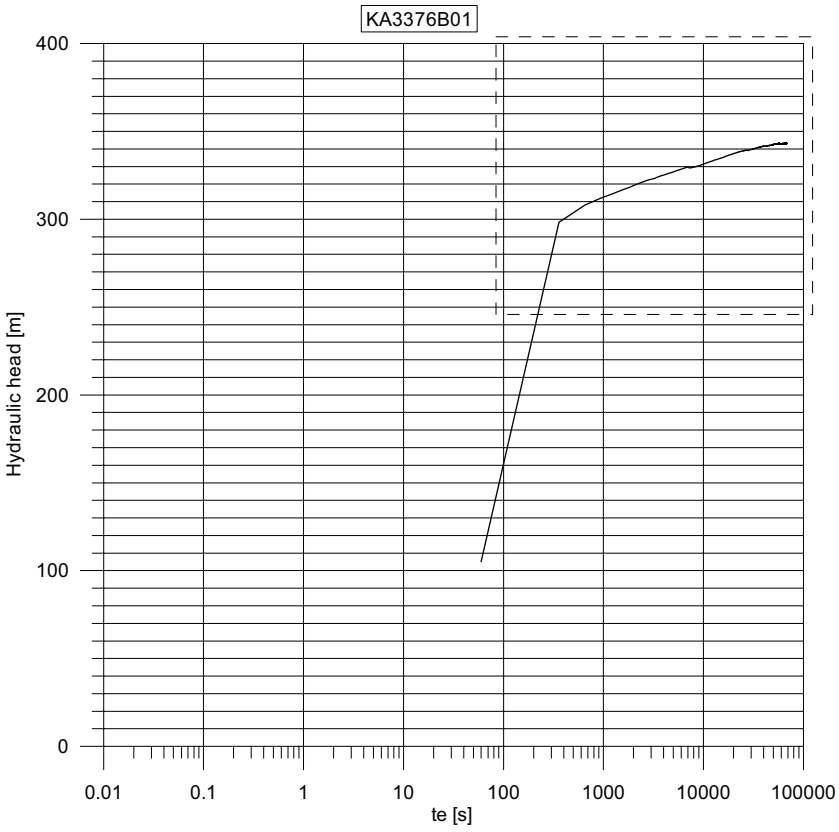

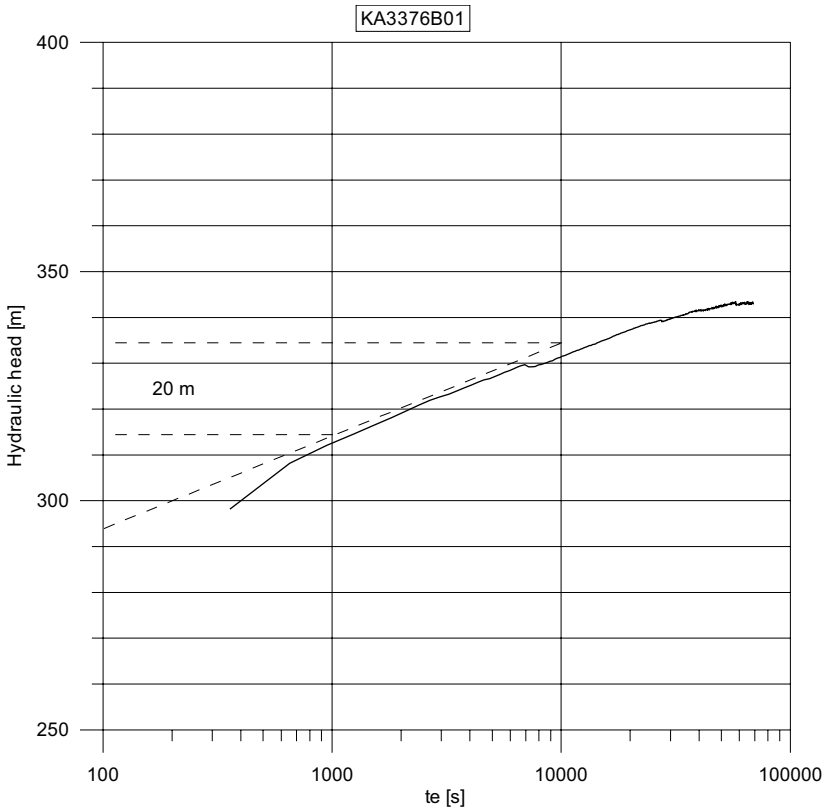

Q = 96.3 L/min = 1.60E-3 m^3/s
ds'' = 20 m
T = 0.183*Q/ ds'' = 1.47E-5 m^2/s
h(te = 86221 s) = 343 m

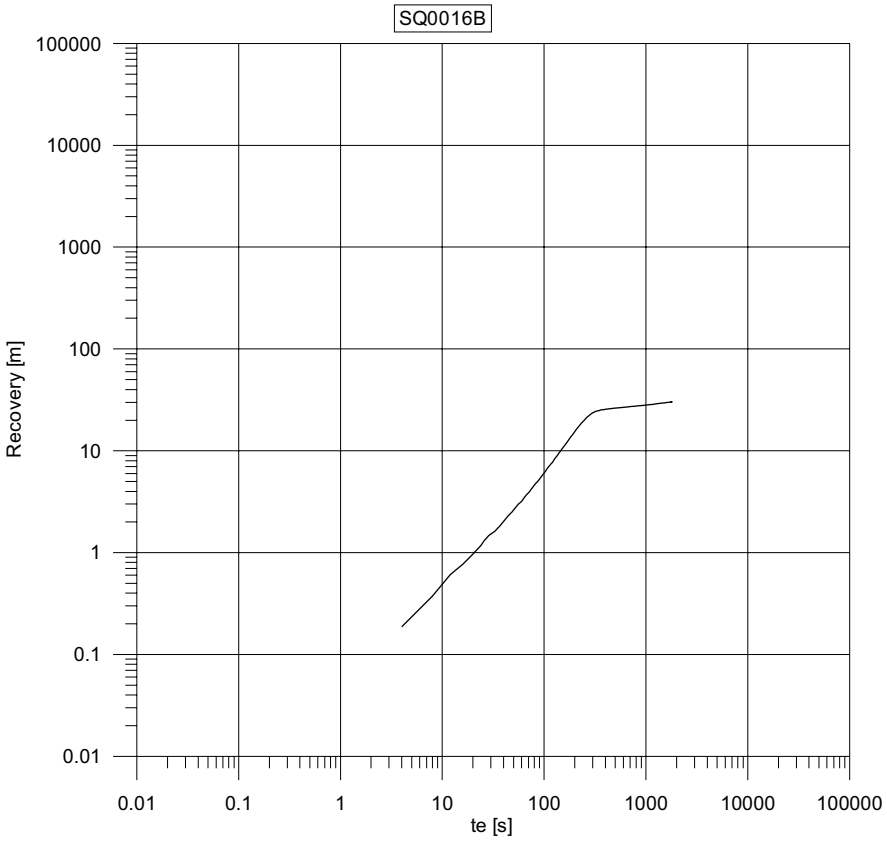

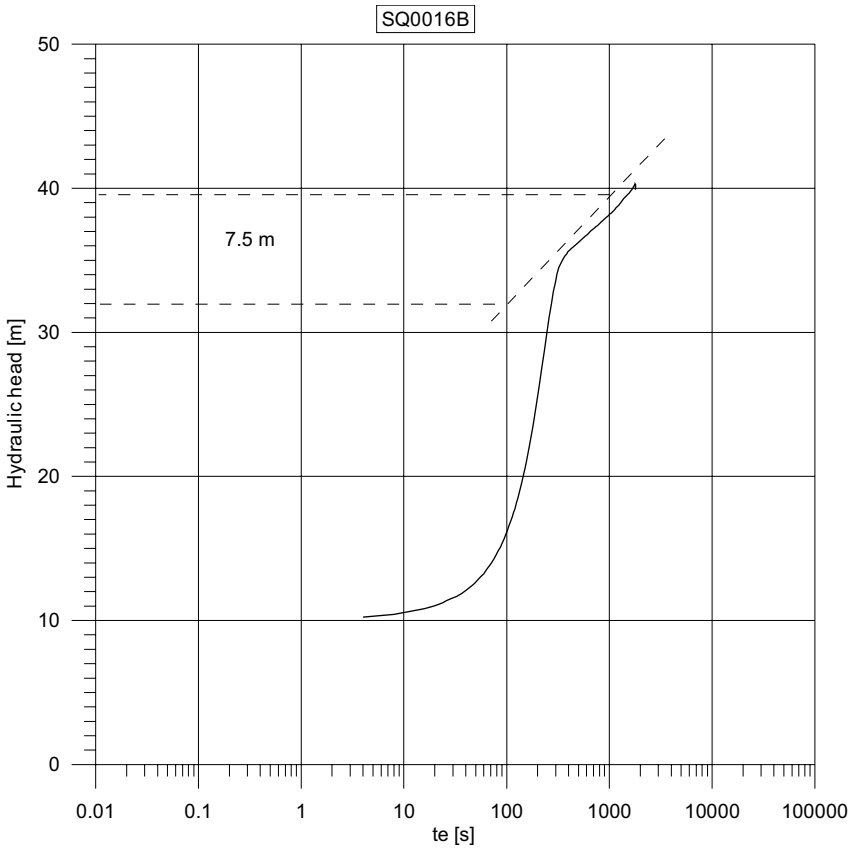

SQ0016B
Q = 0.06 L/min = 1.0E-6 m^3/s
ds'' = 7.5 m
T = 0.183*Q/ ds'' = 2.4E-8 m^2/s

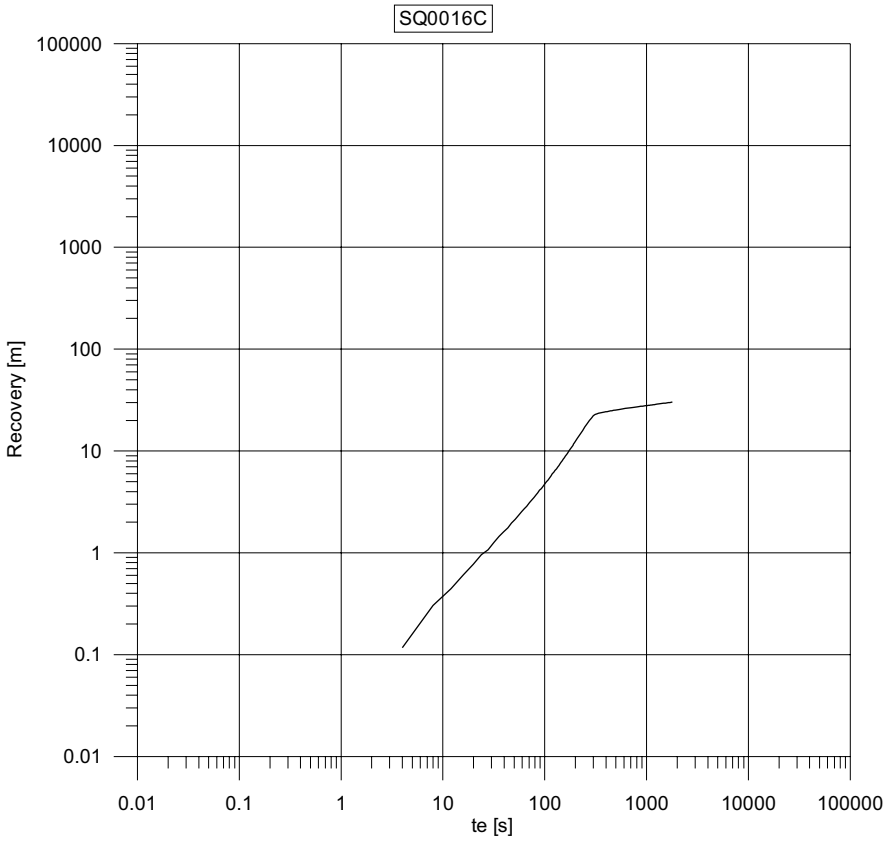

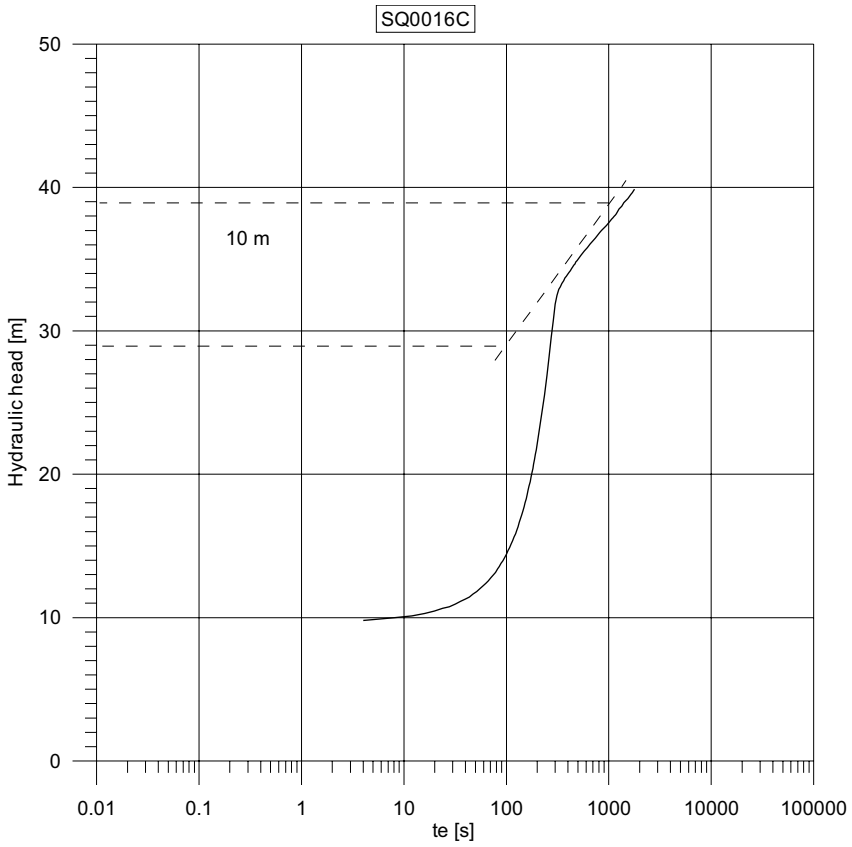

SQ0016C
Q = 0.09 L/min = 1.5E-6 m^3/s
ds'' = 10 m
T = 0.183*Q/ ds'' = 2.7E-8 m^2/s

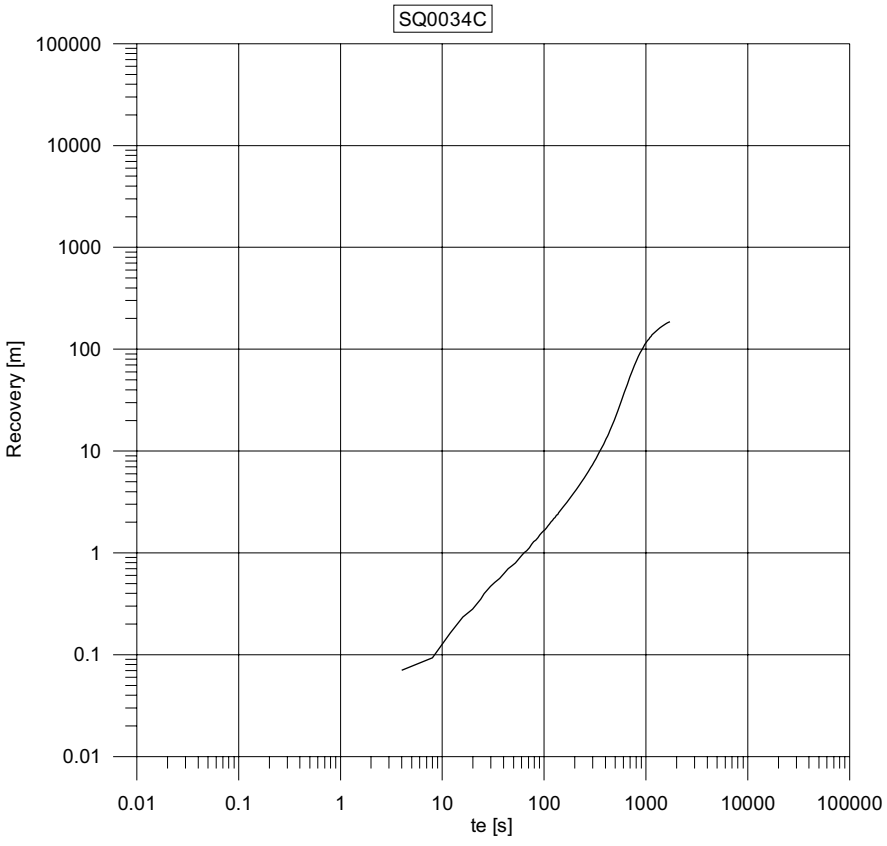

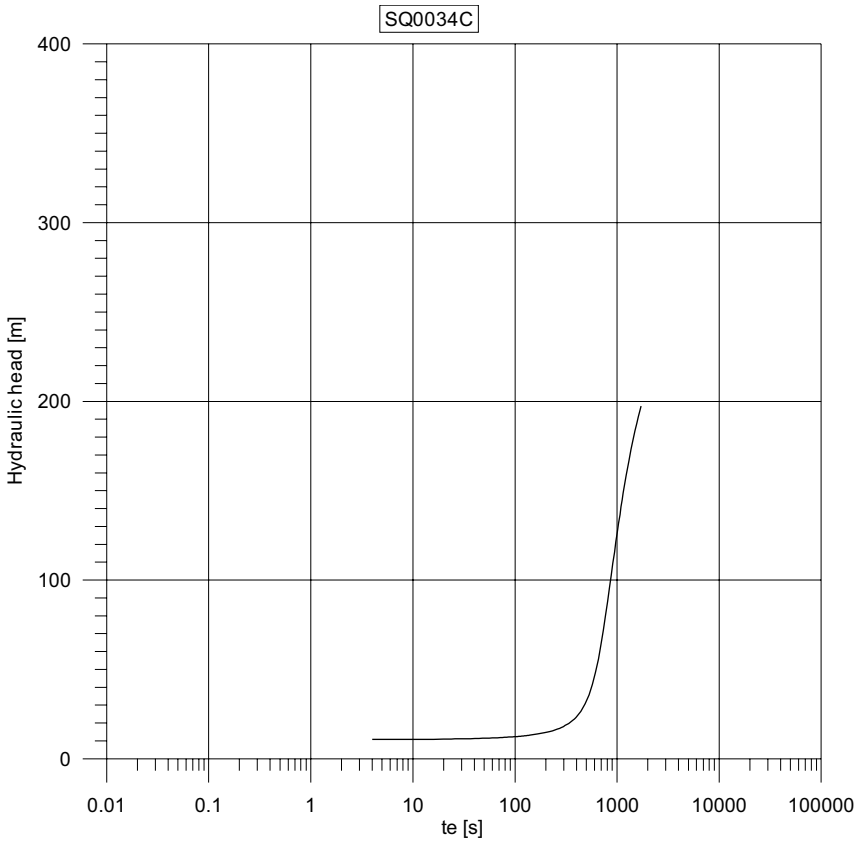
SQ0034C
Hydraulic head [m]
400
300
200
100
0
0.01
0.1
1
10
100
1000
10000
100000
te [s]

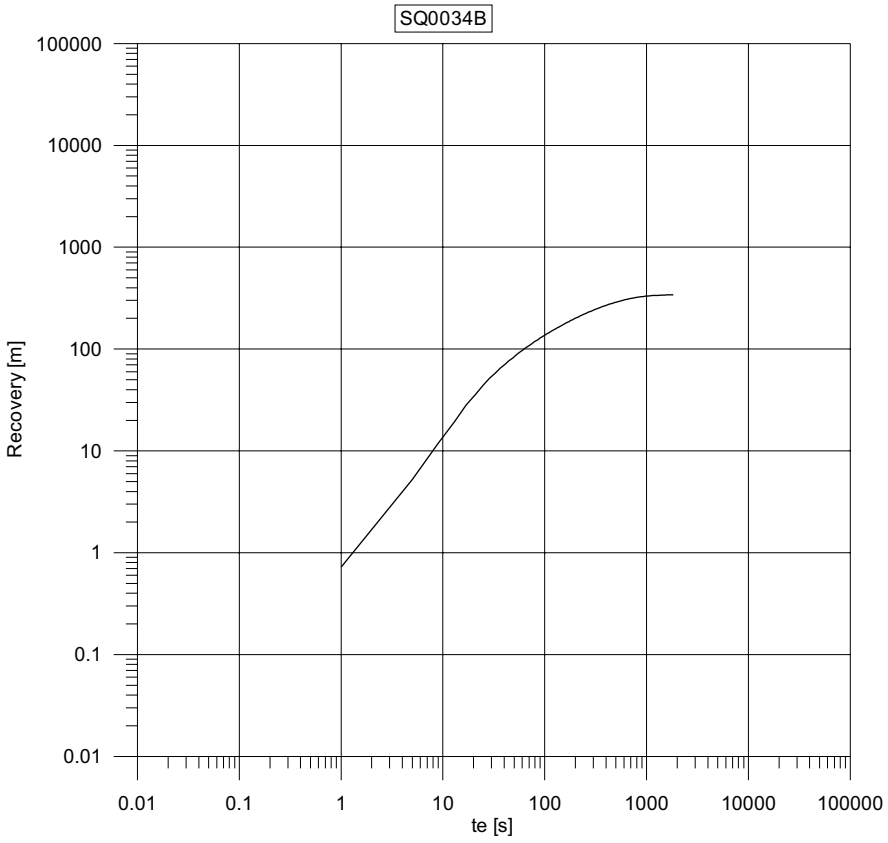
SQ0034B
Recovery [m]
100000
10000
1000
100
10
1
0.1
0.01
0.01
0.1
1
10
100
1000
10000
100000
te [s]

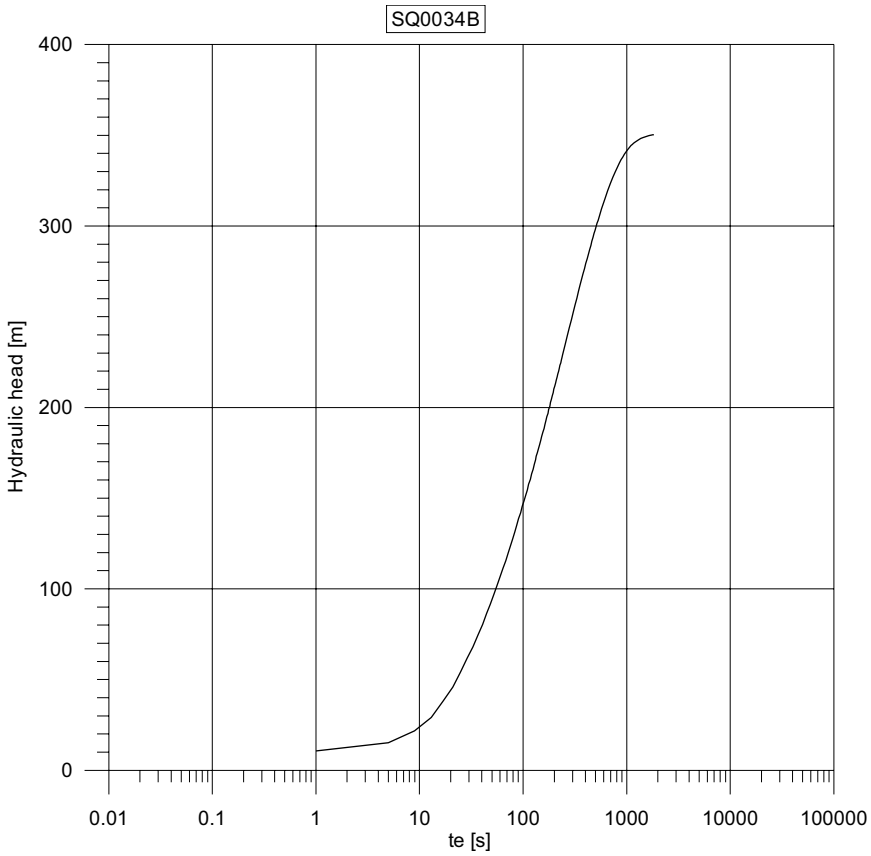

Transmissivities for SQ0034C and SQ0034B not evaluated.

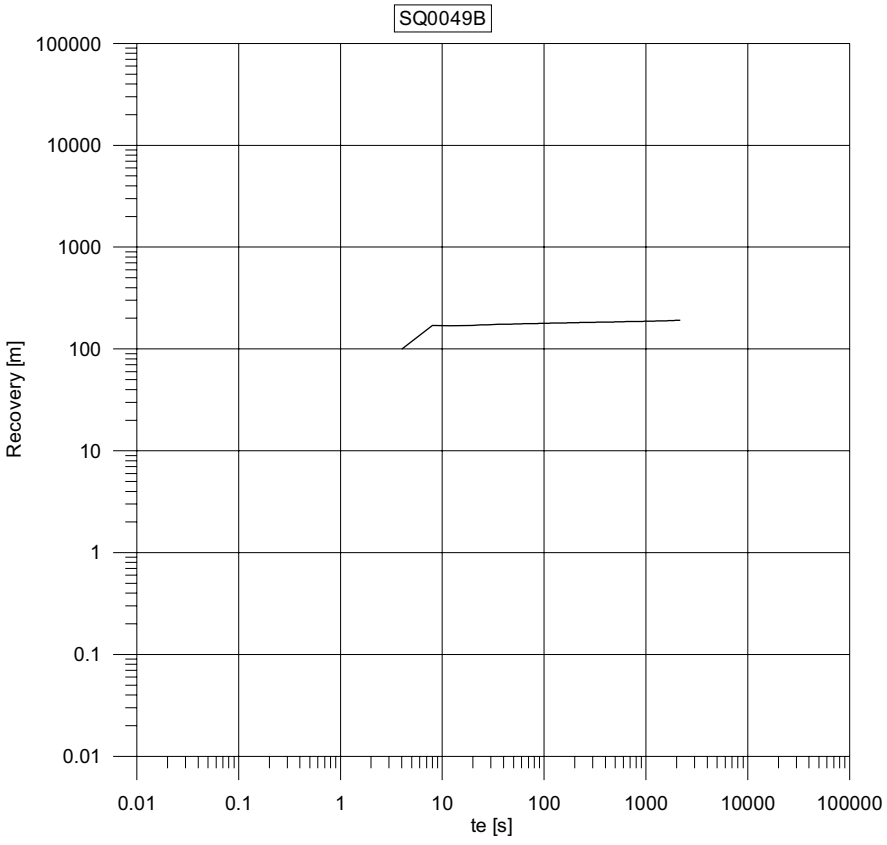

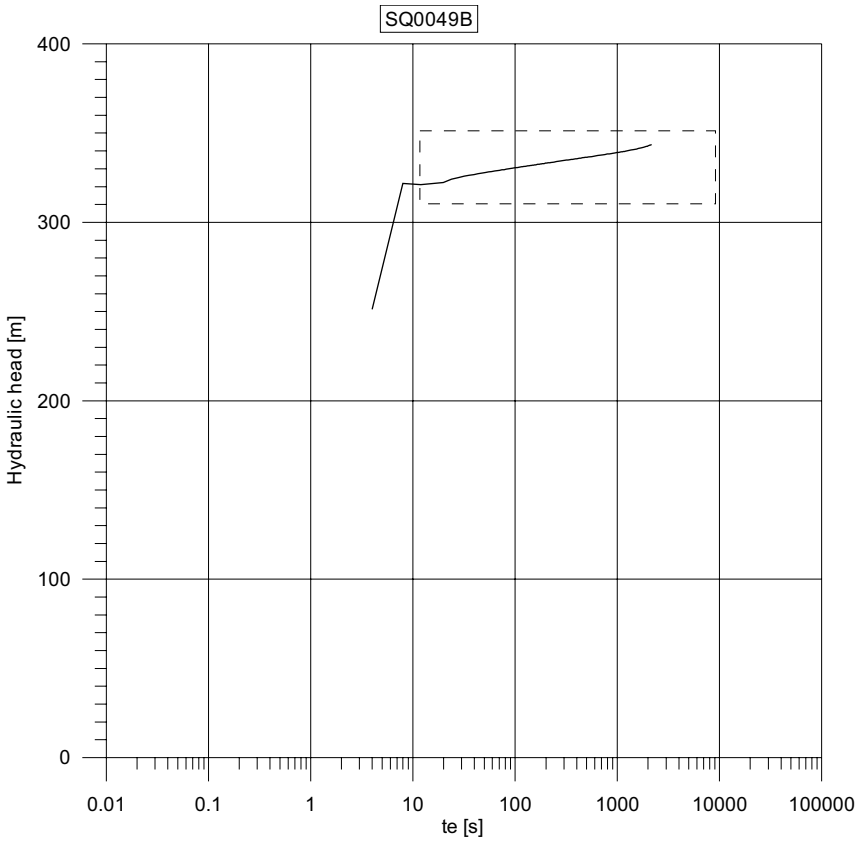

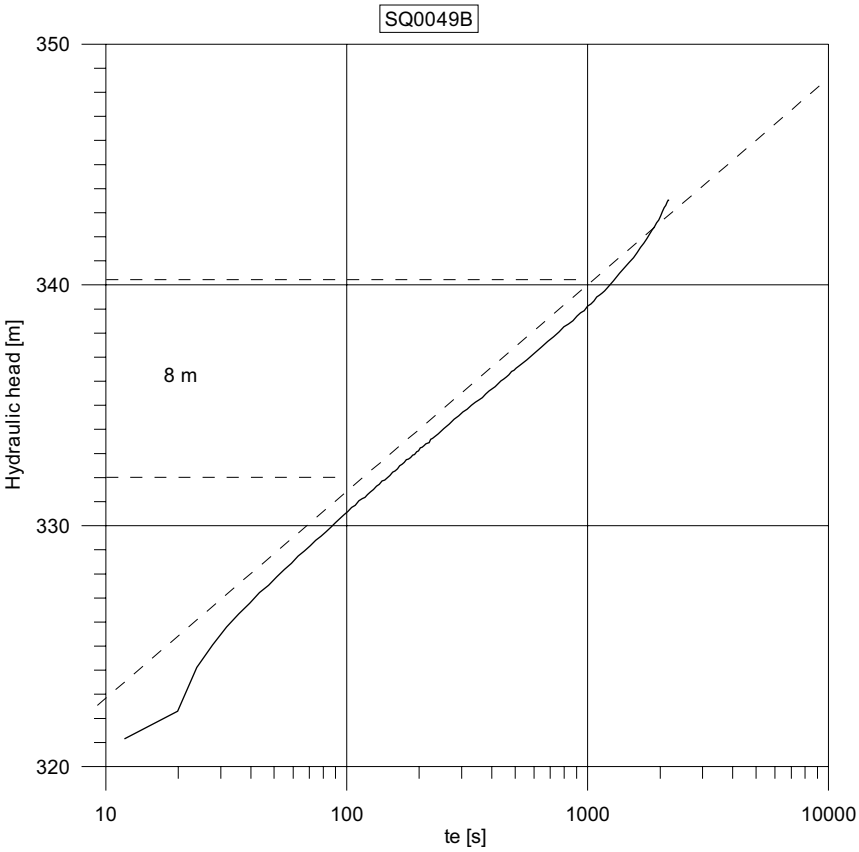

SQ0049B
Q = 33 L/min = 5.5E-4 m^3/s
ds'' = 8 m
T = 0.183*Q/ ds'' = 1.3E-5 m^2/s

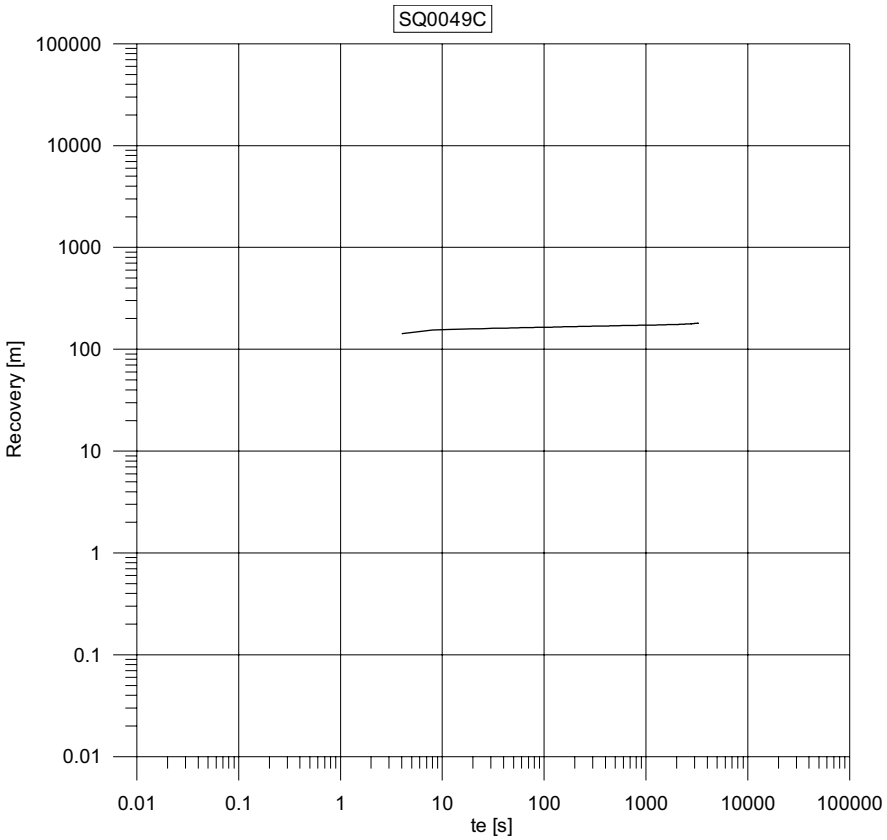
SQ0049C
Recovery [m]
100000
10000
1000
100
10
1
0.1
0.01
0.01
0.1
1
10
100
1000
10000
100000
te [s]

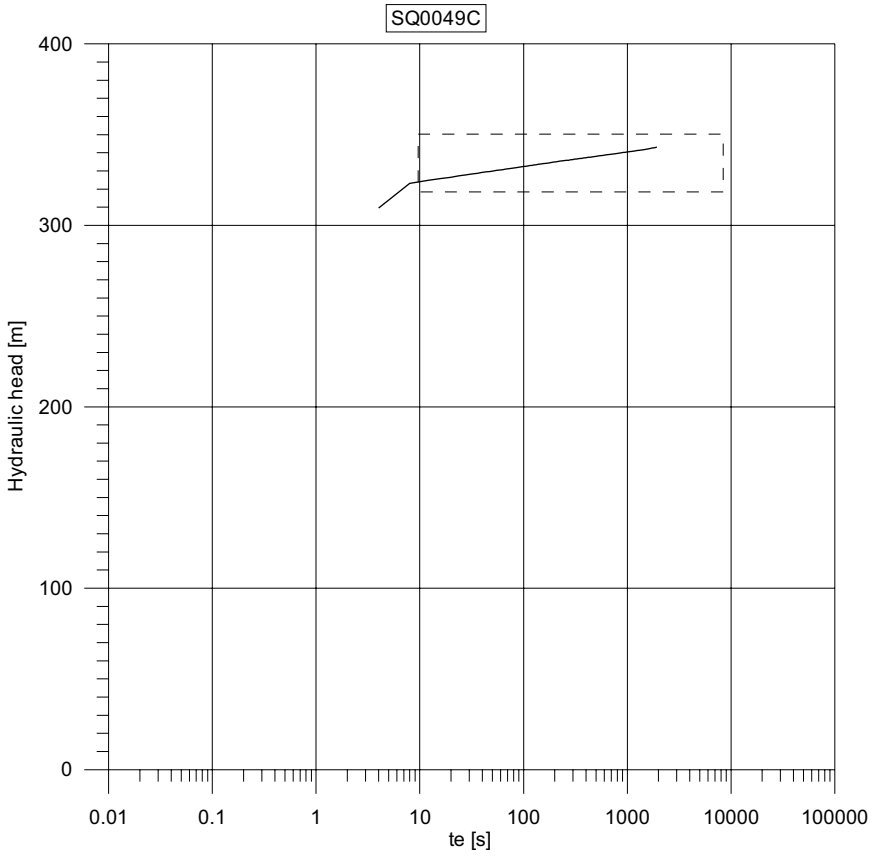
SQ0049C
Hydraulic head [m]
400
300
200
100
0
0.01
0.1
1
10
100
1000
10000
100000
te [s]

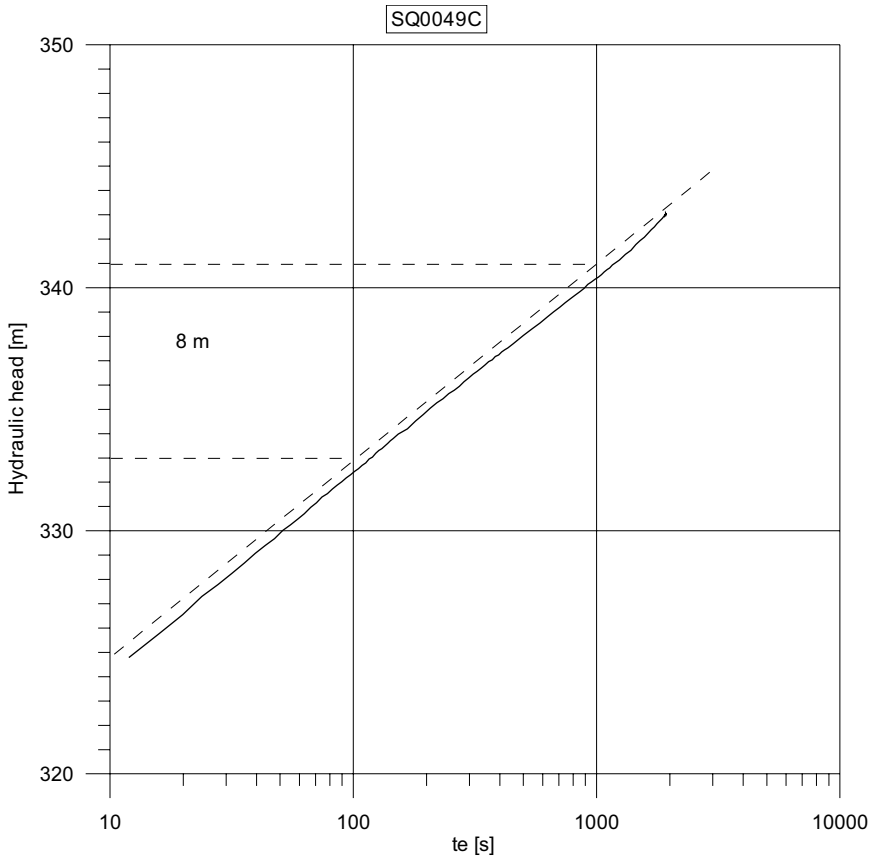

SQ0049C
Q = 33 L/min = 5.5E-4 m^3/s
ds'' = 8 m
T = 0.183*Q/ ds'' = 1.3E-5 m^2/s

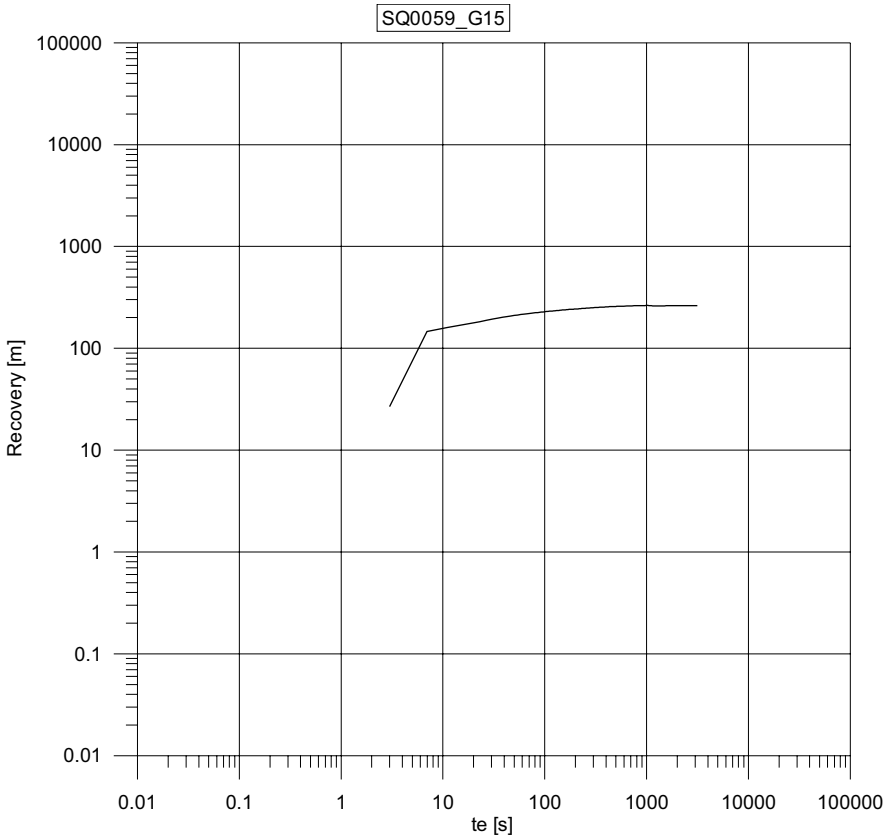

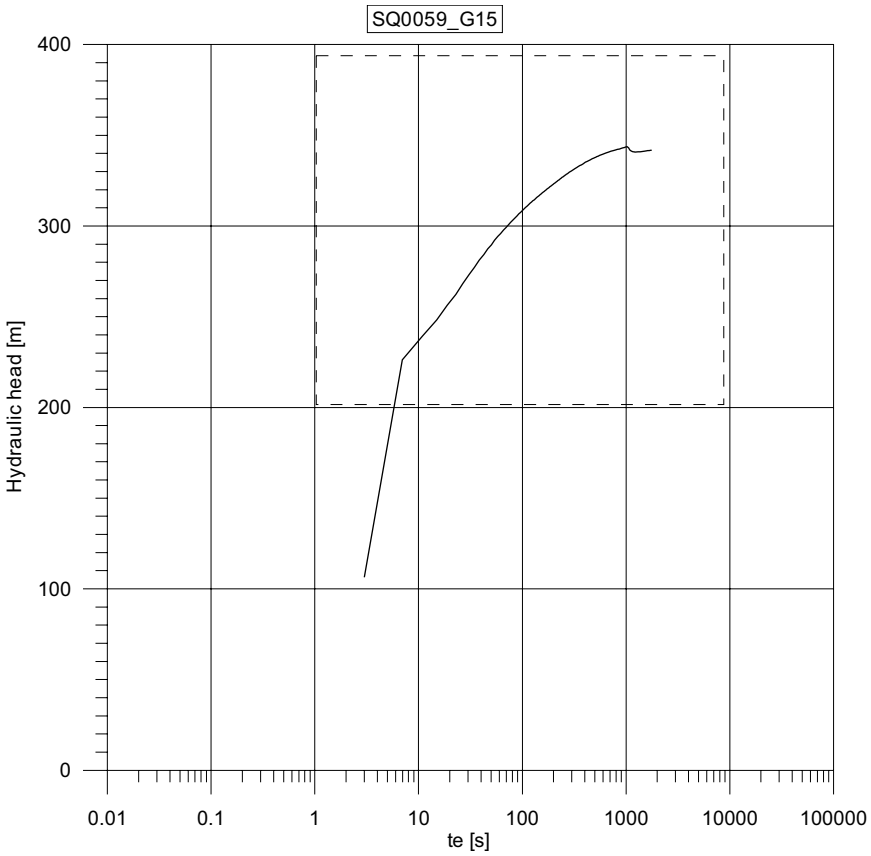

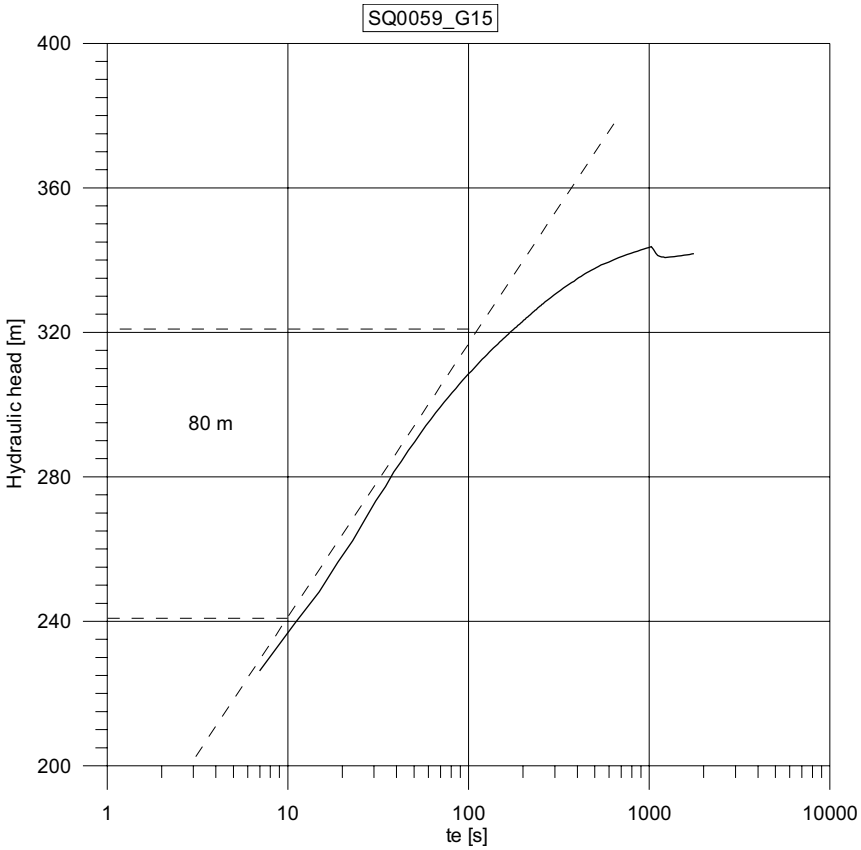

SQ0059_G15
Q = 28 L/min = 4.7E-4 m^3/s
ds'' = 80 m
T = 0.183*Q/ ds'' = 1.1E-6 m^2/s

Appendix F

Inflow during drilling and estimated hydraulic apertures – percussion drilled probe boreholes

Table F-1. Inflow, specific capacity and estimated hydraulic apertures based on inflow during drilling, SQ0016B (7 sections). No inflows are >2 L/min and are therefore not included in the geometrical model (RVS).

Section no	Section	Length [m]	dQ [L/min]
	0–4.6	4.6	0
	4.6–7.6	3	0
	7.6–10.6	3	0
	10.6–13.6	3	0
	13.6–16.6	3	0
	16.6–19.6	3	0
	19.6–22.6	3	0.045*

*Total inflow, difficult to determine location.

Table F-2. Inflow, specific capacity and estimated hydraulic apertures based on inflow during drilling, SQ0016C (7 sections). No inflows are >2 L/min and are therefore not included in the geometrical model (RVS).

Section no	Section	Length [m]	dQ [L/min]
	0–4.6	4.6	0
	4.6–7.6	3	0
	7.6–10.6	3	0
	10.6–13.6	3	0
	13.6–16.6	3	0
	16.6–19.6	3	0
	19.6–22.6	3	0.01*

*Total inflow, difficult to determine location.

Table F-3. Inflow, specific capacity and estimated hydraulic apertures based on inflow during drilling, SQ0034C (6 sections). No inflows are >2 L/min and are therefore not included in the geometrical model (RVS).

Section no	Section	Length [m]	dQ [L/min]
	0–4.6	4.6	0
	4.6–7.6	3	0
	7.6–10.6	3	0
	10.6–13.6	3	0
	13.6–16.6	3	0
	16.6–19.6	3	0.025*

*Total inflow, difficult to determine location.

Table F-4. Inflow, specific capacity and estimated hydraulic apertures based on inflow during drilling, SQ0034B (6 sections). No inflows are >2 L/min and are therefore not included in the geometrical model (RVS).

Section no	Section	Length [m]	dQ [L/min]
	0–4.6	4.6	0
	4.6–7.6	3	0
	7.6–10.6	3	0
	10.6–13.6	3	0
	13.6–16.6	3	0
	16.6–19.6	3	0.825*

*Total inflow, difficult to determine location.

Table F-5. Inflow, specific capacity and estimated hydraulic apertures based on inflow during drilling, SQ0049B (9 sections). Inflows >2 L/min are written in bold and are used for the geometrical model (RVS).

Section no	Section	Length [m]	dQ [L/min]	dQ [m^3/s]	Q/dh [m^2/s] dh: 343 m	b(Q/dh) [μm]
	0–4.6	4.6	0	0	0	0
	4.6–7.6	3	0	0	0	0
B1	**7.6–10.6**	**3**	**45**	**7.50E–04**	**2.19E–06**	**151**
	10.6–13.6	3	0	0	0	0
B2	**13.6–16.6**	**3**	**105**	**1.75E–03**	**5.10E–06**	**201**
	16.6–19.6	3	0	0	0	0
	19.6–22.6	3	0	0	0	0
	22.6–25.6	3	0	0	0	0
	25.6–26.6	1	0	0	0	0

Table F-6. Inflow, specific capacity and estimated hydraulic apertures based on inflow during drilling, SQ0049C (9 sections). Inflows >2 L/min are written in bold and are used for the geometrical model (RVS).

Section no	Section	Length [m]	dQ [L/min]	dQ [m^3/s]	Q/dh [m^2/s] dh: 343 m	b(Q/dh) [μm]
	0–4.6	4.6	0	0	0	0
	4.6–7.6	3	0.9	1.50E–05	4.37E–08	41
C1	**7.6–10.6**	**3**	**39.1**	**6.52E–04**	**1.90E–06**	**145**
C2	**10.6–13.6**	**3**	**80**	**1.33E–03**	**3.89E–06**	**184**
C3	**13.6–16.6**	**3**	**180**	**3.00E–03**	**8.75E–06**	**240**
	16.6–19.6	3	0	0	0	0
	19.6–22.6	3	0	0	0	0
	22.6–25.6	3	0	0	0	0
	25.6–26.6	1	0	0	0	0

Table F-7. Inflow, specific capacity and estimated hydraulic apertures based on inflow during drilling, G15 (6 sections). Inflows >2 L/min are written in bold and are used for the geometrical model (RVS).

Section no	Section	Length [m]	dQ [L/min]	dQ [m^3/s]	Q/dh [m^2/s] dh: 343 m	b(Q/dh) [μm]
	0–4.6	4.6	0	0	0	0
	4.6–7.6	3	0	0	0	0
G15_1	**7.6–10.6**	**3**	**3**	**5.00E–05**	**1.46E–07**	**61**
	10.6–13.6	3	0	0	0	0
G15_2	**13.6–16.6**	**3**	**6.6**	**1.10E–04**	**3.21E–07**	**80**
G15_3	**16.6–18.0**	**1.4**	**27.6**	**4.60E–04**	**1.34E–06**	**129**

Table F-8. Inflow, specific capacity and estimated hydraulic apertures based on inflow during drilling, SQ0059 S_C1 (8 sections). No inflows are >2 L/min and are therefore not included in the geometrical model (RVS).

Section no	Section	Length [m]	dQ [L/min]
	0–4.6	4.6	0
	4.6–7.6	3	0
	7.6–10.6	3	0
	10.6–13.6	3	0
	13.6–16.6	3	0
	16.6–19.6	3	1
	19.6–22.6	3	0
	22.6–25.6	3	0.6

Table F-9. Inflow, specific capacity and estimated hydraulic apertures based on inflow during drilling, SQ0059 S_B2 (8 sections). No inflows are >2 L/min and are therefore not included in the geometrical model (RVS).

Section no	Section	Length [m]	dQ [L/min]
	0–4.6	4.6	0
	4.6–7.6	3	0
	7.6–10.6	3	0
	10.6–13.6	3	0
	13.6–16.6	3	0
	16.6–19.6	3	0
	19.6–22.6	3	0.5
	22.6–25.6	3	0

Appendix G

Decision analysis for Fan 1

To make the decision regarding most suitable design with information from the probe holes three different designs, A, B and C were calculated. This section demonstrates how the decision for recommendation of design was based without going into details about the different designs or calculations.

To support the decision the calculated results presented in Table G-1 were known for three different design concepts. All three were accepted in terms of expected inflow.

To support the decision the Analytical Hierarchy Process (AHP) was used. As object the Choice of design was chosen, as criteria Grouting time, Volumes and Variance in result and as sub-criteria the three design choices are chosen.

Of the criteria, volumes and variance in result are considered to be the most important issues since they are connected to the requirements. Grouting time is considered less important since it is connected only to production.

Based on the analysis grouting design A is the most favourable.

Table G-1 Calculated results for the three evaluated designs of grouting.

Design	Grouting time	Volumes	Variance in result
A	2 grouting rounds =>long total time	600	0%
B	3700	5300	1%
C	2520	1920	10%

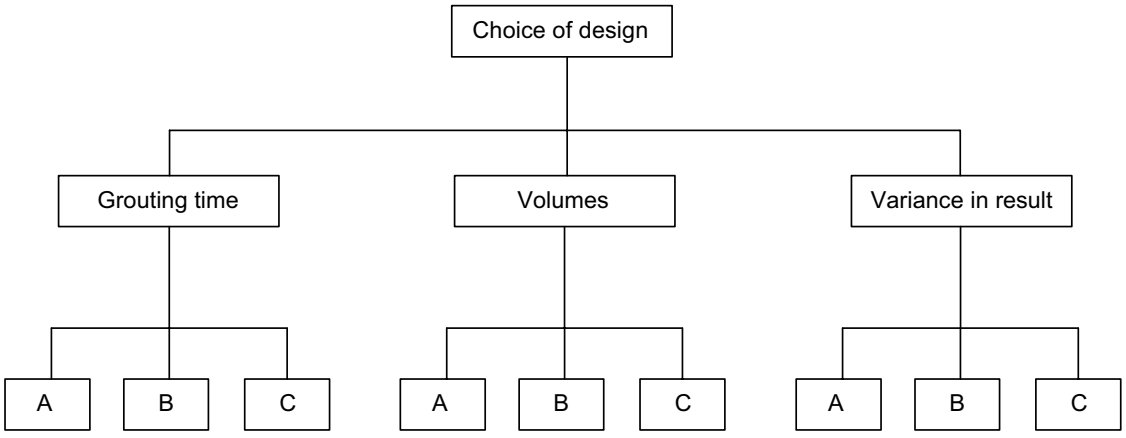

Figure G-1. *Illustration of the AHP structure for the decision.*

Appendix H

Inflow during drilling and estimated hydraulic apertures – grouting boreholes

Table H-1. Inflow during drilling, Fan 1:1.

Borehole/ Section	Inflow [L/min] 0–4.6m	4.6–7.6m	7.6–10.6m	10.6–13.6m	13.6–15.6m	Qtot
H4	0	0	0	3	42	45
C3	0	0	28	23	0	51
A2	0	1	0	119	12	132
A1	0	0	1	8	3	12
I5	0	0	132	0	0	132
G11	0	0	48	0	12	60
G10	0	0	24	0	72	96
D6	0	0	0	0	84	84
B7	0	0	12	10	122	144
B8	0	0	0	36	108	144
G9	0	0	5	5	44	54

Median Qtot: 84 L/min, Qtot/dh: 4.1E–6 m^2/s, b(Qtot/dh): 187 µm,

Fraction <2 L/min: 0/11=0

Median Qmax: 72 L/min Qmax/dh: 3.5E–6 m^2/s, b(Qmax/dh): 177 µm

Table H-2. Estimated hydraulic apertures based on inflow, Fan 1:1.

Borehole/ Section	Estimated hydraulic aperture [µm] 0–4.6m	4.6–7.6m	7.6–10.6m	10.6–13.6m	13.6–15.6m
H4	0	0	0	61	148
C3	0	0	129	121	0
A2	0	43	0	210	98
A1	0	0	45	84	61
I5	0	0	217	0	0
G11	0	0	155	0	98
G10	0	0	123	0	177
D6	0	0	0	0	187
B7	0	0	98	92	211
B8	0	0	0	141	203
G9	0	0	73	73	150

Table H-3. Inflow during drilling, Fan 1:2.

Borehole/ Section	Inflow [L/min] 0–4.6m	4.6–7.6m	7.6–10.6m	10.6–13.6m	13.6–15.6m	Qtot
I19	0	0	0	1.5	0.9	2.4
C15	0	0	0	24	0	24
I20	0	0	0	0	0.3	0.3
C16	0	0	0	21.6	0	21.6
D21	0	0	1	0	1.8	2.8
A14	0	0	0	0	0.1	0.1
D22	0	0	0	1	0	1
H17	0	0	0	2.4	0	2.4
B23	0	0	0.48	0	0.7	1.2
A13	0	0	1	6	2	9
B24	0	1	0	0	8	9
H18	0	0	0	1.3	1.7	3
B25	0	0	0	3	1.2	4.2
A12	0	0	0	0	1.8	1.8
G26	0	0	0	1	2	3
G31	0	0	0	0	0	0
G30						7.8
G29						0
G27						7.2
G28						7.2

Median Qtot: 2.9 L/min, Qtot/dh: 1.4E–7 m^2/s, b(Qtot/dh): 61 µm (20 bore holes),

Fraction <2 L/min: 7/20=0.35

Median Qmax: 1.8 L/min, Qmax/dh: 8.7E–8 m^2/s, b(Qmax/dh): 52 µm (16 bore holes)

Table H-4. Estimated hydraulic apertures based on inflow, Fan 1:2.

Borehole/ Section	Estimated hydraulic aperture [µm] 0–4.6m	4.6–7.6m	7.6–10.6m	10.6–13.6m	13.6–15.6m
I19	0	0	0	49	41
C15	0	0	0	123	0
I20	0	0	0	0	29
C16	0	0	0	119	0
D21	0	0	43	0	52
A14	0	0	0	0	21
D22	0	0	0	43	0
H17	0	0	0	57	0
B23	0	0	33	0	38
A13	0	0	43	77	54
B24	0	43	0	0	85
H18	0	0	0	46	51
B25	0	0	0	61	45
A12	0	0	0	0	52
G26	0	0	0	43	54
G31	0	0	0	0	0

Table H-5. Inflow during drilling, Fan 2:1.

Borehole/ Section	Inflow [L/min] 0–4.6m	4.6–7.6m	7.6–10.6m	10.6–13.6m	13.6–16.6m	16.6–18m	Qtot
G18	0	0	15	0	0	0	15
G19	0	0	9.9	0	0	0	9.9
G20	0	0	0	0	6.6	6.2	12.8
G17	0	0	2	0	4	12.6	18.6
A1	0	0	0	0	0	0	0
G16	0	0	4	0	0	32	36
A2	0	0	0	0	0	2.4	2.4
G15	0	0	3	0	6.6	27.6	37.2
A3	0	0	0	0	12.6	0	12.6
B14	0	0.5	0	0.5	0	2.6	3.6
A4	0	0	0	0.5	2.5	2.2	5.2
B13	0.5	0	0	0.5	0	2.6	3.6
C5	0	1.5	0	3.3	31.2	0	36
D10	0	0	0.5	3.4	0	0	3.9
B12	0	1	0	0	0	6.2	7.2
H6	0	0	0	0	22.8	0	22.8
D11	0.5	0	0.5	0	0	1.3	2.25
H7	0	0.5	0	0	19.9	0	20.4
I8	0	0	0.5	0	0	1.8	2.3
I9	0	3.6	0.6	0	0	0	4.2
I21	0	0	0	0	0	36	36

Median Qtot: 9.9 L/min, Qtot/dh: 4.8E–7 m^2/s, b(Qtot/dh): 91 µm, Fraction <2 L/min: 1/21=0.05

Median Qmax: 6.6 L/min, Qmax/dh: 3.2E–7 m^2/s, b(Qmax/dh): 80 µm

Table H-6. Estimated hydraulic apertures based on inflow, Fan 2:1.

Borehole/ Section	Estimated hydraulic aperture [µm] 0–4.6m	4.6–7.6m	7.6–10.6m	10.6–13.6m	13.6–16.6m	16.6–18m
G18	0	0	105	0	0	0
G19	0	0	91	0	0	0
G20	0	0	0	0	80	78
G17	0	0	54	0	68	99
A1	0	0	0	0	0	0
G16	0	0	68	0	0	135
A2	0	0	0	0	0	57
G15	0	0	61	0	80	129
A3	0	0	0	0	99	0
B14	0	34	0	34	0	59
A4	0	0	0	34	58	55
B13	34	0	0	34	0	59
C5	0	49	0	63	134	0
D10	0	0	34	64	0	0
B12	0	43	0	0	0	78
H6	0	0	0	0	121	0
D11	34	0	34	0	0	46
H7	0	34	0	0	115	0
I8	0	0	34	0	0	51
I9	0	65	36	0	0	0
I21	0	0	0	0	0	141

Appendix J

Grouting Data

Table J-1. Grouting data in Fan 1 grouting round 1.

Hole number	Grouted volume [l]	Grouting time [min]	Median sealing effect [%]
A1	154	41	–
A2	113	5	–
C3	198	26	–
H4	189	14	–
I5	184	5	–
D6	156	28	–
B7	177	8	–
B8	180	5	–
G9	115	31	–
G10	115	17	–
G11	53	17	–
Total	1634	197	93

Table J-2. Grouting data in Fan 1 grouting round 2.

Hole number	Grouted volume [l]	Grouting time [min]	Median sealing effect [%]
A12	124	67	–
A13	140	49	–
A14	51	9	–
C15	224	56	–
C16	191	51	–
H17	129	43	–
H18	136	71	–
I19	78	35	–
I20	47	2	–
D21	87	39	–
D22	45	24	–
B23	77	38	–
B24	137	35	–
B25	232	59	–
G26	149	71	–
G27	178	52	–
G28	161	45	–
G29	54	7	–
G30	220	66	–
G31	77	35	–
Total	2537	854	98

Table J-3. Grouting result in Fan 2.

Hole number	Grouted volume [l]	Grouting time [min]	Median sealing effect [%]
A1	50	5	–
A2	61	6	–
A3	192	38	–
C4	169	43	–
C5	173	19	–
H6	203	17	–
H7	196	19	–
I8	35	20	–
I9	49	12	–
D10	13	6	–
D11	22	16	–
B12	133	45	–
B13	78	5	–
B14	42	18	–
G15	164	24	–
G16	156	23	–
G17	171	55	–
G18	153	37	–
G19	127	34	–
G20	107	18	–
I21	162	20	
Total	2456	480	96

Table J–4. Inflow in control holes in Fan 1.

Hole number	Inflow [l/min]
G6	0
C4	0.1*
G3	0.24
I5	0.1*
Total	0.44

*) Estimated since too low to be accurately measured.

Table J-5. Inflow in control holes in Fan 2.

Hole number	Inflow [l/min]
G1	0.5
I2	0.7
I3	0.5
G4	0.7
Total	2.4

Appendix K

Compilation of borehole data and tunnel mapping using RVS

The figures in this appendix include

- The core borehole and extrapolated fractures based on inflow from Posiva Flow Log and strike/dip of the closest fracture (based on BIPS and core mapping) for inflow number:
  - 4/47.66 m (Figure K-2a–d)
  - 8/50.42 m (Figure K-3a–d)
  - 9/51.78 m (Figure K-4a–d)
  - 11/57.00 m (Figure K-5a–d)
  - 12/58.09 m (Figure K-6a–d)
  - 19/65.48 m (Figure K-7a–d)
- Probe boreholes.
- Grouting boreholes (for boreholes where at least one section exceeds an inflow of 2 L/min).
- Data from tunnel mapping (fractures indicated by blue lines either exhibited flow, drip or were found humid when mapping the tunnel after excavation).

For probe and grouting boreholes the following colours are used:

<2 L/min: green

>2 L/min: blue

The largest section inflow of a borehole: red

Figure K-1 presents an overview showing the core borehole, the grouting Fans 1:2 and 2:1 and results from tunnel mapping.

For some of the figures on the following pages, the image (excluding the tunnel) has been rotated to get a view parallel to the extrapolated fracture. This way, all intersected sections are visible. Going through the four images for each extrapolated fracture, the first one (e.g. 4_47.66-1) shows the core borehole, a grouting fan, the extrapolated fracture and data from tunnel mapping, blue lines indicate conductive fractures. Figures 4_47.66-2 to 4_47.66-4 present Fan 1:1, 1:2 and 2:1 respectively. By studying these images, the successive sealing of the rock can be identified.

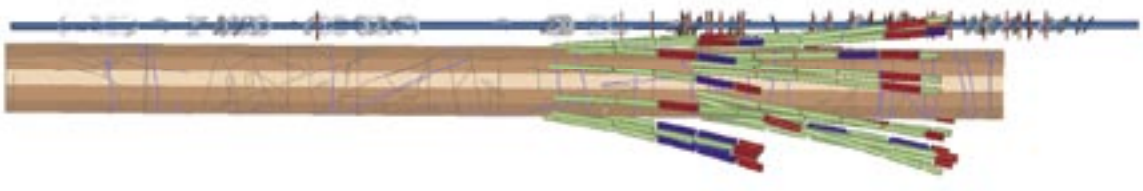

Figure K-1. *Overview showing the core borehole (grey discs represent fractures and red lines inflow from Posiva Flow Log), the grouting Fans 1:2 and 2:1 are seen (colours explained above) and results from tunnel mapping (blue fracture traces indicate conductive fractures).*

Figure K-2 a–d. Extrapolated fracture for inflow number 4/47.66 m

Figure K-2 (a–d) below shows the extrapolated fracture based on inflow number 4. For b) 4_47.66-2, the first conductive sections of the grouting boreholes are those found where a fracture from inflow number 4 intersects the grouting boreholes. After grouting of Fan 1:1, see c) 4_47.66-3, all inflows are below 2 L/min. The second Fan, 2:1, see d) 4_47.66-4, do not intersect this extrapolated fracture.

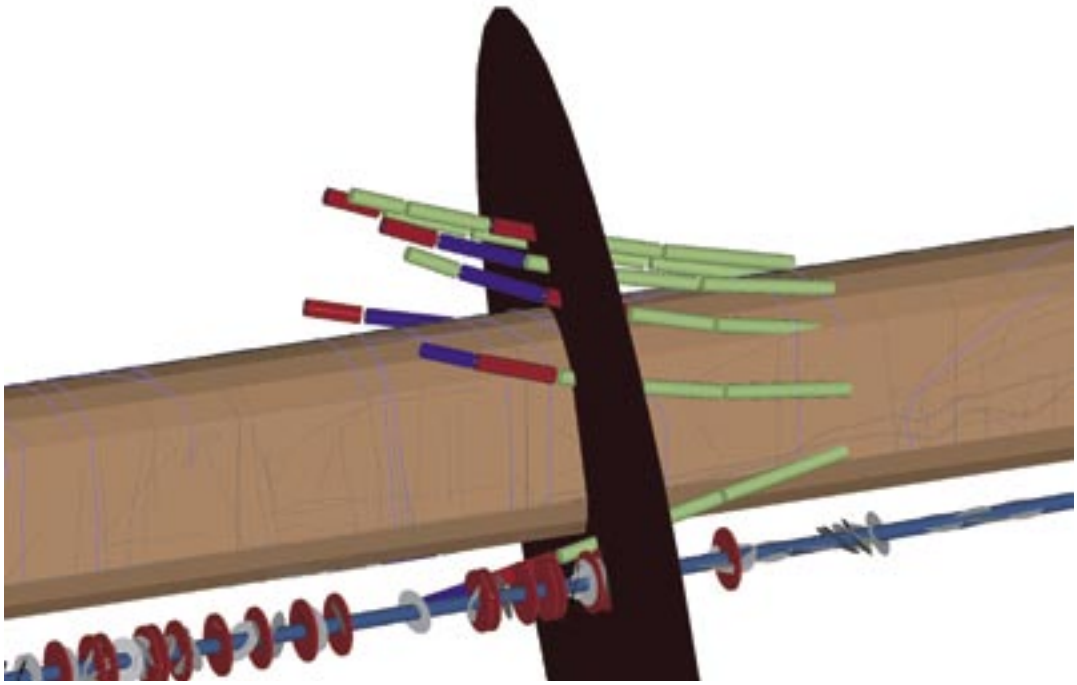

Figure K-2a. *4_47.66-1 core borehole, fan 1:1 (section inflow > 2 L/min) and tunnel mapping.*

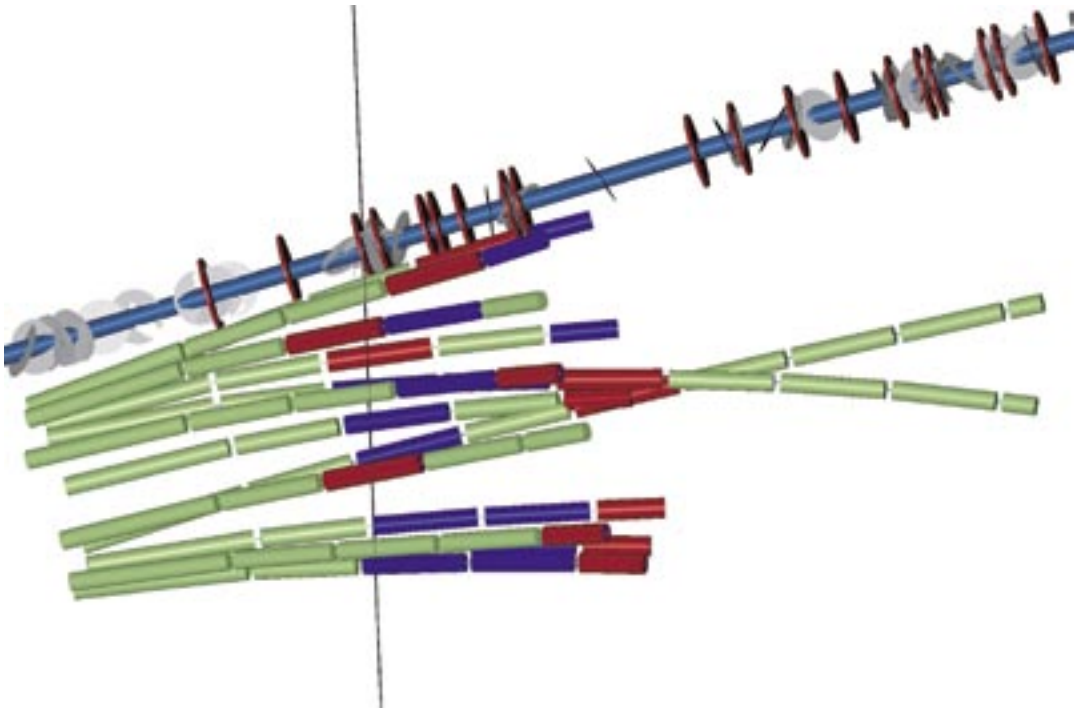

Figure K-2b. *4_47.66-2 core borehole, probe boreholes SQ0049B and SQ0049C and fan 1:1 (section inflow > 2 L/min).*

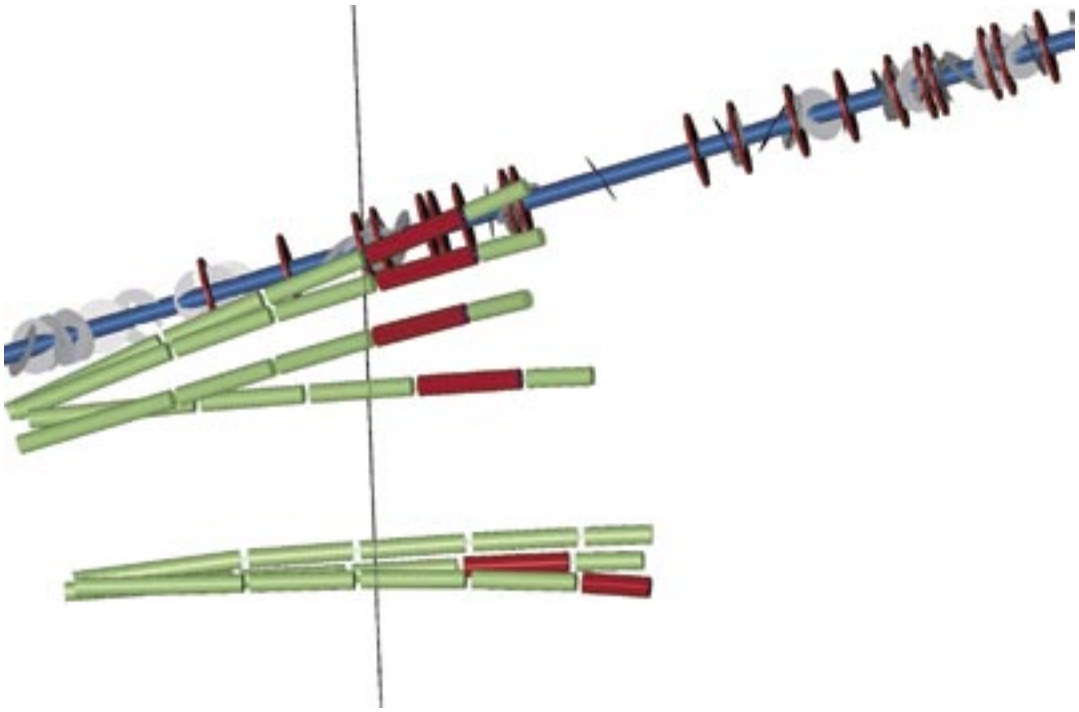

Figure K-2c. *4_47.66-3 core borehole and fan 1:2 (section inflow > 2 L/min).*

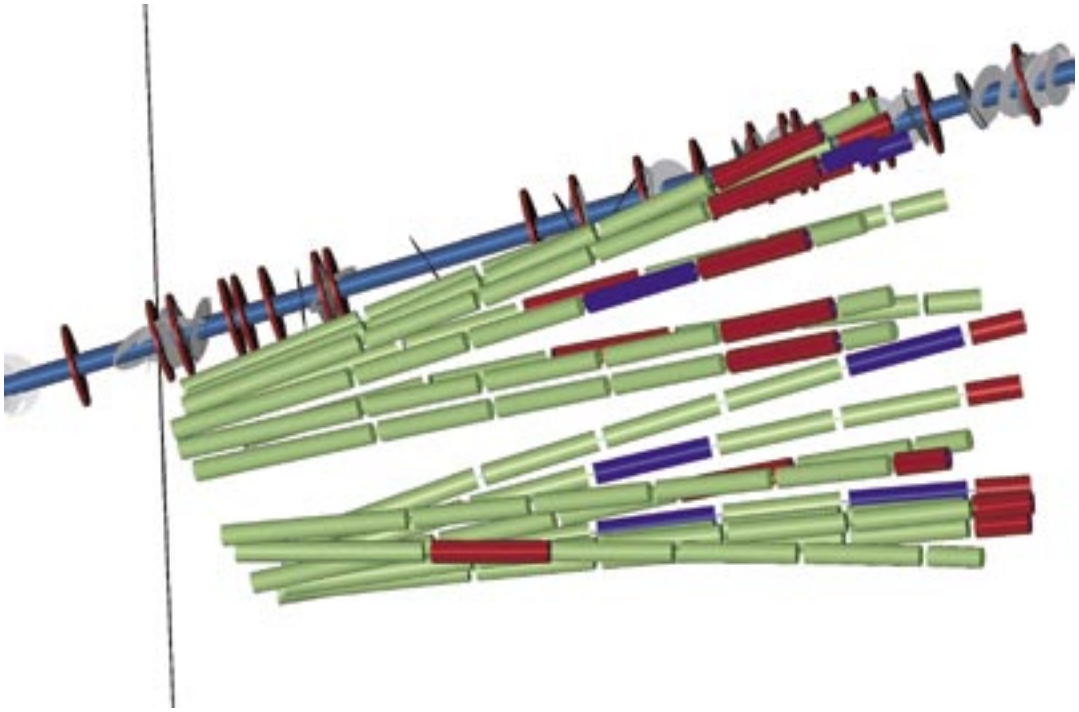

Figure K-2d. *4_47.66-4 core borehole and fan 2:1 (section inflow > 2 L/min).*

Figure K-3 a–d. Extrapolated fracture for inflow number 8/50.42 m

Figure K-3 (a–d) below shows the extrapolated fracture based on inflow number 8. After grouting of Fan 1:1, some of the boreholes have an inflow exceeding 2 L/min. However, after grouting of Fan 1:2 (identified by Fan 2:1, see d) 8_50_42-4) all inflows are below 2 L/min, showing that also the second grouting Fan (1:2) was efficient.

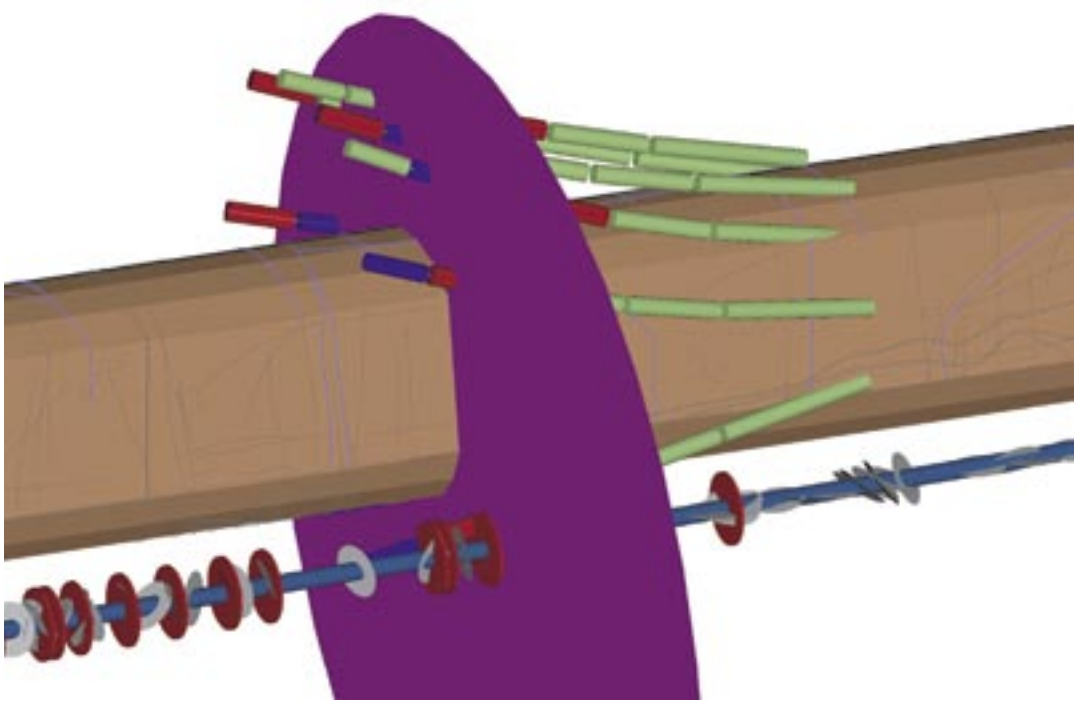

Figure K-3a. *8_50.42-1 core borehole, fan 1:1 (section inflow > 2 L/min) and tunnel mapping.*

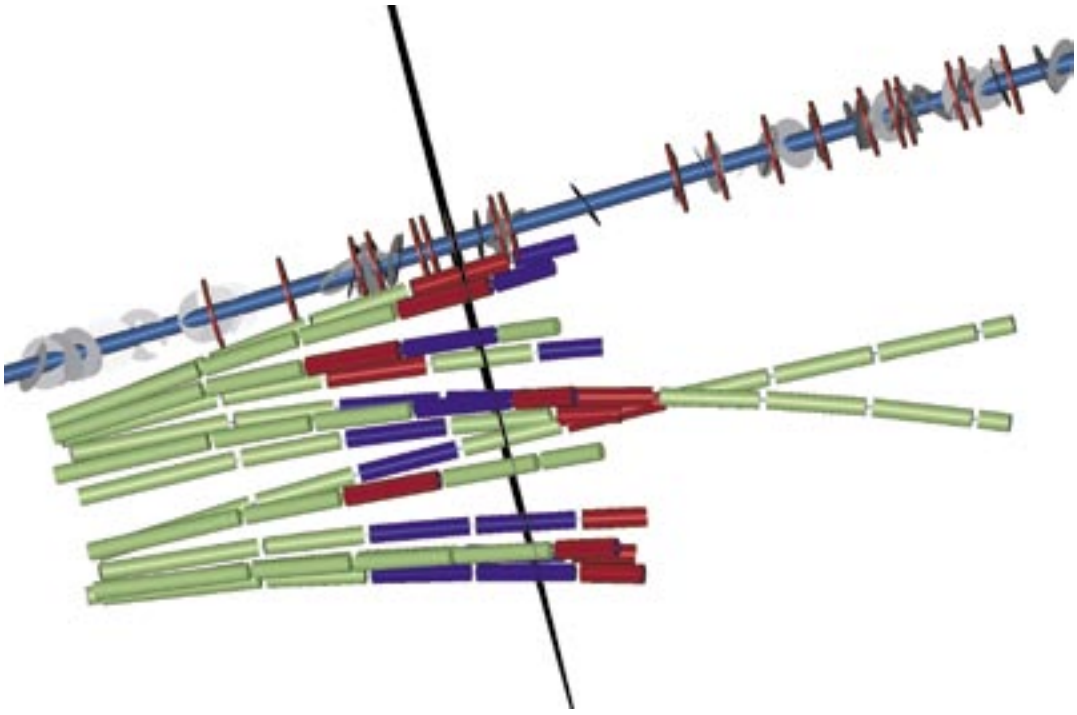

Figure K-3b. *8_50.42-2 core borehole, probe boreholes SQ0049B and SQ0049C and fan 1:1 (section inflow > 2 L/min).*

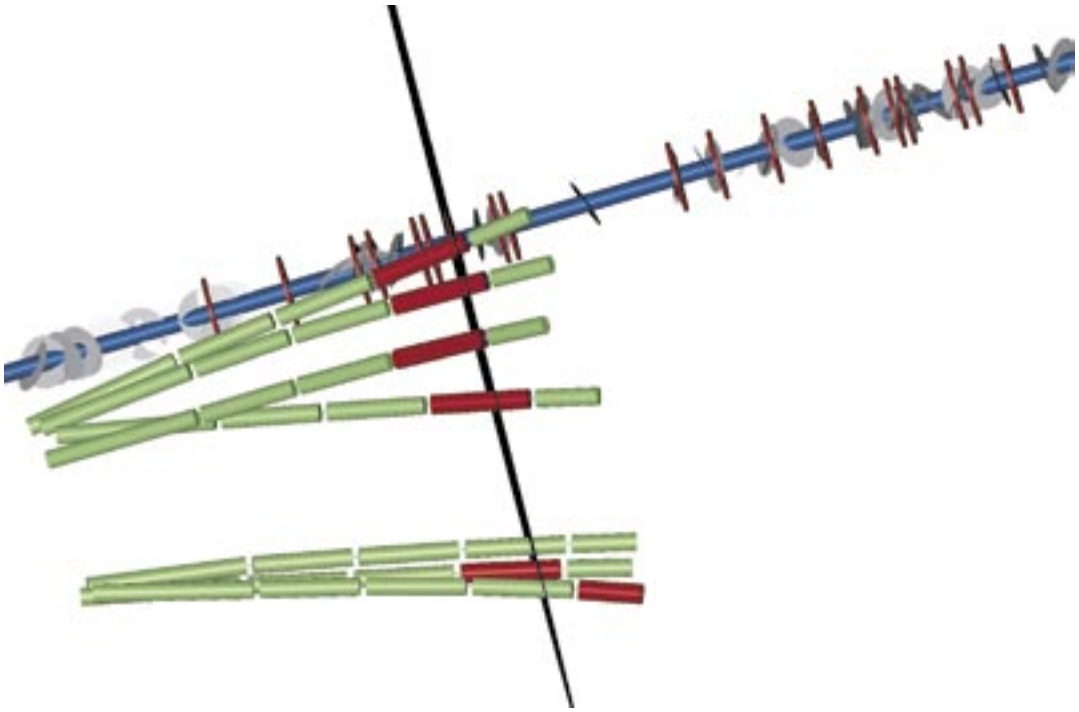

Figure K-3c. *8_50.42-3 core borehole and fan 1:2 (section inflow > 2 L/min).*

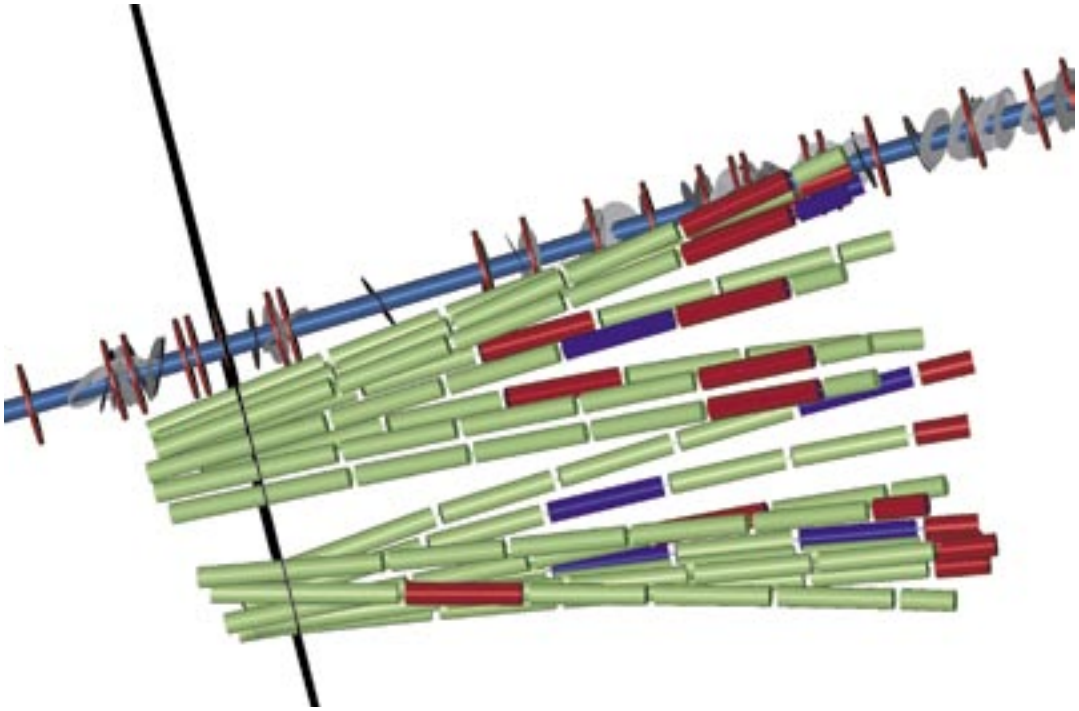

Figure K-3d. *8_50.42-4 core borehole and fan 2:1 (section inflow > 2 L/min).*

Figure K-4 a–d. Extrapolated fracture for inflow number 9/51.78 m

Figure K-4 (a–d) below shows the extrapolated fracture based on inflow number 9. The fracture that was extrapolated based on inflow number 9, also intersects the two probe boreholes (SQ0049B and SQ0049C) at their most conductive sections (150 and 180 L/min respectively, to be compared to 11 L/min for inflow 9). Further, these inflows are well above what would be expected from the grouting boreholes (median inflow approximately 40 L/min, see Appendix L). Figures (9_51.78-1 to 9_51.78-3, Fan 1:1 and 1:2) indicate that few of the grouting boreholes are actually intersecting the extrapolated structure. The tunnel mapping indicates another possible explanation since a trace of a conductive fracture is seen in the roof of the tunnel at this location. This fracture could possibly be intersected by few of the grouting boreholes or the probe boreholes only. Even so, see d) 9_51.78-4 (Fan 2:1) show that only one section intersected by the fracture has an inflow exceeding 2 L/min for Fan 2:1. The grouting application seems to have been successful and deviations between modelled grout take and actual grout take may be explained by a larger fracture being grouted via less conductive fractures or a less conductive part of the fracture.

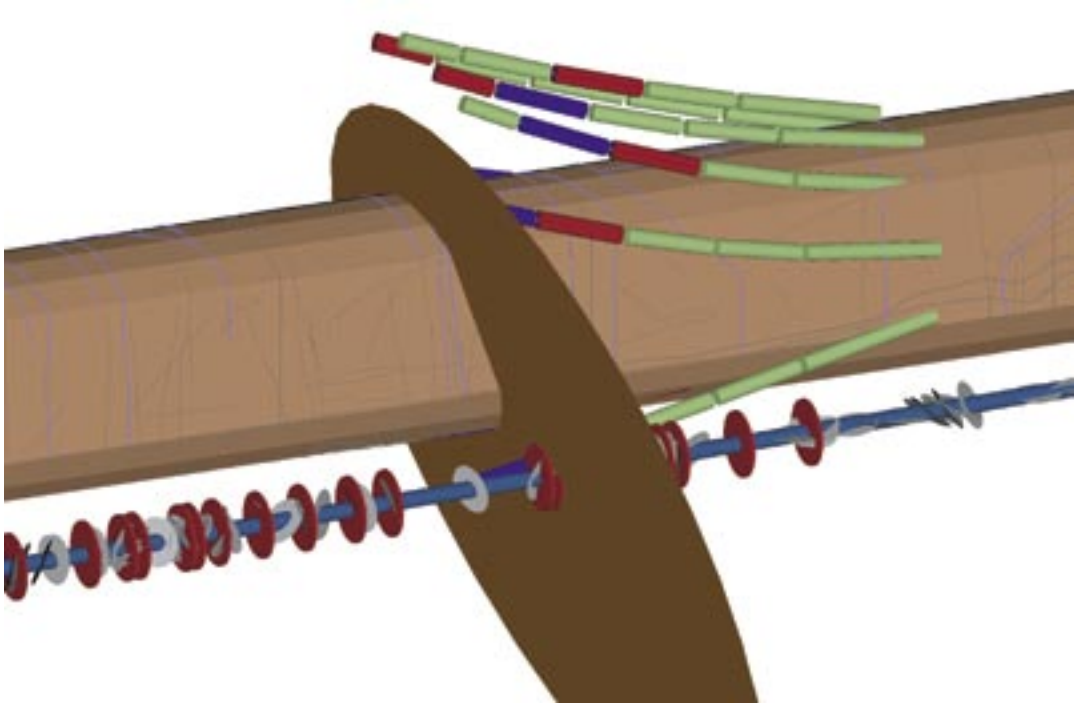

Figure K-4a. *9_51.78-1 core borehole, fan 1:1 (section inflow > 2 L/min) and tunnel mapping.*

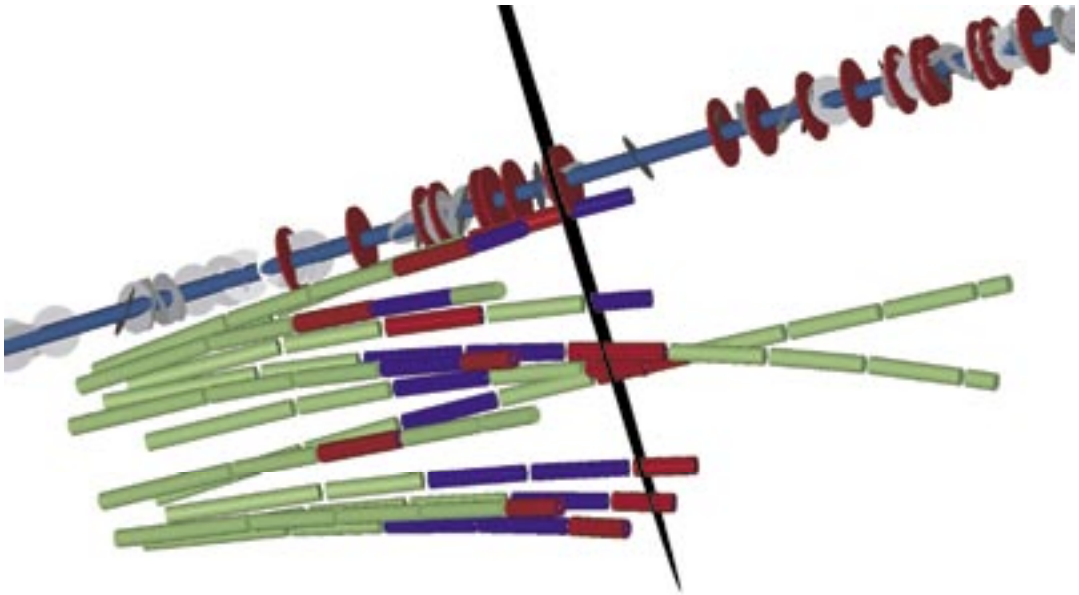

Figure K-4b. *9_51.78-2 core borehole, probe boreholes SQ0049B and SQ0049C and fan 1:1 (section inflow > 2 L/min).*

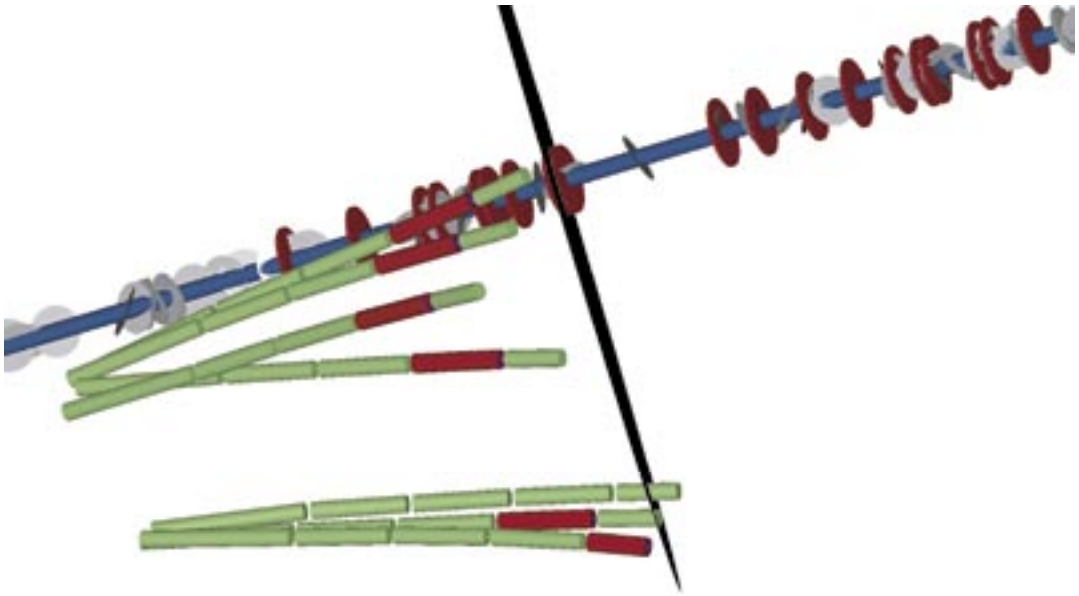

Figure K-4c. *9_51.78-3 core borehole and fan 1:2 (section inflow > 2 L/min).*

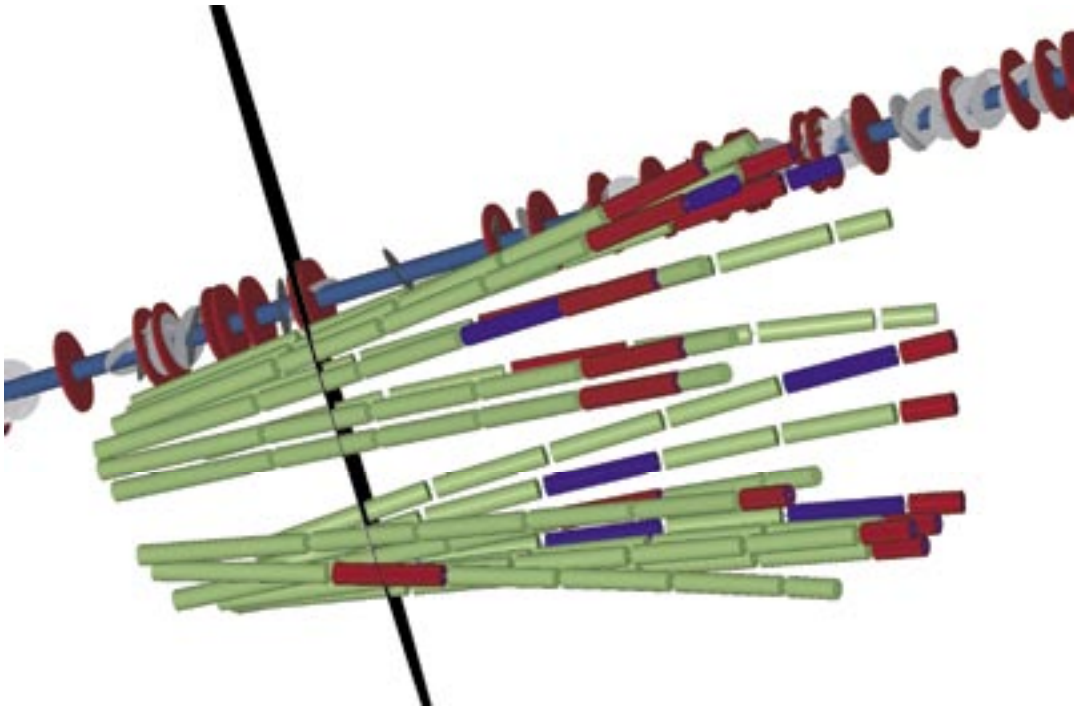

Figure K-4d. *9_51.78-4 core borehole and fan 2:1 (section inflow > 2 L/min).*

Figure K-5 a–d. Extrapolated fracture for inflow number 11/57.00 m

Figure K-5 (a–d) below shows the extrapolated fracture based on inflow number 11. This fracture was not identified by probe boreholes SQ0049B and SQ0049C. One reason for this can be the large inflows at the position of inflow 9 actually hiding smaller inflows further along the borehole. Very few of the intersected sections have inflows exceeding 2 L/min, see d) 11_57_00-4, and the tunnel mapping indicates no conductive fracture (blue fracture trace) in the immediate vicinity of this fracture.

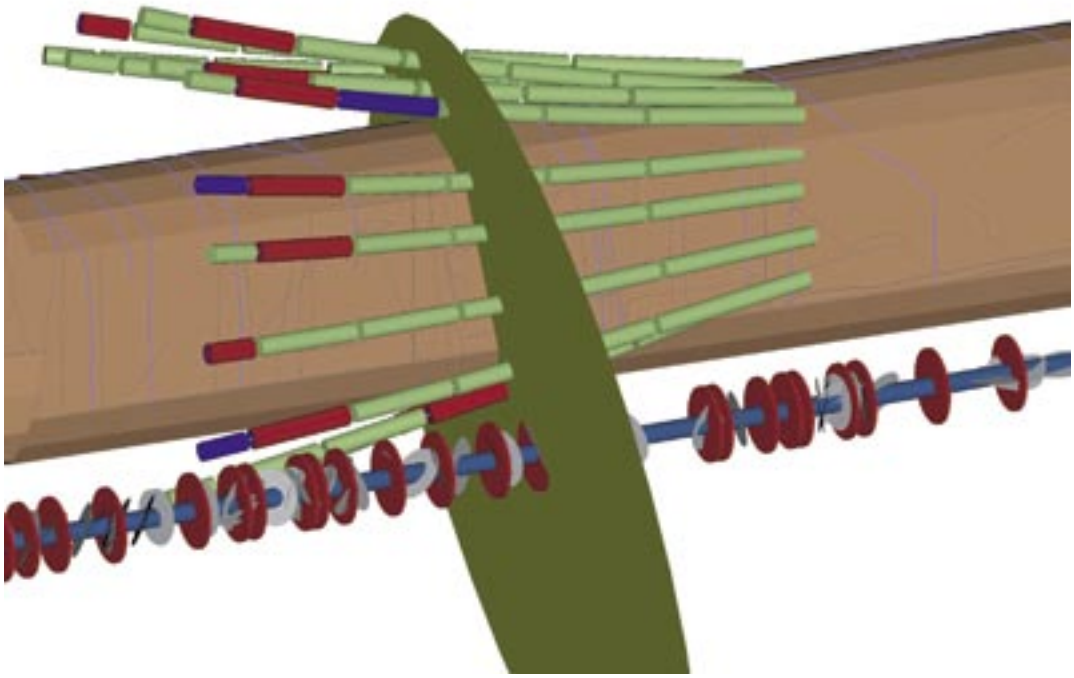

Figure K-5a. *11_57.00-1 core borehole, fan 2 (section inflow > 2 L/min) and tunnel mapping.*

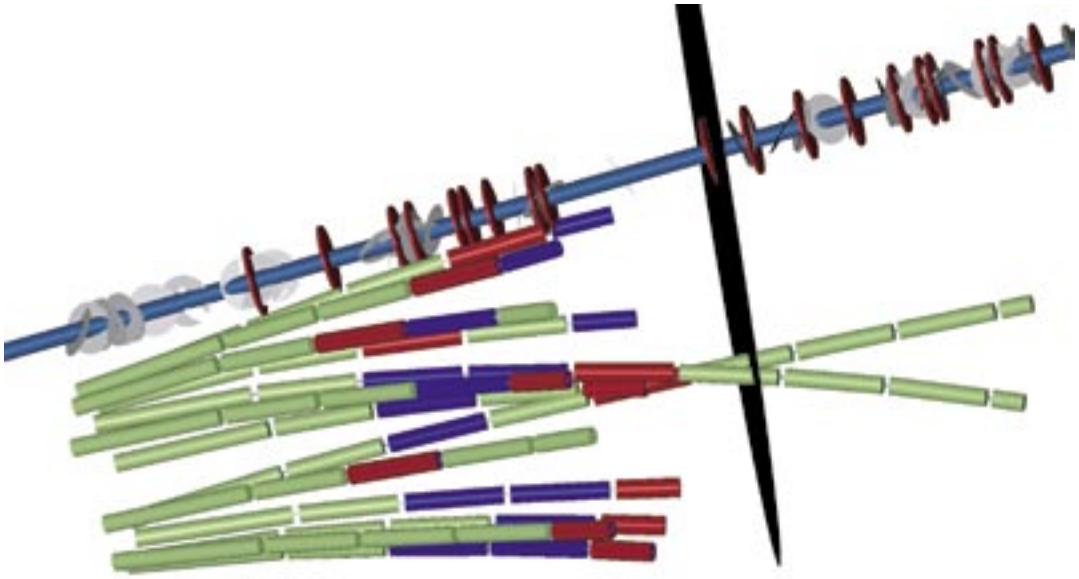

Figure K-5b. *11_57.00-2 core borehole, probe boreholes SQ0049B and SQ0049C and fan 1:1 (section inflow > 2 L/min).*

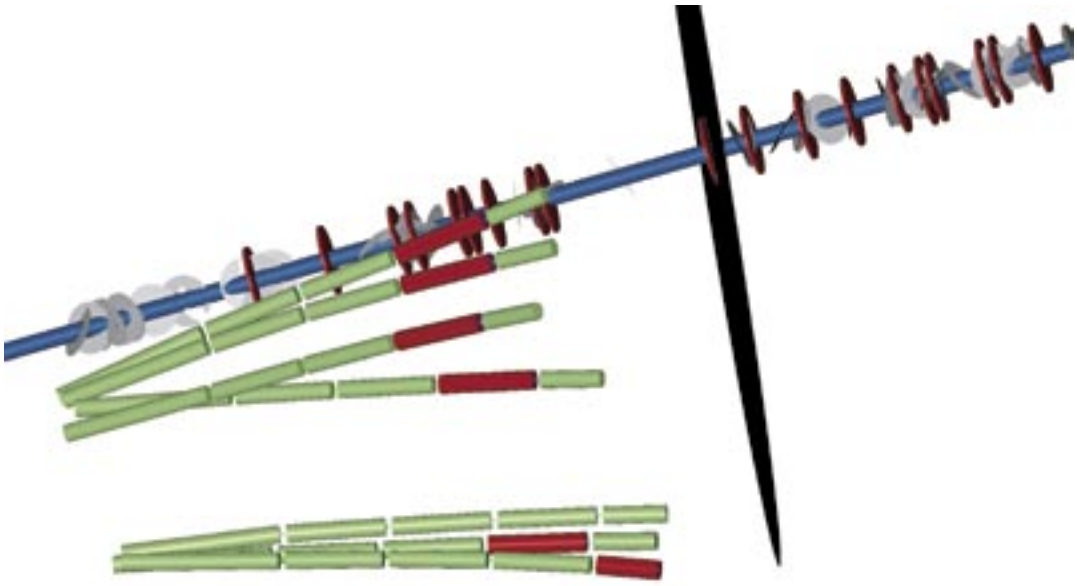

Figure K-5c. *11_57.00-3 core borehole and fan 1:2 (section inflow > 2 L/min).*

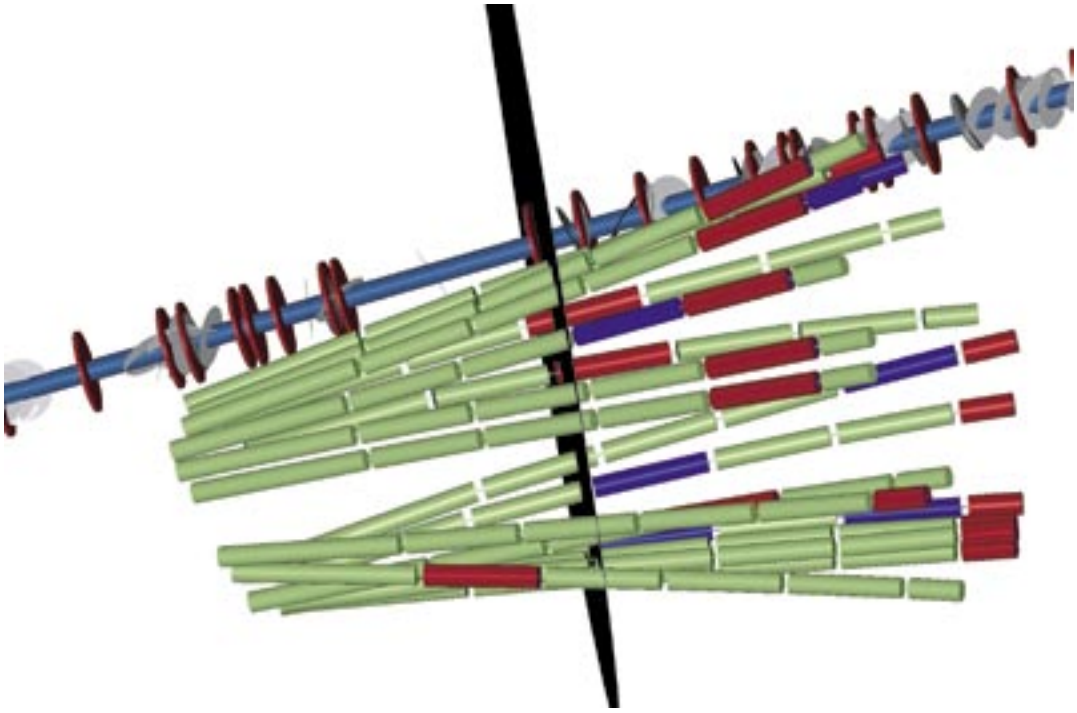

Figure K-5d. *11_57.00-4 core borehole and fan 2:1 (section inflow > 2 L/min).*

Figure K-6 a–d. Extrapolated fracture for inflow number 12/58.09 m

Figure K-6 (a–d) below shows the extrapolated fracture based on inflow number 12. This fracture as well as the above was not identified by probe boreholes SQ0049B and SQ0049C. Here, however, some of the sections have inflows exceeding 2 L/min and in the vicinity of the intersected fracture, the tunnel mapping shows a conductive fracture in the roof of the tunnel.

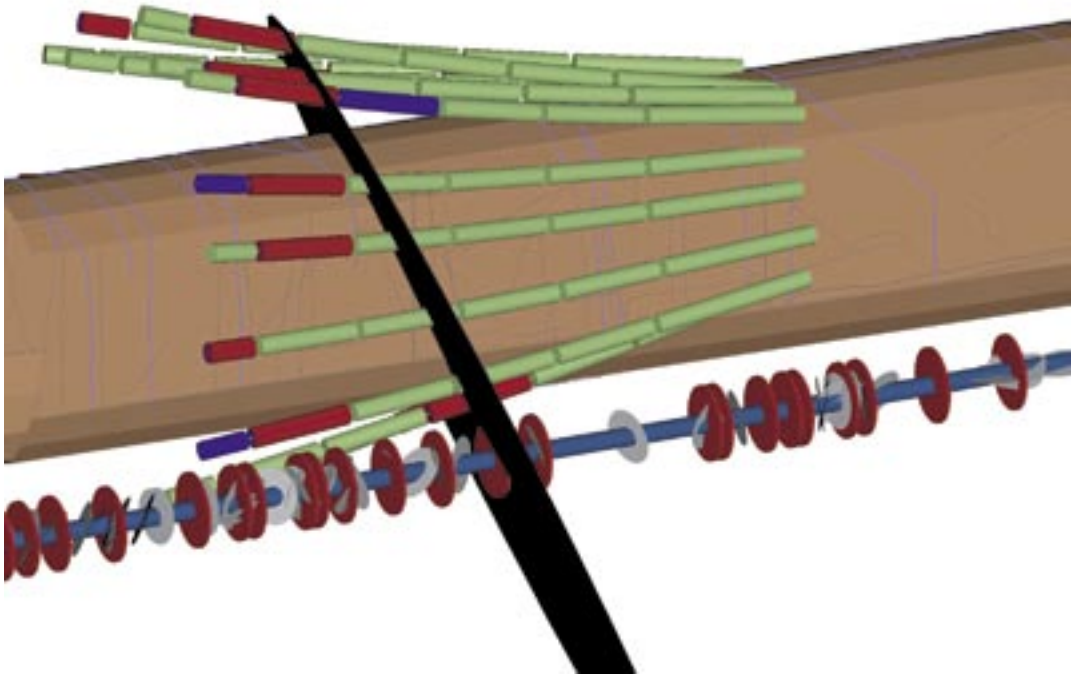

Figure K-6a. *12_58.09-1 core borehole, fan 2 (section inflow > 2 L/min) and tunnel mapping.*

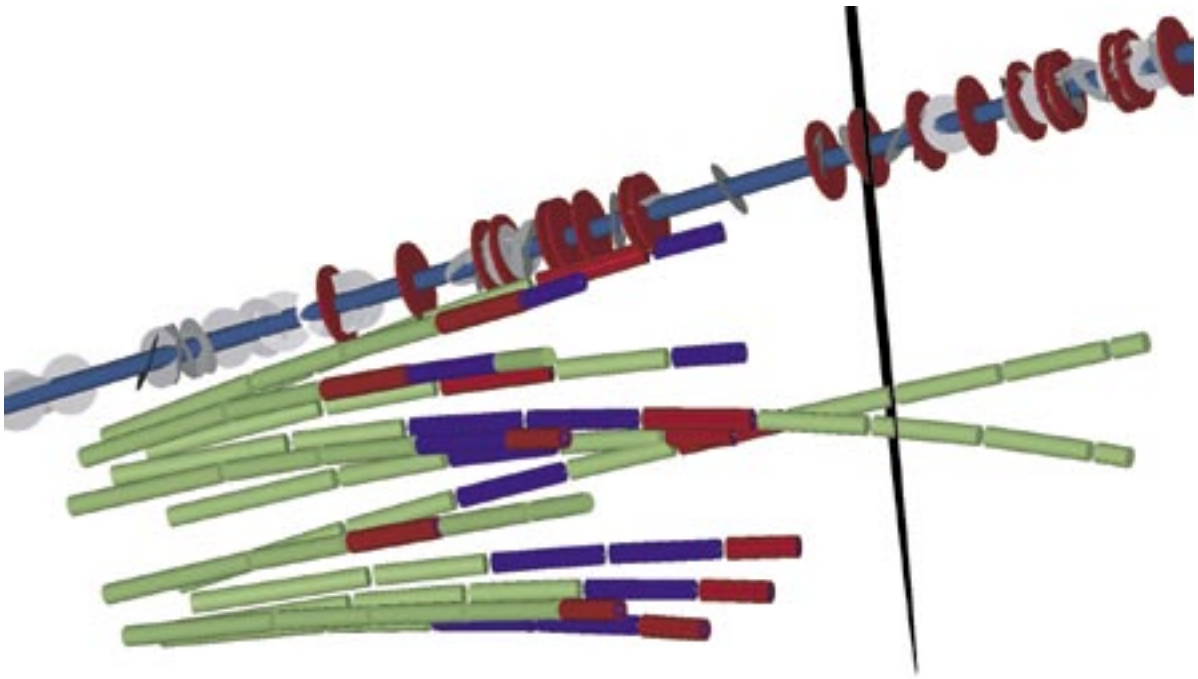

Figure K-6b. *12_58.09-2 core borehole, probe boreholes SQ0049B and SQ0049C and fan 1:1 (section inflow > 2 L/min).*

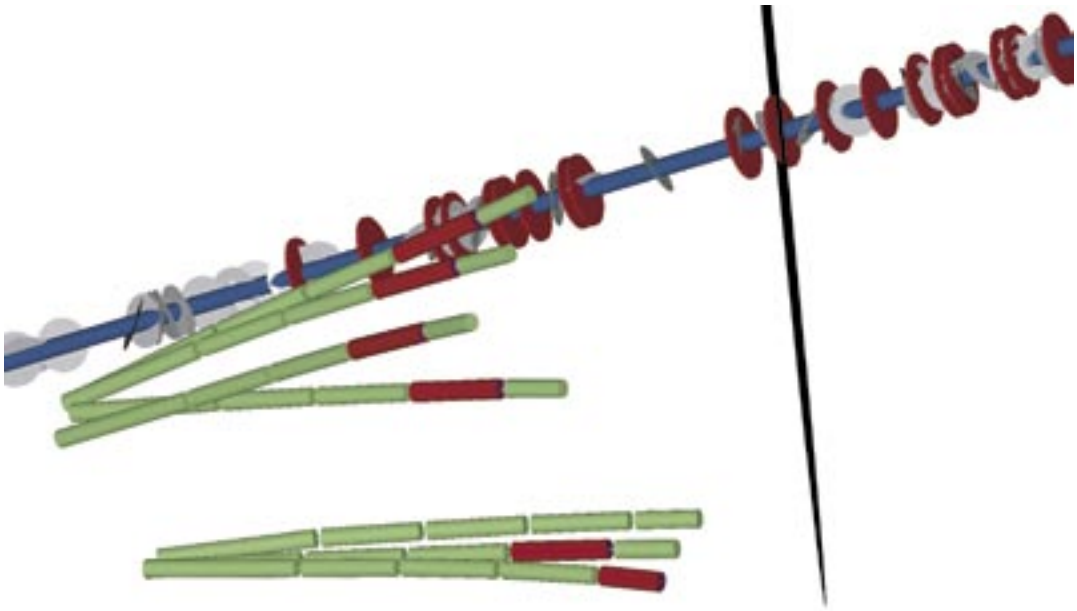

Figure K-6c. *12_58.09-3 core borehole and fan 1:2 (section inflow > 2 L/min).*

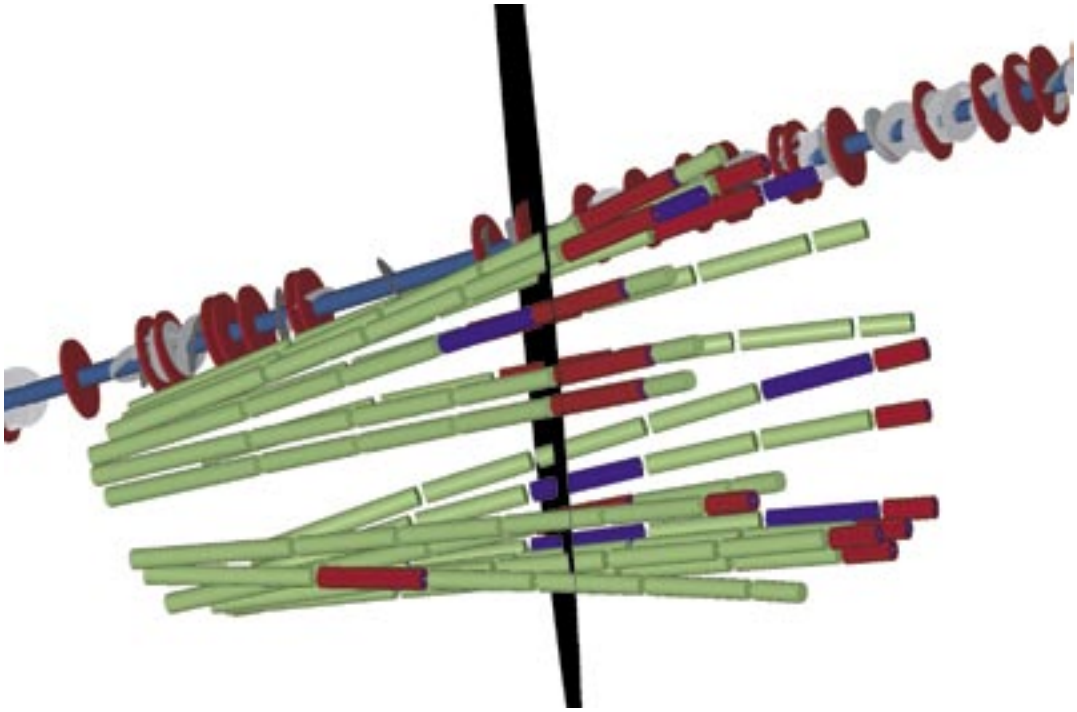

Figure K-6d. *12_58.09-4 core borehole and fan 2:1 (section inflow > 2 L/min).*

Figure K-7 a–d. Extrapolated fracture for inflow number 19/65.48 m

Figure K-7 (a–d) below shows the extrapolated fracture based on inflow number 19. A fracture is identified by tunnel mapping at this location. Only few of the sections intersected by the fracture have inflows exceeding 2 L/min.

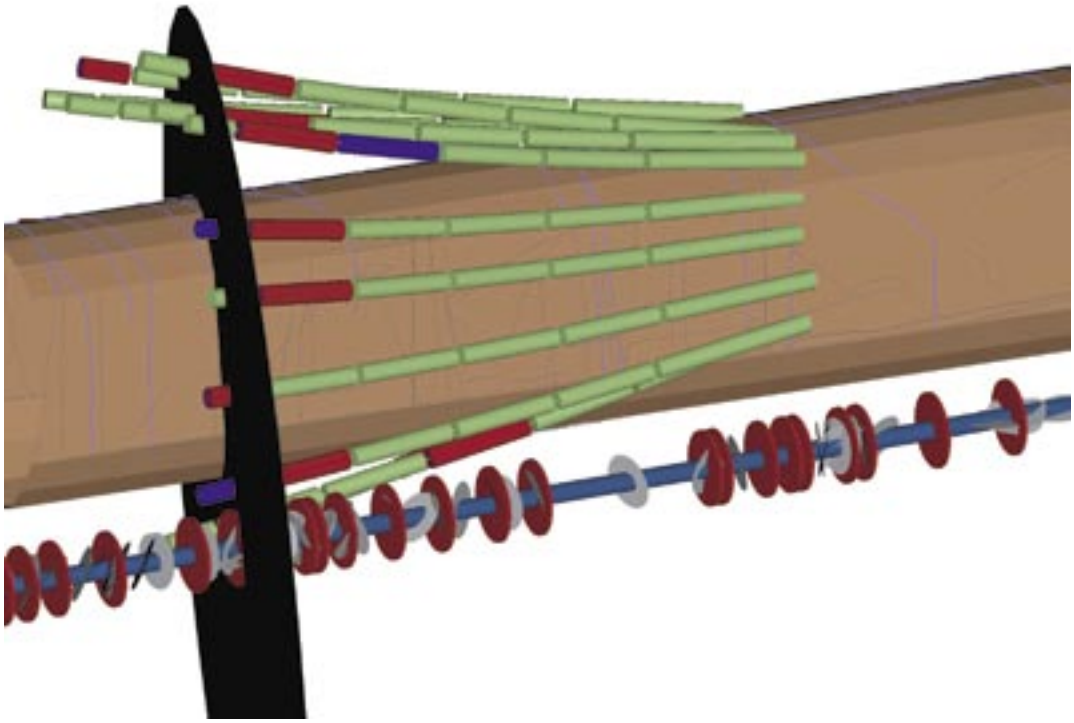

Figure K-7a. *19_65.48-1 core borehole, fan 2 (section inflow > 2 L/min) and tunnel mapping.*

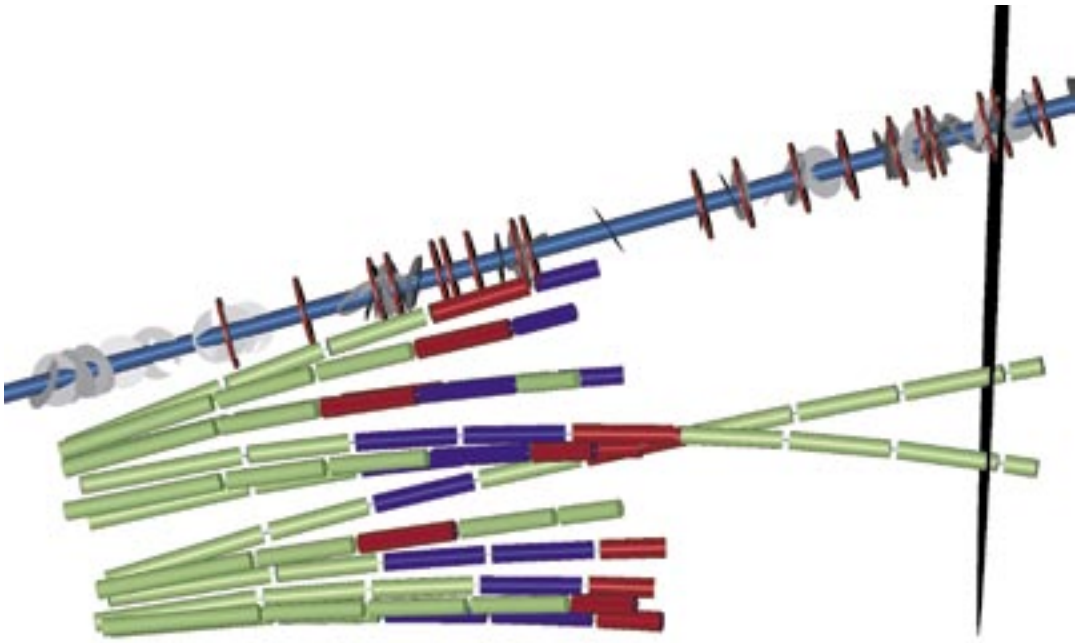

Figure K-7b. *19_65.48-2 core borehole, probe boreholes SQ0049B and SQ0049C and fan 1:1 (section inflow > 2 L/min).*

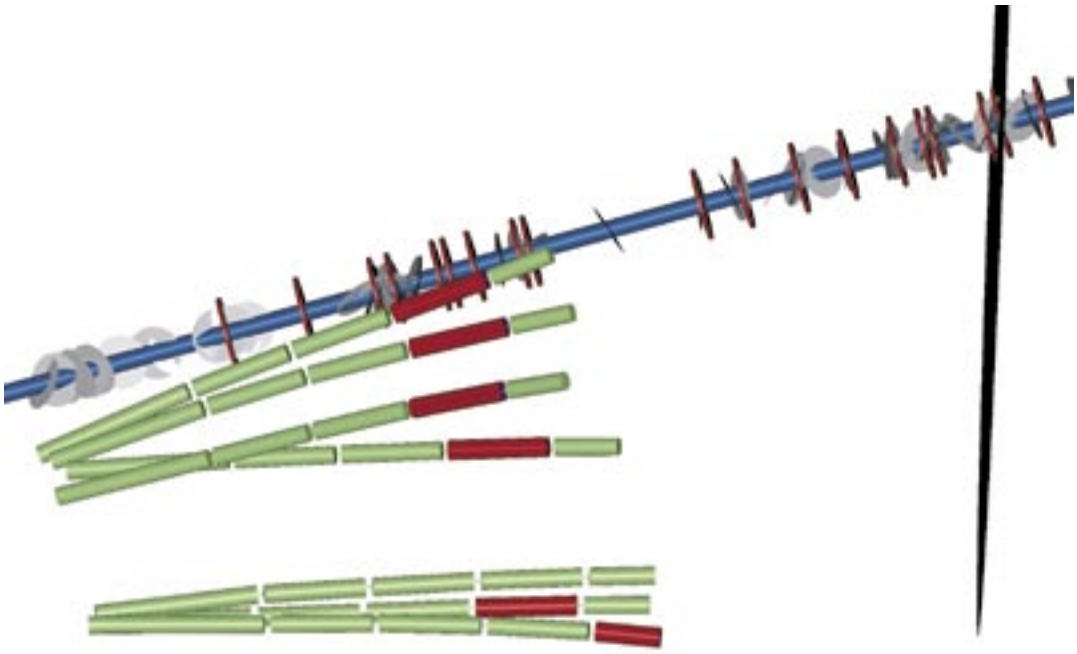

Figure K-7c. *19_65.48-3 core borehole and fan 1:2 (section inflow > 2 L/min).*

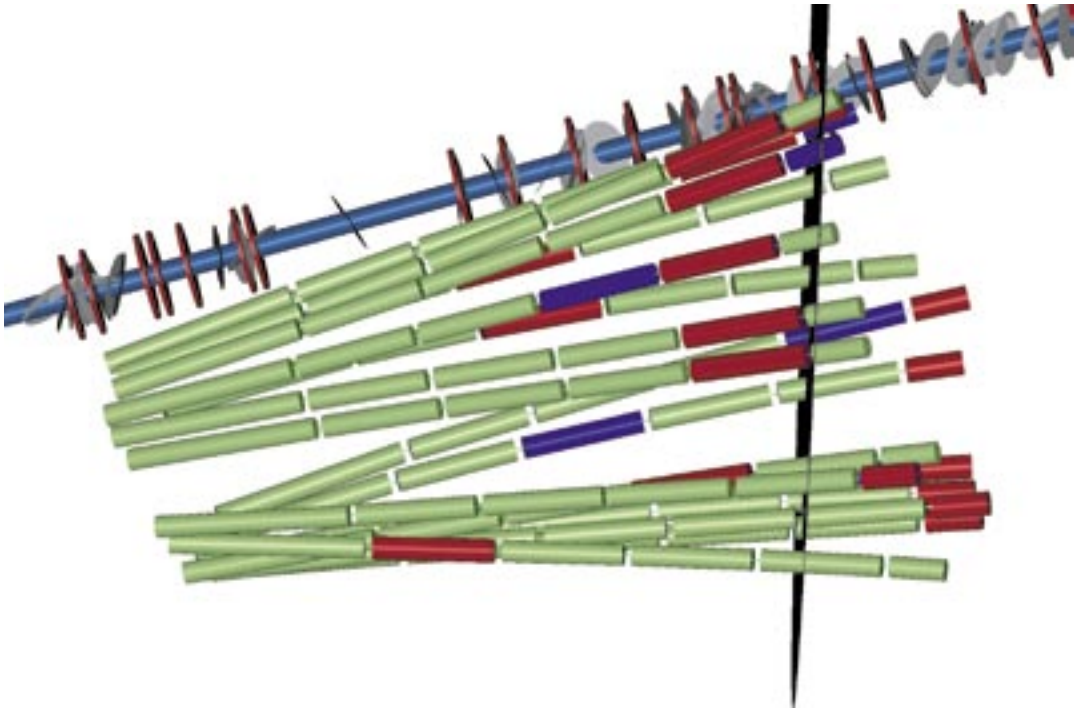

Figure K-7d. *19_65.48-4 core borehole and fan 2:1 (section inflow > 2 L/min).*

Boreholes vs tunnel mapping

Finally, what can be said about observations in boreholes compared to tunnel mapping? Fracture based on inflow 4 seems to intersect a structure that changes direction and is not going completely straight through the tunnel. One (two) conductive fractures are seen in the vicinity of extrapolated fracture based on inflow number 8. One fracture (which is divided into two along the tunnel wall) is seen in the vicinity of the extrapolated fracture number 9. Based on BIPS and core mapping of the core borehole, two approximately parallel fractures (strike/dip 129.6°/69.3 ° and 123.2 ° /70.4 ° respectively) at a distance of 0.1 m were also seen in the core borehole. In front of this (these) fractures, a blue fracture trace is seen in the roof only. This fracture is one possible explanation for the large inflows into the probe boreholes (SQ0049B and SQ0049C). At the location of the fracture based on inflow number 11, tunnel mapping identifies no conductive fracture and for inflow number 12, a fracture trace thought to be conductive is seen in the roof only. Appendix L shows that very few of the borehole sections for the fracture based on inflow 11 gave any significant inflow, which is in agreement with the tunnel mapping. Finally, a blue fracture trace is seen in the vicinity of the fracture based on inflow number 19. To conclude, tunnel mapping identifies possible conductive fractures for all predicted conductive fractures based on the core borehole except the one based on inflow no 11. However, for the location of inflow number 11, the grouting boreholes and tunnel mapping show similar results.

Section inflows for extrapolated fractures

Appendix L

Section inflows for extrapolated fractures based on strike and dip of the fracture found closest to the location of inflow (from BIPS and core logging) using RVS.

		4_47_66 Section	4_47_66 Inflow	8_50_42 Section	8_50_42 Inflow	9_51_78 Section	9_51_78 Inflow	11_57_00 Section	11_57_00 Inflow	12_58_09 Section	12_58_09 Inflow	19_65_48 Section	19_65_48 Inflow
Fan 1:1	H4	3	**0**	4	**3**	-	**-**	-	**-**	-	**-**	-	**-**
	C3	3	**28**	4	**23**	-	**-**	-	**-**	-	**-**	-	**-**
	A2	3	**0**	4	**119**	-	**-**	-	**-**	-	**-**	-	**-**
	A1	3	**1**	4	**8**	4	**8**	-	**-**	-	**-**	-	**-**
	I5	3	**132**	4	**0**	-	**-**	-	**-**	-	**-**	-	**-**
	G11	3	**48**	4	**0**	5	**12**	-	**-**	-	**-**	-	**-**
	G10	3	**24**	4	**0**	5	**72**	-	**-**	-	**-**	-	**-**
	D6	3	**0**	4	**0**	-	**-**	-	**-**	-	**-**	-	**-**
	B7	3	**12**	4	**10**	-	**-**	-	**-**	-	**-**	-	**-**
	B8	3	**0**	4	**36**	5	**108**	-	**-**	-	**-**	-	**-**
	G9	3	**5**	4	**5**	5	**44**	-	**-**	-	**-**	-	**-**
	B (probe)	3	**45**	4	**0**	5	**105**	6	**0**	6	**0**	8	**0**
	C (probe)	3	**39.1**	4	**80**	5	**180**	6	**0**	7	**0**	8	**0**
Fan 1:2	C15	3	**0**	4	**24**	-	**-**	-	**-**	-	**-**	-	**-**
	C16	3	**0**	4	**21.6**	-	**-**	-	**-**	-	**-**	-	**-**
	H17	3	**0**	4	**2.4**	-	**-**	-	**-**	-	**-**	-	**-**
	A13	3	**1**	4	**6**	-	**-**	-	**-**	-	**-**	-	**-**
	B24	3	**0**	4	**0**	-	**-**	-	**-**	-	**-**	-	**-**
	B25	3	**0**	4	**3**	5	**1.2**	-	**-**	-	**-**	-	**-**
	G26	3	**0**	4	**1**	5	**2**	-	**-**	-	**-**	-	**-**
Fan 2:1	G18	-	**-**	1	**0**	1	**0**	3	**15**	3	**15**	5	**0**
	G19	-	**-**	1	**0**	1	**0**	3	**9.9**	3	**9.9**	5	**0**
	G20	-	**-**	1	**0**	1	**0**	3	**0**	3	**0**	6	**6.2**
	G17	-	**-**	1	**0**	1	**0**	2	**0**	3	**2**	5	**4**
	G16	-	**-**	1	**0**	1	**0**	2	**0**	3	**4**	5	**0**
	A2	-	**-**	1	**0**	2	**0**	3	**0**	4	**0**	6	**2.4**
	G15	-	**-**	1	**0**	1	**0**	2	**0**	4	**0**	5	**6.6**
	A3	-	**-**	1	**0**	2	**0**	3	**0**	4	**0**	6	**0**
	B14	-	**-**	1	**0**	1	**0**	3	**0**	3	**0**	5	**0**
	A4	-	**-**	1	**0**	2	**0**	3	**0**	4	**0.5**	6	**2.2**
	B13	-	**-**	1	**0.5**	1	**0.5**	3	**0**	3	**0**	5	**0**
	C5	-	**-**	1	**0**	2	**1.5**	3	**0**	5	**31.2**	6	**0**
	D10	-	**-**	1	**0**	2	**0**	3	**0.5**	4	**3.4**	5	**0**
	B12	-	**-**	1	**0**	1	**0**	3	**0**	3	**0**	5	**0**
	H6	-	**-**	1	**0**	2	**0**	3	**0**	5	**22.8**	6	**0**
	H7	-	**-**	1	**0**	2	**0.5**	3	**0**	5	**19.9**	6	**0**
	I9	-	**-**	1	**0**	2	**3.6**	3	**0.6**	4	**0**	5	**0**
	I21	-	**-**	1	**0**	2	**0**	3	**0**	4	**0**	5	**0**

median Q	5	5	44	0	0.25	0	
median Q/dh	2.4E-07	2.4E-07	2.1E-06		1.2E-08		
median b(Q/dh)	73	73	150		27		
section inflows > 2L/min	6	7	5	2	7	5	
section inflows < 2L/min	5	4	6	19	14	16	
total n□mber of sections	11	11	11	21	21	21	
fraction < 2L/min	0.45	0.36	5/11 intersected	0.90	0.67	0.76	